A SMART MECHATRONIC BASE ISOLATION SYSTEM USING EARTHQUAKE EARLY WARNING

A thesis submitted in fulfillment of the requirements for the degree of Doctor of Philosophy

Yan-Shing Lin

School of Engineering
College of Science, Engineering and Health
RMIT University
Melbourne, Australia
September 2019

DECLARATION

I certify that except where due acknowledgement has been made, the work is that of the author alone; the work has not been submitted previously, in whole or in part, to qualify for any other academic award; the content of the thesis is the result of work which has been carried out since the official commencement date of the approved research program; any editorial work, paid or unpaid, carried out by a third party is acknowledged; and, ethics procedures and guidelines have been followed.

Yan-Shing Lin

30/9/2019

ACKNOWLEDGEMENTS

Indeed, the study of a doctoral degree and the writing of a doctoral dissertation can be regarded as two of the significant challenges in life. Although the process is arduous, it is very interesting and memorable.

First of all, I would like to thank my supervisor Ricky Chan for leading me into the field of structural control. With careful guidance and assistance, not only I successfully did complete my studies, but I also learned how to face difficulties and challenges.

Secondly, I would like to thank Nuwantha Fernando, another of my supervisors, for providing professional support in the field of control engineering. Thanks for not giving up and helping me in frustration, so that I can successfully complete this interdisciplinary research topic.

Thirdly, I would like to thank my family and partner Cynthia for the support, encouragement, and companionship in my study way. Without these, I may not be able to finish this road.

Finally, I would like to thank RMIT University for all support, including enthusiastic staff, professional educators, and software/hardware support.

CONTENTS

LIST OF FIGURES

LIST OF TABLES

ABSTRACT

Earthquake is one of the most devastating natural disasters. In the last few decades, many seismic mitigation techniques have been developed. They include passive, semi-active and active control which have been proven their effectiveness in events of earthquakes. Among them, base isolation has been regarded as a mature technology and commercialisation is common in earthquake-prone countries. This technology decouples the main structure from its foundation and effectively lengthens the natural period of vibration, away from resonance vibration. However, the lateral stiffness of base isolation devices is generally too low to resist serviceability lateral forces such as wind and flood which may cause unacceptable lateral movements of the structure. Added lateral stiffness and/or damping is usually required. On the other hand, the Earthquake Early Warning (EEW) system which uses different arrival time of seismic P and S waves is readily available in Japan, Taiwan, parts of China and Europe. This technology offers more possibilities for improvement of earthquake mitigation technique.

This project develops a smart mechatronic base isolation system which can be triggered by the EEW system. It uses the earthquake early warning signals and nearby monitoring signals to determine the situation and automatically switches to the appropriate anti-seismic mode. In the first phase of research, a one-dimensional system is developed and tested on an electrical shake table. A prototype smart mechatronic base isolation system is developed. In this prototype design, electromagnetic shear keys which lock the base isolator are released either by simulated EEW signals or on-site accelerometers. The advantage of this design gives

the main structure a very strong stiffness under in-service condition (i.e. when there is no ground motion) while maximizing the effectiveness of base isolation when ground motion is anticipated. The system is fully automated, and the main structure is re-entered once ground motion ceases. In the second stage, a two-dimensional base isolation, created by low-friction linear bearings is developed and activation of base isolation is carried out by linear actuators. In the third stage, the system is developed further. Light Detection and Ranging (LIDAR) sensors are added to monitor position of base isolator in real-time, an active control strategy is added into the microcontroller and actuation is carried out by stepper motors. Using the feedbacks provided by the sensor the active base-isolation system re-position the main structure in real-time. The research presented in this thesis opens up new opportunities in future seismic risk mitigation of civil structures. By connecting the EEWS and mechatronic devices, the performance of traditional base isolation system can be enhanced.

Keywords: *earthquake early warning; base isolation; smart structures; internet of things; sensor; controller*

CHAPTER 1

INTRODUCTION

1.1 Background of Seismic Structural Control

Earthquakes occur every day. Most of them are small or occur in remote areas such as the sea floor that most people do not feel them. In areas with relatively concentrated populations, earthquakes of magnitude 5 or above may cause enormous casualties such as the earthquake in Central Nepal in 2015, Kyushu in Japan in 2016 and Sichuan in China in 2017. In the past, we have always stressed that the stiffer the structure, the more it is resistant to earthquakes. Shock-resistant structure is an important part of traditional building technology. It strengthens the walls and load-bearing columns and adds strength supplements to form a strong building. However, with the progress of civilisation and the development of science and technology, we have learned to isolate/reduce the power of earthquakes and developed further construction technology: seismic-free technology and seismic technology.

Among these technologies, base isolation is regarded by earthquake experts as one of the most important achievements of earthquake engineering in decades. Isolation devices are

typically positioned at the base or at a certain location of the structure to isolate or reduce the transmission of earthquake energy to the superstructure. Thereby, this technique ensures the safety of buildings during an earthquake. Nowadays, numerous isolation devices have been studied and widely applied to provide a sufficiently safe isolation system between the superstructure and the foundation of the building [1]. They are broadly divided into two categories, namely elastomeric and sliding. Elastic bearings are usually composed of alternating rubber and steel plates. The rubber material provides damping elastic force, and the steel plates enhance vertical load capacity. Moreover, the lead core is added to some devices for further damping enhance. Recent developments and applications are summarized in [2]; Sliding isolation uses sliding material in the isolation layer such as low friction coefficient material, so that the upper structure of the foundation can only transmit limited earthquake force to achieve protecting the superstructure. The characteristic of low friction coefficient isolator is that the natural vibration period of the whole system before sliding is the same as the structural period. When sliding, the stiffness of the isolation layer is zero, and the natural vibration period of the whole system becomes infinite, so the sliding isolation can avoid any seismic waves. Related research and discussion are discussed in [3].

In general, base isolation systems reduce horizontal stiffness of a structure and avoid the dominant excitation frequency of earthquakes. However, wind loadings on structure attract considerable attention, particularly for base isolated structures whose elasticity is sensitive to wind excitations [4]. Henderson et al [5] discussed that the wind effect on base isolation indicates that the base isolation may amplify the response to the wind. Chen et al [6] conducted a statistical analysis to different base isolated structures to confirm the displacement response of wind. Liang et al [7] analysed the floor acceleration response of a

base isolated building to different average wind speeds to discuss the habitability of base isolated building.

To solve the problem, Soong and Costantinou [8] explain how to introduce control strategies into civil engineering. Some kinds of forces from device adapt the main structure. Passive and active control represent innovative technologies for protection of structures against wind, earthquakes and other external loads. Thereby base isolation system may be improved by controlling engineering, and it has been investigating for years. Ramallo et al [9] proposed a smart base isolation strategy using magnetorheological (MR) dampers, and Yoshioka et al [10] experimentally demonstrate H-square (H^2)/Linear–quadratic–Gaussian (LQG) damping strategy by a base-isolated two-degree-of-freedom building model with MR damper installed between the base and the ground. Chang et al [11] applies the active control technique by three actuators to a base isolated three-story two-bay steel building. Shook et al [12] do a comparative analytical and experimental study of several algorithms for the control of seismically excited base isolated structures.

Although active control strategies theoretically solve the external load problem, there are still some difficulties in the process of the actual construction of the active control base isolation system such as construction cost, the energy required for the system operation [13, 14] and the thermal shutdown of the actuator [15]. The compromise is to consider semi-active control which combines the advantages of active control and passive control. Various devices have been studied which involve (i) Stiffness control devices [16]; (ii) Electro-rheological dampers/magneto-rheological dampers [17]; (iii) Friction control devices [18]; (iv) Fluid viscous devices [19]; and (v) TMDs and TLDs [20]. However, semi-active control still has

limitations [21-23] that cannot be ignored such as (i) Modelling error; (ii) Time delay; (iii) Limited sensor and controller; (iv) Parameter uncertainties and system identification.

Further, smart control includes control algorithms and actuators as well. The biggest difference is that no precise model of structure is needed. Control algorithm uses the system output feedback to adjust the system parameters, and then actuators accurately execute control. The principle is basically the same as the active control, but the system will achieve optimal control through repeated self-improvement. Cheng et al [24] demonstrated many applications to highlight the importance of system adaptability. Kim et al [25] proposed a new bio-inspired controller which developed through the integration of a brain emotional learning (BEL) algorithm. Amezquita-Sanchez et al [26] reviewed the main smart control applications to illustrate the pros and cons of smart actuators and control strategies tendencies.

1.2 Research Motivations

Throughout the history of mankind, earthquakes remain one of the most devastating natural disasters. In recent large earthquakes such as the 2011 Tohoku, Japan, 2011 Christchurch, New Zealand and the 2015 earthquake in Nepal, tens of thousands of lives were lost and their economical and societal costs are enormously large. The Earthquake Early Warning (EEW) System is a promising technology that attempt to mitigate earthquake risks by providing warning messages to industries, public transportation such as rail companies, and to the general public via television, radio and personal communications. Japan is the first country in the world to implement a nationwide EEW system. The Japan Meteorological Agency (JMA) commenced the EEW service to advanced users in 2006 and the general public since 2007. The principle of EEW is that by utilising a sophisticated network of

seismometers, those located close to epicentre will detect P-waves of ground motion. At the seismic station, seismic intensity is instrumentally estimated considering accelerogram, amplitudes, frequency and durations [27]. The estimation is transmitted to JMA in real-time basis and then broadcasted to the public. P-waves travel faster than the more destructive S-wave, and the EEW may provide early warning, in the order of seconds to minutes, providing the valuable time to reduce seismic risks such as turning off certain industrial processes, reducing the speed of trains and the time to evacuate from buildings.

On the other hand, with the advances of engineering technologies in the last hundred years, various strategies and methods have proven to enhance civil structures capabilities of withstanding earthquake loads. Among these technologies, base isolation is an effective technique, and it is generally accepted that it is a mature technology for seismic protection of civil structures. Base isolation systems shift the natural periods of the structures to long period range, typically to 2-4 seconds by physically decoupling the foundation and its superstructure. The decoupling is achieved by a number of techniques, and various base isolator designs have been studied and now available commercially that Warn et al [28] summarizes recent developments and applications.

Indeed, base isolation systems reduce horizontal stiffness of a structure and avoid the dominant excitation frequency of earthquakes. Wind effects on base isolated structures are a practical concern, particularly for lightweight structures. Henderson et al [29] carried out wind tunnel tests on base isolated structures. Wind effects may cause unacceptably large displacement to the main structure. The topic has been studied by Chen et al [30] and concluded that hurricane wind loads on a certain base isolators may experience excessive displacements. Vulcano [31] compared earthquake and wind dynamic responses of

base-isolated buildings and concluded that serviceability – floor acceleration is a problem under strong wind and may cause discomfort to occupants. To mitigate the issue, Love et al [32] proposed the use of tuned liquid damper to reduce the motion of a base isolated structure. Base isolation system can be improved by control strategies that some kinds of active forces is delivered to the main structure. Smart base-isolation has been researched in the last two decades. However, base isolation systems with active control may imply difficulties in practical implementation. In particular, the force-delivering devices such as hydraulic actuators [33] will need to be switched on. Earthquake events are relatively rare in nature and having the system turned on will incur problems such as overheating and other maintenance issues [34]. For semi-active controlled systems, for example, the use of MR dampers [10], the problem of large power consumption seemed to be solved. However, semi-active control still requires careful system identification, tuning and control algorithm are complex to implement.

Finally, following the above, the possibilities offered by EEWS may not be just an alert to the public. In highly urbanized areas, the time required to evacuate the entire building is much longer than the time provided by the EEWS [35]. In contrast, the protection of critical systems and the activation of seismic mechanisms appear to be more helpful to reducing losses and increasing the community resilience after earthquake.

This project proposes the smart mechatronic base isolation system with the use of EEW signal provided by seismic stations which can immediately improve the structural responses subjected to the earthquake. Four conceptual frameworks of the proposed system are described and demonstrated by laboratory-scaled proof-of-concept experiments. The proposed system has the following advantages:

(1) It possesses high lateral stiffness and strength in service condition, therefore,

wind-effects on main structure does not cause excessive displacement;

(2) Precise model of the structure is unnecessary. System executes the control strategy through the information from EEWS and network of sensors.

(3) It is mechanically re-centred, does not rely on elastic stiffness of dampers or concave surfaces;

(4) It facilitates the use of linear motion guides, thus enable very low-friction base isolation and large design displacement; and

(5) The comprehensive acceleration caused by the earthquake on the building is lower, and people in the building feel more comfortable.

The conceptual design is presented, and subsequently an experimental investigation is described.

1.3 Objective and Scope

The concept of control engineering is introduced into structural design. Several structural responses, monitoring, mechatronics and seismic strategies are studied. This research is limited by the site and large scaled testing facilities. This research focuses on experimentally achieving a smart base isolation system in a small and simple version. Simulations and verifications will be respectively carried out on MATLAB, Arduino controller and a small-scale earthquake simulator. The concept of smart control is applied to the traditional Base Isolation. This includes detection, control and actuation. Based on the suddenly environmental alteration detected by either network of sensors or the Earthquake Early Warning (EEW), the actuators are activated to immediately respond to the change via isolating the building from the foundation to improve the engineering properties. Sensitivity, reliability and accuracy of signal

are also studied to include all scenarios. Then some potential controlling method will be investigated and demonstrated as a conceptual experiment. Finally, four historical earthquakes are practically simulated by shake table to verify the performance of proposed system and discussed results.

The project will be achieved in four objectives. The first one is to conceptually develop a new mechatronic smart base isolation system that can be electronically triggered by either network of sensors or the Earthquake Early Warning System (EEWS). Many possibilities for combining structures with machines are discussed and defined herein, including the structure of the building, the seismic simulation of shake table, the specifications of controller, transmission protocols and the flows of proposed base isolation system. Secondly, such system is theorized using fundamentals of structural dynamics and control theories. Degree of freedom, equation of motion, structure model, relationship between friction and displacement, and control algorithm will be mathematically described to initially explore the system's possibilities and expected results. Next is to verify such system experimentally via a scaled experiment. Proposed systems will be achieved in a small but scaled lab version and the shake table will scaled simulate four major earthquakes: (1)1994 Northridge, (2)1995 Kobe, (3)1979 El-Centro and (4)1992 Mendocino (data provide by Quanser Shake table II). Moreover, wireless sensors are mounted on the structure to record seismic responses at different locations. Finally, data is analysed on Matlab to compare the structure response and system performance under different conditions.

1.4 Research Questions

RQ1. What benefits do mechatronics and control systems add to the base isolation systems?

RQ2. How to effectively trigger the base isolation system by Earthquake Early Warning System and network of accelerometers?

RQ3. How to improve engineering properties of the isolators?

RQ4. Does active control help improve the base isolation system?

1.5 Organization of Thesis

This dissertation shows how mechatronics and earthquake early warning can be added to traditional base isolation system. The organization of this thesis is as follows.

Chapter 2 reviews the literature in detail. Firstly, the structural control in the seismic structure is reviewed and divided into three types: passive control, active control and semi-active control. Next, earthquake early warning system and its possible applications are described. The final part focuses on reviewing the mathematical model of base isolation structure and describing its state equations for time domain.

Chapter 3 introduces the monitoring of seismic structural response. It is used to trigger the proposed base isolation system and then implemented through the Arduino control platform. Through this chapter, for monitoring, several available signals (including sources, correctness and sensitivity), hardware designs (including control platform, circuit and sensors) and software designs (including system flow, decision making and network communication) can be roughly understood.

In Chapter 4, we begin to demonstrate the proposed smart base isolation system. The first is to introduce the design concept and then propose the required experimental setups and instruments. A six-story building model is built and then installed on the base isolation system. The isolator uses two parallel low friction linear motion roller guides (also called

linear stages). The system uses Arduino control platform to receive external signals (EEW and sensor networks) and then commands the actuators to perform output. In 4-1 section, actuators act as shear keys which firmly connect the foundation in normal time. The system only activates when an earthquake is detected and then the actuators disconnect the foundation as performing traditional base isolation system. As a result, the proposed system reduces the structural response and enhance the resistance in serviceability conditions such as strong winds.

Further, the base isolation system in Chapter 4 also considers the direction of earthquakes and the possibility of actual application. Another two parallel linear stages are mounted vertically on two parallel linear stages that means the building model can slide in two dimensions. In 4-2 section, electromagnets are tried to be used as the shear keys which follows the principle of attraction of the same polarity to connect the foundation in normal time. The system activates when an earthquake is detected, and then the electromagnets are discharged to disconnect the foundation. Moreover, earthquakes in different directions are simulated to test for structural response. As a result, the proposed system reduces the structural responses, but electromagnets are not recommended because the problem of overheating which can affect the magnetic force. In 4-3 section, the next part is installing four linear motors below the building on the foundation. A frame is built around the building which allows the linear motor to extend to secure the building in normal time and pull back when earthquake comes. Experiment result shows that the system can perform well when the earthquake at the beginning of the earthquake is small.

In Chapter 5, the concept of active control is introduced. Sensors continuously detect structural responses as system input, and stepper motors are used to perform system output.

Control algorithm is adopted to stabilise the building during an earthquake. Building model is mounted on two parallel linear stages and touched by stepper motors. System operates all the time against environmental disturbances such as earthquake and wind, and the building always centres to the origin. However, experiments have shown that the PID controller can only effectively maintain the structure within the system range but not improve the structural response caused by the earthquake.

Chapter 6 summarizes the thesis and discusses the future work.

CHAPTER 2

LITERATURE REVIEW

2.1 Structural Control in Seismic Structure

With the development of multidisciplinary cooperation, controlling applications in civil engineering for earthquake resistance have been gradually valued. Early, scholars focus on materials selection to strengthen the building via the characteristics such as strength, stiffness and toughness, but the damaged structure is usually impossible to be 100 % repaired [36] after earthquake because of the difficulty of construction and the changes of characteristics. Recently, the concepts of control are introduced into civil engineering and separated into two methods: passive control and active control. By reducing the input or the effect of the seismic force, the ability of damping can be effectively increased to achieve the target of isolation. At first, passive control had been widely applied to many buildings by the applications of energy dissipation and isolation. This technology is to allow the seismic force to enter the structure and then utilise the certain implements such as bracing, shear wall, dampers, isolation or energy dissipation device to absorb/isolate seismic force [37]. Next, the concept of active

control includes detection, control and actuation [8]. Based on the suddenly environmental alteration detected by sensors, the controller can switch on the actuators to immediately respond to the change via reaction force to reduce the seismic response. Finally, semi-active control combines the advantages of passive control and active control. Active control adjusts the properties of the passive control device using less control force based on the sensors' data to achieve optimal vibration control [38]. Overall, semi-active control is more stable and consumes less energy.

2.1.1 Passive Control

To reduce the damage of the earthquake to the building and improve safety, in the building structure, a nonlinear component is installed to consume the energy at the time of the earthquake. According to the damping technology applied by each building, it is mainly divided into two different damping strategies: resistant and isolation. Resistant technology is the use of a number of devices or structures in a building to absorb energy, such as beams and columns, shear walls or absorbers; isolation technology is to specially equip with an isolation layer to install isolation pads or dampers, so as to isolate most of the seismic energy.

Common resistant structures mainly include steel structure, steel-concrete structure, frame structure, shear wall and brick-concrete structure. First of all, steel structure is a structure composed of steel materials which is light in weight and convenient in construction but has poor corrosion resistance and is non-refractory [39]. It is widely used in large buildings such as the Bird's Nest Stadium in China, the Eiffel Tower in France and the Golden Gate Bridge in the United States. Secondly, material of steel-concrete structure is reinforced concrete, for example, a mixture of steel, cement, gravel and water. This structure has good

seismic performance and durability, and is often used in high-rise residential and villas, but the cost is relatively high [40]. Thirdly, frame structure is composed of beams and columns connected by rebars. Beams and columns can work together to resist the horizontal and vertical loads of the building, but the wall in this structure does not bear the weight [41] and is only for the protection and separation. Fourthly, reinforced concrete wall are used to replace the beams and columns in the frame structure that can bear the internal forces caused by various loads but unfortunately cannot be applied to large space buildings [42]. This structure is called Shear wall. Finally, brick-concrete structure is a structure consisting of a small part of reinforced concrete and most of the brick wall. The resistance to pressure is high, but the bending and shear resistance are poor [43] which result in weak seismic performance. In conclusion, the resistant structure still has to bear most energy of the earthquake that this technology is just used as the second defence.

The base isolation technology is one of the mature high-tech technologies which makes possible for buildings to not collapse in earthquake. Building with isolation technology only experiences a magnitude 5.5 earthquake when a magnitude 8 earthquake comes [1]. This technology not only reduces the damage caused by the earthquake, but also protects the decoration and important equipment. At present, because of the different materials of the isolation layer, it can be divided into three specific methods: rubber isolation bearing, sliding isolation, and damper isolation. However, it is worth noting that the design and construction of the isolation structure must be very rigorous, because the isolation layer is the extension of the column. Once the structure is flawed, it will cause irreparable damage to the main structure after the earthquake [44].

In the early 20th century, the concept of Tuned Mass Damper (TMD) was proposed [45] which uses tuned methods to reduce the vibration. However, TMD system still has some shortcomings. First, the vibration control is very sensitive to the frequency of the earthquake. If the optimal frequency of TMD system deviates from the seismic frequency by more than 5%, the control effect will decrease by about 30% [46]. Next, the substructure mass of TMD system has a great influence on the structural control ability. If the mass is insufficient, the control effect is usually poor [47]. Finally, TMD system mainly responds to linear frequencies and vibrations, so TMD system is ineffective for seismic control [48] because the structure may enter nonlinear frequencies and vibrations when earthquake comes.

2.1.2 Active Control

Active control technology is activated by external disturbances or internal responses. System continuously reads data from the sensors, and then calculates the required force for actuators to output. The control force which outputs to the structure will change the motion characteristics of the structure, thereby reducing the vibration response of the structure. Since the force of active control can change by the detected seismic wave, the seismic effect is basically independent of the seismic wave characteristics. So the seismic performance is better than the passive control. However, actuators usually requires huge energy or several devices to drive that makes this technology difficult to achieve in practical construction [34]. At present, the more mature active control technologies are: Hybrid Mass Damper (HMD), Active Mass Driver (AMD), Active Tendon System (ATS) and Active Bracing System (ABS) [49].

First of all, to improve the performance of passive control Tuned Mass Damper (TMD), Hybrid Mass Damper (HMD) was proposed [50] which is a combination of TMD and active control actuators. The system has the reliability of fail-safe, which means that TMD system can still play its passive control role and effect when HMD system fails [51]. When the time that the environmental disturbance is small, HMD system can switch to TMD system mode that active control actuator stops working to save energy and prolong its life.

Next, AMD system controls the motion of the inertial mass to convert the vibration energy of the structure into the energy consumption of the movement of the AMD mass. The springs and dampers in the system can reduce the movement of the mass and allocate the proportion of various forces in the controlling process. The resultant force is the active control force applied by the AMD system to the structure. Although AMD mass is lighter than TMD and AMD system is more effective, the construction and the maintenance of AMD system are still more expensive and this technology involves reliability issues [52].

Last but not least, ATS system is similar to ABS system. Active control tendons/braces are placed on the facade of the building to effectively change the stiffness of the structure based on the data reads by sensors, and then enhance the seismic capacity of the structure. The earliest ATS models and dynamic characteristics were proposed in [53], and then Soong's team improved and designed better results [54, 55]. Similarly, the concept of ABS was first proposed in [56], and finally a two-way ABS control system was implemented by the Soong team [54, 55].

2.1.3 Hybrid Control and Semi-active Control

Hybrid control and semi-active control focuses on the controlling of the properties of passive system device. Sensors continuously collects data from external disturbances and internal structural reactions, and then changes the stiffness or damping coefficient of the structure in real time with less control force to reduce the structural response to achieve the seismic target. In other words, hybrid control and semi-active control can be said to be a combination of passive control and active control. The main difference is that the hybrid control applies active control to regulate the natural motion of passive control, while the purpose of active / semi-active control is to improve the control effect to the structure. The most common hybrid control is dominated by Hybrid Mass Damper (HMD), and the common semi-active control systems include Active Variable Stiffness (AVS), Active Variable Damping (AVD) and Active Variable Stiffness and Damping (AVSD).

The HMD system adds Active Mass Damper system (AMD) to Tuned Mass Damper system (TMD). Unlike the AMD system that is directly attached to the structure, the AMD system is added to the TMD system so that it can be very small and light (about 10% to 15% of the mass of the TMD) [24]. Hybrid control mainly depends on the natural vibration of the TMD system, and the main goal of the AMD system here is to adjust the dynamic characteristics of the TMD system. The energy required by the HMD system and the force required to execute the control can be much smaller than the AMD system, but the equipment size and construction space requirements are high which is an application problem [57].

AVS system is activated by the sensors' data to quickly lock the device to adjust the stiffness of the system, thereby reducing the response of the earthquake. Experiments in [58] show that the device of AVS system is relatively simple, requiring only a small amount of

control force to change the parameters of the structure, and the performance is obvious. However, the design and application of AVS system is still difficult because the stiffness of the structure itself is large, while the control device can only increase the stiffness. In other words, AVS system can work better in a less stiffness structure [59].

Similarly, AVD system is activated by sensor data to quickly adjust the damping coefficient to make the damping force close to the optimal control force, thereby achieving the semi-active control close to the active control. Here, the semi-active variable damping device requires the ability of continuously changing of damping force. Common dampers include controllable damping-viscous damper [60], magnetorheological fluid damper [61], electrorhelogical damper and piezoelectric friction damper [62].

Finally, AVSD system is actually a combination of AVS system and AVD system. The basic principle is to actively adjust the controllable passive device to achieve the optimal structural stiffness or damping based on the data read from sensors, so that the structural response during earthquake reduces as small as possible to achieve the seismic target. In [63], experiment shows that the displacement of the floor can be improved by more than 40%, and the acceleration can be improve by more than 25%.

In conclusion, semi-active control combines the advantages of passive control and active control to quickly control the structure but requires only a small amount of energy to operate. In addition, the costs of construction and maintenance are lower, which is currently the most accepted seismic control method.

2.2 Earthquake Early Warning System

From 2003 to 2007, Japan officially developed the Earthquake Early Warning (EEW) System and set up stations at frequent earthquakes areas throughout the country. The principle of EEWS is to utilise a complex network of observation stations and the time difference of seismic waves. As shown in Figure 2-2-1, when an earthquake occurs, the high frequency compressional P-waves which travel fastest (about 6-7 km/sec) and it is the first body wave which will be detected by a seismic station. The more destructive surface waves (S-waves) is slower and takes a longer time to arrive. According to the characteristics of the P wave (Primary Wave) in the seismic wave which is 1.73 to 1.85 times faster than the S wave (Secondary Wave) [64], after detecting the P wave, the seismic information such as the acceleration, amplitude, frequency and duration [27] are broadcasted to the whole country through radio waves which transmit much faster (about 300,000 km/sec). However, there are still some problems in EEWS. First, EEWS is only effective for the areas 70 kilometres away from the epicentre, and the areas within 70 kilometres is a blind zone for EEWS [65]. It is impossible to receive an earthquake warning before the arrival of strong earthquake. Second, EEWS uses the first 3 seconds of the P wave to make an estimate [66]. The earthquake scale is calculated from the main wave, and then the earthquake scale and maximum displacement are integrated to estimate the distance from the epicentre. Therefore, limited information possibly causes the EEWS to be inaccurate.

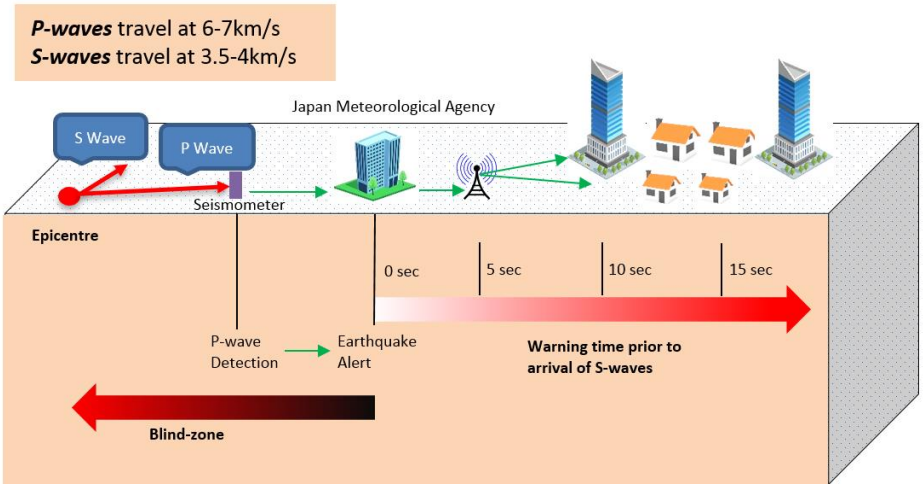

Figure 2-2-1 Schematic Diagram of Earthquake Early Warning system

In Japan, EEW can provide earthquake warnings from a few seconds to a few minutes, providing coping time to response to the earthquake. Recently, there are many applications aiming at reducing larger earthquake disasters, such as shutting down system operations, reducing the speed of transportation, opening all exits and evacuating personnel [67]. Future applications should focus more on automation, with a view to doing more things in a limited amount of time, for example, activating devices, shutting down systems, and closing pipelines.

2.3 Mathematical Model of Dynamic System of Base Isolation Structure

First, the structure is assumed to be undamaged and linear, and no relative movement between base and foundation is assumed. The shear building model is commonly adopted which assume the floor slabs are infinitely rigid and simplifies the n-level structure into

n-degree of freedom. The motions of the rigid floor plate are confined to two translations and one rotational motion. When the rigid-diaphragm assumption is made, a multi-degree of freedom system with DOF equals to n. Under 1-dimensional wind excitation, the following equation of motion can be written:

(1) $\mathrm{M}\ddot{\mathrm{x}} + \mathrm{C}\dot{\mathrm{x}} + \mathrm{K}\mathrm{x} = \mathrm{W}$

where x is the relative displacement vector. M, C, and K are $n \times n$ mass, damping and stiffness matrices respectively. W is an $(n \times 1)$ wind-excitation vector.

Then the addition of traditional base isolation layer causes relative movement between the building and the foundation. Equation of motion is written as follows.

(2) $\mathrm{M}_{bi}\ddot{\mathrm{x}} + \mathrm{C}_{bi}\dot{\mathrm{x}} + \mathrm{F}_{bi} = -\mathrm{M}_{bi}\Gamma\ddot{x}_g$

where x is a vector of relative displacements corresponding to the degree of freedom. M_{bi} is mass matrix in which it contains m_b $(n+1 \times n+1)$. C_{bi} is the corresponding damping matrix. Γ is a column of ones and $\ddot{x}_g$ is one-dimensional ground acceleration. F is the resilience force of the system. For a linear system F=Kx where K is the stiffness matrix. However, in a base isolated structure, the resilience force F will demonstrate some nonlinearity due to the base isolation system. Thus, we may write,

(3) $\mathrm{F} = \mathrm{K}\mathrm{x} + \gamma f_f$

where γ is a location matrix indicating the location of base isolation (which is at the base in this case), and f_f is a nonlinear frictional force of the base isolation device. The Bouc-Wen resilience model [68] has been used to model elastomeric types [69] and sliding type [70] base isolators. Here, we assume a friction-based sliding isolation system and the frictional force (f_f) is assumed proportional to weight of the main structure, the Bouc-Wen model can be written as,

(4) $f_f = \mu W Z$

where W is the weight of structure, m is the coefficient of friction and Z is a dimensionless parameter which is defined below:

(5) $Y\dot{Z} = A\dot{x} - \gamma|\dot{x}|Z|Z|^{n-1} - \beta\dot{x}|Z|^n$

where x is the relative displacement of dynamic system, Y is the elastic deformation, while A, b, g and n control the shape of hysteresis. Equation (4) and (5) may readily be coupled with equations of motion in a dynamic system.

CHAPTER 3

SEISMIC STRUCTURAL RESPONSE MONITORING

When an earthquake occurs, the high frequency compressional P-waves which travel fastest, and it is the first body wave which will be detected by a seismic station. The more destructive surface waves (S-waves) is slower and takes a longer time to arrive. The EEW makes use of this time difference. Seismic waves travel at 4-7 kilometres per second [71] which is significantly slower than the electromagnetic wave which travel at speed of light (300,000 km/sec). Thus, EEW observes the occurrence and P-waves by a network of seismometers distributed through the country, and system quickly analysis ground motion data and disseminate warning messages prior to the arrival of the S-waves [67].

In this experiment, the seismic monitoring system collects data from the network of sensors and EEWS from internet, and then filter out the important information. These sensors are placed at critical locations in the structure to detect the structural responses via controller. Data sensed from the sensors can be used for active control as the input of the algorithm or to

act as a trigger factor to activate the base isolation system. This chapter focuses on the seismic structure response monitoring system, which uses the EEWS from internet and the network of sensors to collect the seismic information.

3.1 Seismic Monitoring System Architecture

For the smart base isolation system to be activated, predefined trigger events are needed . A combination of sensors form the seismic monitoring system. In this project, the system has two trigger events: the signals from the EEWS and the network of sensors where the information is organized by Arduino control platform with Ethernet shield and sensors. The Ethernet shield is expanded on the controller, and as shown in Figure 3-1-1, according to the requirement, the sensors are set at different locations around the structure.

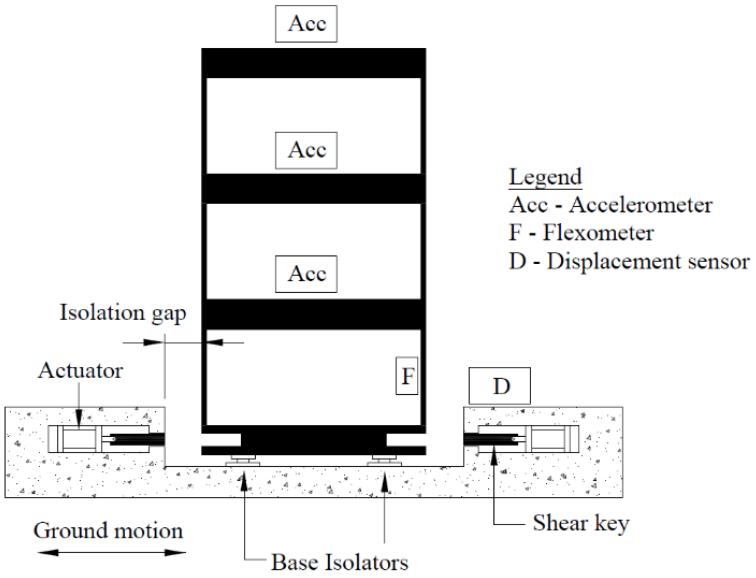

Figure 3-1-1 Seismic Monitoring System Architecture

When an earthquake is detected, the observatory sends the earthquake signals immediately via the EEWS. The changed flag of EEWS is read by Ethernet shield from internet and then a signal is sent to the microcontroller to activate the system. Due to the fact that EEWS contains a blind zone where no early warning may be given due to proximity of epicentre [72], on-site monitoring of ground acceleration is required to ensure activation of base-isolation system as backup plan. Here, ground movement is constantly monitored by accelerometers set at the foundation level around the building. More accelerometers can effectively avoid accidental triggering of system due to malfunctions, signal noises from electronic instrumentation and local disturbance such as vibrations from vehicular traffic [73]. Once acceleration above a predetermined threshold is detected, the system is triggered. Moreover, displacement sensor constantly measures the displacement of base relative to its original position. Once the ground movement ceases the system will reset and push the building back to the origin. Since the devices are lightweight in comparison to the total gravity weight of the structure, the mechanism and its associated mechanical parts will be simple and inexpensive. Unlike conventional control systems, the proposed system does not require a very meticulous control strategy to be implemented. This enables a much lower cost of computational effort, hardware requirement and maintenance that a low-cost electronic controller board will suffice. In addition, malfunctioning of control system will not cause any damage or significant effect onto the structure. Long term maintenance will be easy and inexpensive.

3.2 Hardware Circuit Design

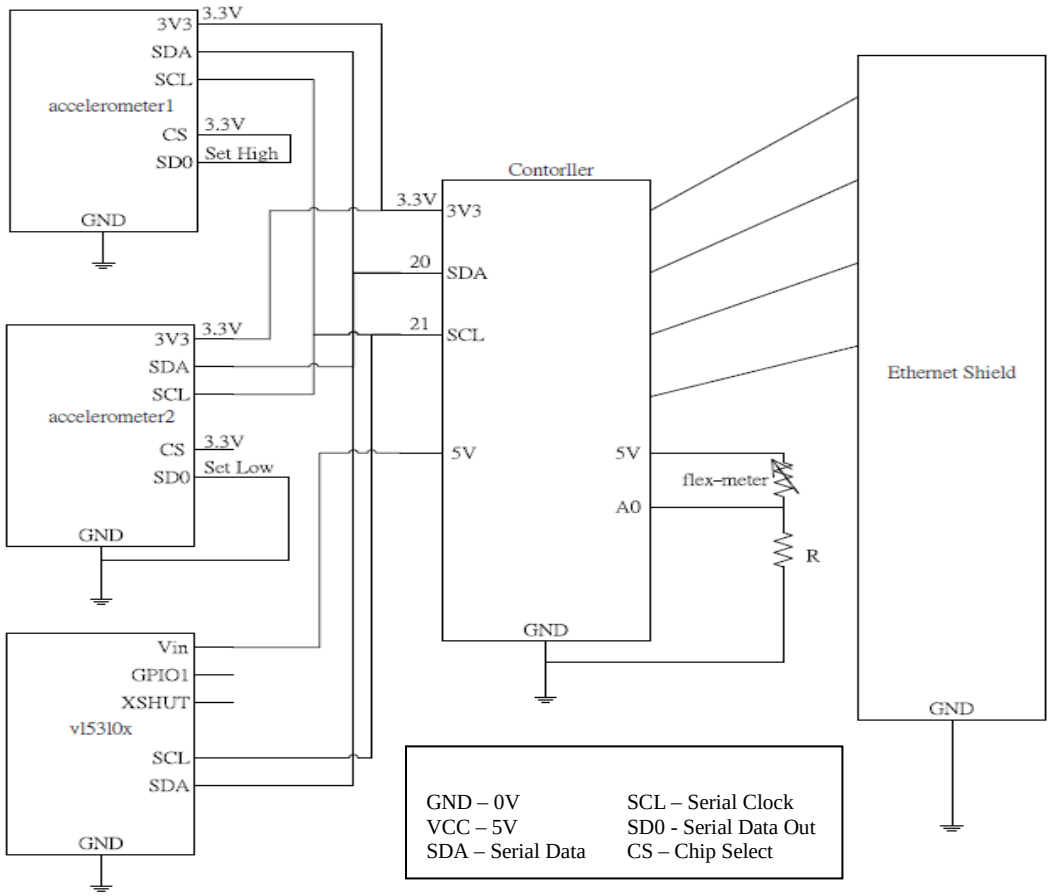

Figure 3-1-2 Circuit Design of Seismic Monitoring System

This section describes the hardware design of the seismic monitoring system. As shown in Figure 3-1-2, through the Arduino control platform, the seismic information collected from the system is used to trigger the proposed smart base isolation system. Here, the control platform and requirements, available seismic information, and network communications are listed and introduced.

3.2.1 Control Platform and Requirement

The seismic monitoring system is controlled by a microcontroller board (ATmega3289 clocked at 18MHz) called Arduino MEGA 2560 where baud rate can be set from 300 Hz to 115200 Hz. As shown in the left of Figure 3-2-1, this platform has 54 sets of digital input/output ports (14 of which can be used for PWM output), 16 analog inputs and a 16 MHz crystal oscillator [74]. Because of the built-in bootloader, it can be burned directly via USB instead of other external burners. The power supply can be powered by USB directly or by using an AC-to-DC adapter or battery. Moreover, the platform is inexpensive (about $38) and small in size. Its extensive library supports the execution of a variety of controllers, sensors and algorithms, so users can achieve their goals with minimal cost and complete design logic, making this platform much ideal for lab-scale machine experiments.

Arduino MEGA 2560

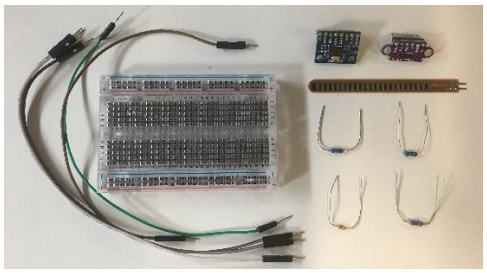

Electronic Materials

Figure 3-2-1 Arduino MEGA2560 and Electronic Materials

For the requirement of the seismic monitoring system, the sensors used are accelerometers, flex-meters and distance sensors. Here, external power supply is not necessary, and Ethernet shield will be discussed later in the network communication section.

Therefore, the electronic materials are controllers, sensors, wires, resistors and breadboards as shown in the right of Figure 3-2-1.

3.2.2 Accelerometers, Flex-Meters and Distance Sensor

3.2.2.1 Accelerometer (ADXL345)

The model of the accelerometer in this project is ADXL345 which is a small, low-power three-dimensional accelerometer with a measurement range of ±16g and a data output format of 16-bit binary complement [75]. It can be executed by Arduino control platform via SPI or I2C communication protocols. Its resolution can achieve up to 3.9mg/LSB to measure not only static acceleration of gravity but also measure the dynamic acceleration caused by motion or hitting. In other words, this sensor can detect if the device is tilted or moving.

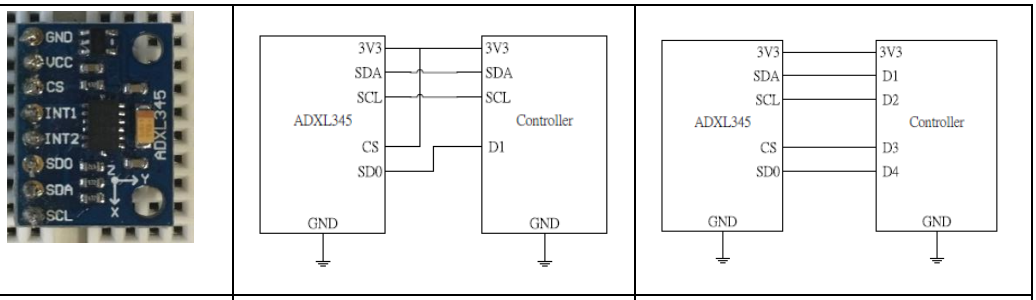

Accelerometer ADXL345	I2C Protocol Pin Diagram	SPI Protocol Pin Diagram

Figure 3-2-2 Accelerometer ADXL345 and Pin Diagram

As shown in the left of Figure 3-2-2, the ADXL345 accelerometer has eight pins: GND, VCC, CS, INT1, INT2, SD0, SDA, and SCL. The GND and VCC pin are responsible for the power supply. The CS pin determines the chip selection. The INT1 and INT2 pin output the interrupt. SDO, SDA, SCL are responsible for the serial transmission. There are two different

wiring methods because of different communication protocols: I2C and SPI. For I2C protocol, the pin diagram is shown in the middle of Figure 3-2-2, and for SPI protocol, the pin diagram is shown in the right of Figure 3-2-2. One thing to note here is to be careful not to make the voltage of the VCC pin higher than 3.6V to avoid burning the chip.

3.2.2.2 Flex-Meter

The flex-meter is actually a kind of variable resistor. One side of the sensor is printed with a polymer ink in which conductive particles are embedded. The ink is bent to cause the internal conductive particles to move away from each other, thereby increasing the resistance. When flex-meter is not bent, it is a 30K ohms resistor. The resistance can increase to 70k ohms at 90 degrees according to the bending angle (up to 90 degrees).

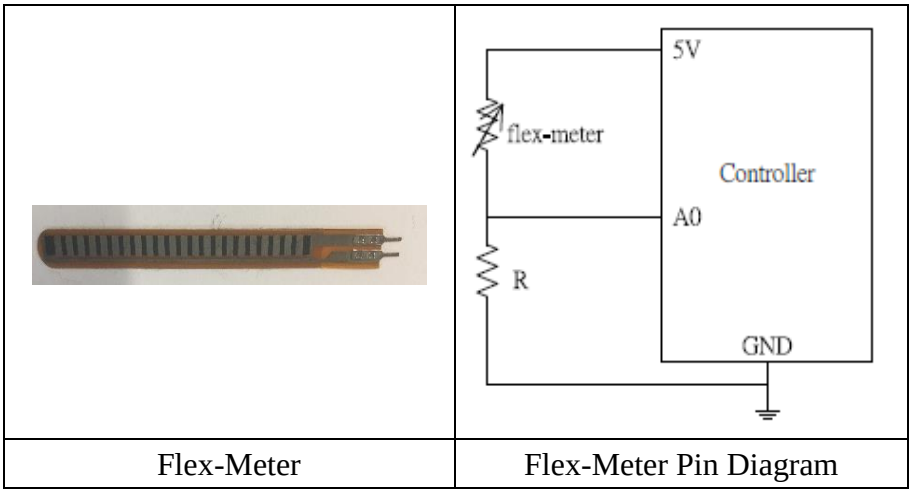

Flex-Meter	Flex-Meter Pin Diagram

Figure 3-2-3 Flex-Meter and Pin Diagram

As shown in Figure 3-2-3, the simplest circuit design of the flex-meter is to use the concept of voltage division. By connecting the flex-meter in series with a fixed resistor, the controller can read the voltage via the theory of series circuit, and then the angle and force of

the bending can be derived according to the datasheet. One thing to note here is the bending direction of the flex-meter is fixed. Bending in the other direction does not produce valid data and may damage the sensor.

3.2.2.3 Distance Sensor

On the Arduino control platform, the vl53l0x is one chose of the high-accuracy distance sensors. Without considering the color or the light reflectivity of the target, this sensor can measure the absolute distance within two meters, and the light source is completely invisible and harmless to the human eye. The measurement method is to use a new generation of time-of-flight (ToF) laser ranging which is a method of measuring distance based on the time difference between the emission and return of infrared light [76]. By using infrared light, it ensures less interference and makes it easier to distinguish natural light for higher performance and stability.

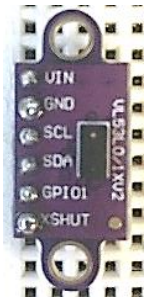

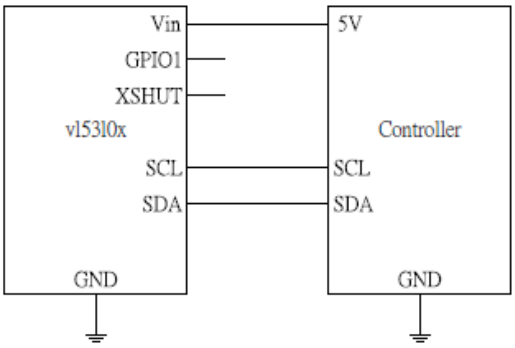

Distance Sensor vl53l0	vl53l0x Pin Diagram

Figure 3-2-4 Distance Sensor vl53l0 and Pin Diagram

As shown in Figure 3-2-4, the VL53L0X sensor has six pins: VIN, GND, SCL, SDA, GPIO1, XSHUT. The GND and VCC pins are responsible for the power supply. SDA, SCL is

responsible for serial transmission. The XSHUT is responsible for turning the sensor on/off. This sensor uses the I2C protocol, and the pin diagram is shown in the right of Figure 3-2-4.

3.2.3 Network Communication

To obtain the signal of EEWS on the Internet, the Ethernet shield is chosen as one of the Arduino expansion boards that allows the Arduino control platform to connect to the Local Area Network (LAN) or the Internet. This package supports TCP/IP Protocols (TCP, UDP, ICMP, IPv4 ARP, IGMP, PPPoE, Ethernet) on the hardware circuit to reduce the burden of Arduino. It can achieve transmission speed up to 100MB / s [77] but only allow up to four connections at the same time. As shown in the left of Figure 3-2-5, the Ethernet shield has six status indicators: TX, RX, COL, FDX, 100, LNK. First, LNK, TX and RX indicate that data is being transmitted/received. COL indicates that a packet collision has occurred. FDX means that the network connection state now is full duplex. 100 indicates that the current transmission speed is 100 MB/s.

Ethernet Shield

Plugged Ethernet Shield on Controller

Figure 3-2-5 Ethernet Shield and Ethernet Shield on Controller

For circuit design, Ethernet Shield has long pin header that can be plugged directly into Arduino control platform (as shown in the right of Figure 3-2-5) and retain the pin layout of the Arduino control platform, allowing users to stack more expansions boards as needed. One thing to note is that the communication protocol between the Arduino controller and ethernet shield is SPI, so communication and memory card read/write cannot both operate at the same time because they share the same SPI bus.

3.3 Software Design

The project will operate on the Arduino control platform, so an Arduino Integrated Development Environment (IDE) is required which includes text editors, code libraries, compilers and test platforms to simplify software development and to identify and minimize coding errors and misspellings. First of all, according to the operating system, the suitable Arduino IDE can be downloaded and installed for free from its official website. After the installation, the Arduino control platform connects the computer via the USB cable and then checks if the corresponding COM port appears. Once the environment is set down, the software design can begin.

Arduino's software design is divided into two functions: setup and loop. The code in the **setup( )** function will only be executed once the power is turned on or after pressing the RESET button, mainly responsible for parameter Initialisation and pin definition. And the code in the **loop( )** function will be looped after the **setup( )** function is executed, mainly responsible for the execution of the main functions and the input/output of the data.

3.3.1 Accelerometer

This project employs two ADXL345 accelerometers for ground motion detection. In this experiment, considering the cost of the wiring and the complexity of the layout, the controller makes serial transmission with sensors via I2C protocol. Under this, according to [78, 79], the ADXL345 accelerometer can simultaneously support read/write of two devices with the pull-up resistor 4.7kΩ. When there is only one accelerometer is used, the SD0 pin is grounded, and the device address is 0x53. Here, the memory address 0xA6 is used for data writing and the memory address 0xA7 for data reading; when using two accelerometers, the SD0 pin is connected to 3.3V, and the device address is 0x1D. Here, the memory address 0x3A is used for writing and memory address 0x3B for reading.

Figure 3-3-1 The Flow Chart of Accelerometer ADXL345

The flow chart of ADXL345 accelerometer is shown in Figure 3-3-1. The software design can be divided into three parts: enabling the I2C protocol, adjusting the mode of sensor, and reading the data. Firstly, in the **setup( )** function, the **Wire.begin( )** command is used to initialise the I2C communication, and then the **Serial.begin()** command is to set the data transmission rate in bits per second (also call baud rate) for serial transmission. Next, via the **Wire.write( )** command, the DATA_FORMAT register 0x31 is for setting the sensing range from ±2g to ±16g, and the POWER_CTL register 0x2D is for switching the mode of

sensor such as measure, sleep and wakeup. Finally, after setting the transmission and the sensor mode, the **Wire.read( )** command in the **loop( )** function is used to continuously read the data from the sensor.

3.3.2 Flex-Meter

The control method of the flex-meter focuses on the concept of voltage division in the parallel circuit, so it is relatively simple in the software design part. However, as the controller's specifications and power supply are different, there will be some errors that need to be corrected, so the range of resistance values related to the bending angle needs more tests to be more accurate.

Figure 3-3-2 The Flow Chart of Flex-Meter

The flow chart of flex-meter is shown in Figure 3-3-2. The software design can be divided into three parts: enabling analog input, reading data, and data comparison. First, in the **setup( )** function, the **Serial.begin( )** command is used to set the data transmission rate, and then the **pinMode( )** command is used to set the pin to perform analog input. Next, in the **loop( )** function, the **analogRead( )** command is used to read the voltage from the analog input to calculate the resistance value. Finally, use the **map( )** command to compare the resistance values to the bend angle of sensor.

3.3.3 Distance Sensor

In this project, the controller makes serial transmission with the sensor via the I2C protocol. Under this, according to [80], the distance sensor can simultaneously support read/write of multiple devices according to the device address. Here, you can use the **lox.begin( )** command to define more device addresses to initialise more distance sensors. One thing to know is that the device address must be different from the default device address (0x29) and must not be lower than 0x7F.

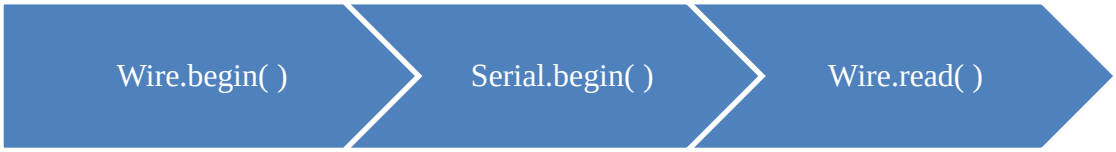

Figure 3-3-3 The Flow Chart of Distance Sensor vl53l0x

The flow chart of the distance sensor is shown in Figure 3-3-3. Software design can be divided into two parts: enabling the I2C protocol and reading data. First, in the **setup( )** function, the **Wire.begin( )** command is used to initialise the I2C transmission, and then the **Serial.begin( )** command is used to set the data transmission rate. Finally, the **Wire.read( )** command in the **loop( )** function is used to continuously read the data from the sensor.

3.3.4 Ethernet Shield

In this project, Ethernet shield is used to read the EEWS signals from the internet. To use the Ethernet expansion board, the Arduino IDE itself already has some basic libraries that can help activate the Ethernet shield, such as Wire.h, SPI.h and Ethernet.h. After setting the

environment, the device parameters have to be ensured that includes mac ID, IP address, IP port, DNS, gateway and subnet. Then the software design can begin.

Figure 3-3-4 Ethernet Shield Flow Chart

The flow chart of Ethernet shield is shown in Figure 3-3-4. The software design can be divided into three parts: enabling SPI transmission, enabling Ethernet shield and data reading. First, in the **setup( )** function, the **SPI.begin( )** and **Serial.begin()** commands are used to set the SPI transmission and data transmission rates. Next, the **Ethernet.begin()** command will activate the Ethernet shield. Finally, in the **loop( )** function, use the **client.read()** command to get the information from the specified ethernet IP address. The only thing to note is that the **client.stop( )** command must be use after all to free the memory for the next communication.

This experiment will perform in the local area network and employ the Ethernet Shield embedded on the controller. The browser acts as the console, and the Ethernet shield acts as the monitoring server. Therefore, the computer operating the browser and the controller with the embedded Ethernet shield must be connected to the same network and assigned IP addresses. As shown in Figure 3-3-5, when no earthquake occurs, the EEWS system shows no earthquake and the base isolation system is off. When an earthquake is detected, the EEWS system updates the seismic flag and then commands the controller to activate the base isolation system.

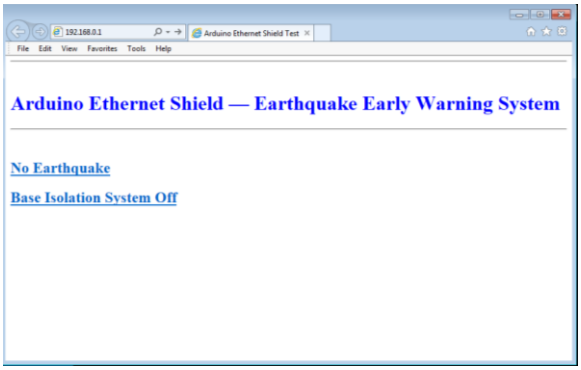

No Earthquake and BI System Off

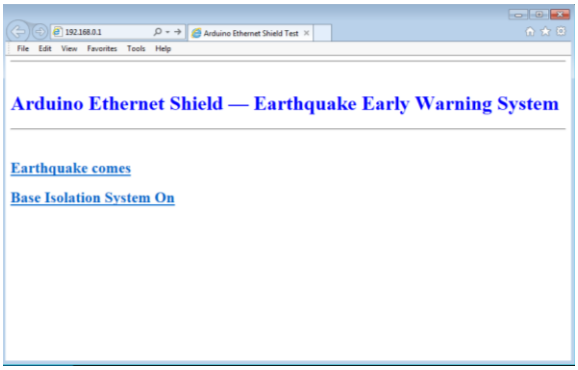

Earthquake Comes and BI System On

Figure 3-3-5 Ethernet Shield Test

3.4 Summary

In this chapter, control platform, sensor fusion and network communication are discussed to combine into a seismic structural response monitoring system. The first section, by the system architecture, provides a general understanding of the building model and sensor positions. The second section is about the specifications of the control platform, the functions of the sensors, and the mechanism of network communication. The last section discusses how to code to manipulate the control platform, sensors, and network communications. After the seismic structural response monitoring system is set up, and then the actuators are added as part of control, the proposed system is complete.

CHAPTER 4

SMART MECHATRONIC BASE ISOLATION SYSTEM

In chapter 4, the proposed system will be demonstrated and validated. Here, EEW is used to activate the base isolation system. The system begins with a conventional passive isolation system, but it is able to physically decouples the structure from its foundation. A multi-degree of freedom system is supported on an isolated base. The isolation system possesses its own stiffness and damping characteristics denoted by k_b and c_b. A flow-chart in Figure 4-1 shows the sequence of operation of the proposed system. During standby condition (i.e. with no ground motion), shear keys are engaged such that the structure is effectively not isolated. The shear keys provide high strength and stiffness against serviceability lateral forces such as design wind loads. When an earthquake is detected by EEW, a signal is sent to the microcontroller to disengage the shear keys from the foundation, and the system becomes passive base-isolated structure. Once acceleration above a predetermined threshold is detected, shear keys are disengaged via actuators. A distance sensor will constantly measure the displacement of structure relative to its original position. Once the ground movement ceases the system will reset and shear keys engage again. Since the shear keys are lightweight in comparison to the total gravity weight of the structure, the mechanism and its associated mechanical parts will be simple and inexpensive. Unlike conventional active or semi-active control systems, the proposed system does not require any control strategy to be implemented.

This enables a much lower cost of computational effort, hardware requirement and maintenance. A low-cost electronic controller board will suffice. The complexity of system identification for the purpose of tuning control strategies can also be avoided. In addition, unlike actively controlled systems, malfunctioning of control system will not cause any damage or significant effect onto the structure. Long term maintenance will be easy and inexpensive.

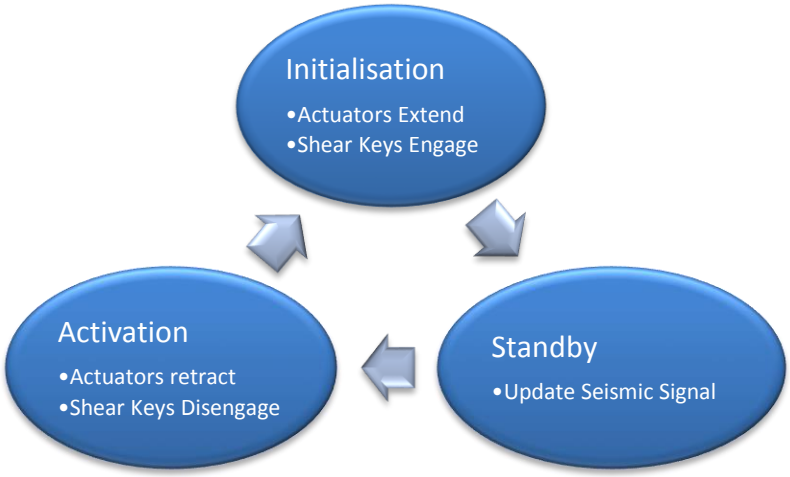

Figure 4-1 Flow Chart of Smart Mechatronic Base Isolation System

4.1 Solenoid Shear Keys

4.1.1 Experimental Setup

A lightweight six-storey frame made of aluminium, timber and acrylic glass is fabricated for this investigation. Four columns made of 5mm thick acrylic glass strips are connected to 3mm thick timber boards which simulate floors. The frame (above the base isolation system) measures 280mm x 225mm x 900mm (height). The bottom storey is braced in out-of-plane direction to avoid torsional motion. The base of the frame is made of a 10mm thick plywood and secured on the shake table. Figure 4-1-1 shows an overview of the experimental setup. Steel blocks are positioned on each floor to simulate floor masses. The total weight of frame

is 5.4kg (excluding base isolation system). The base isolation system is made up of two 16mm diameter linear steel rails and four ball-bearing slide blocks which support base plate of the model frame, as shown in Figure 4-1-2. The linear rail and slide block system is typically used in manufacturing when a high load capacity and a linear motion is required. Figure 4-1-3 shows the close up view of the base isolation. Natural frequencies were determined by experimental modal method and the first three values are: 1.62Hz, 5.94Hz and 11.5Hz. A free vibration test is conducted and its viscous damping ratio (ζ) is 2.85% determined by a fitted exponential curve, as shown in Figure 4-1-4.

The experimental setup is secured on a Quanser Shake Table II which simulates ground motion in one dimension, aligning with the base isolation system. Four scaled historical earthquakes are simulated: 1979 El Centro, 1995 Kobe, 1994 Northridge and 1992 Mendocino (data provide by Quanser Shake table II). The shake table is controlled via MATLAB SIMULINK and an algorithm is implemented to determine the desire position of the shake table measured accelerations yielded on the shake table are equivalent to the recorded values. Responses of the frame are measured independently by four accelerometers positioned at four locations: top of shake table, base (above base isolation), 3rd level and roof as shown. Each earthquake history is repeated three times:

1. "Fixed based" - with the shear key is deployed and the base isolation has been disabled;
2. "BI by EEW" - shear keys are disengaged prior to the ground shaking and base isolation is effective, representing a situation where EEW is effective forecasting the arrival of ground motion, and;
3. "BI by sensor" refer to the situation which the shear keys are disengaged by the controller, when readings from accelerometers exceed the threshold value.

Figure 4-1-1 Overview of Experimental Setup

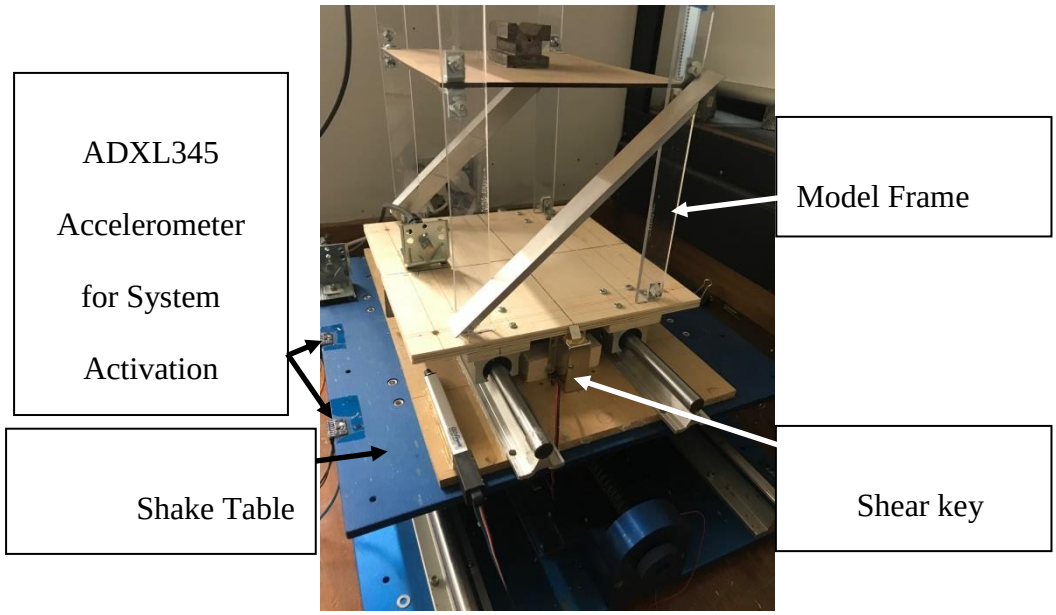

Figure 4-1-2 Side View of Setup

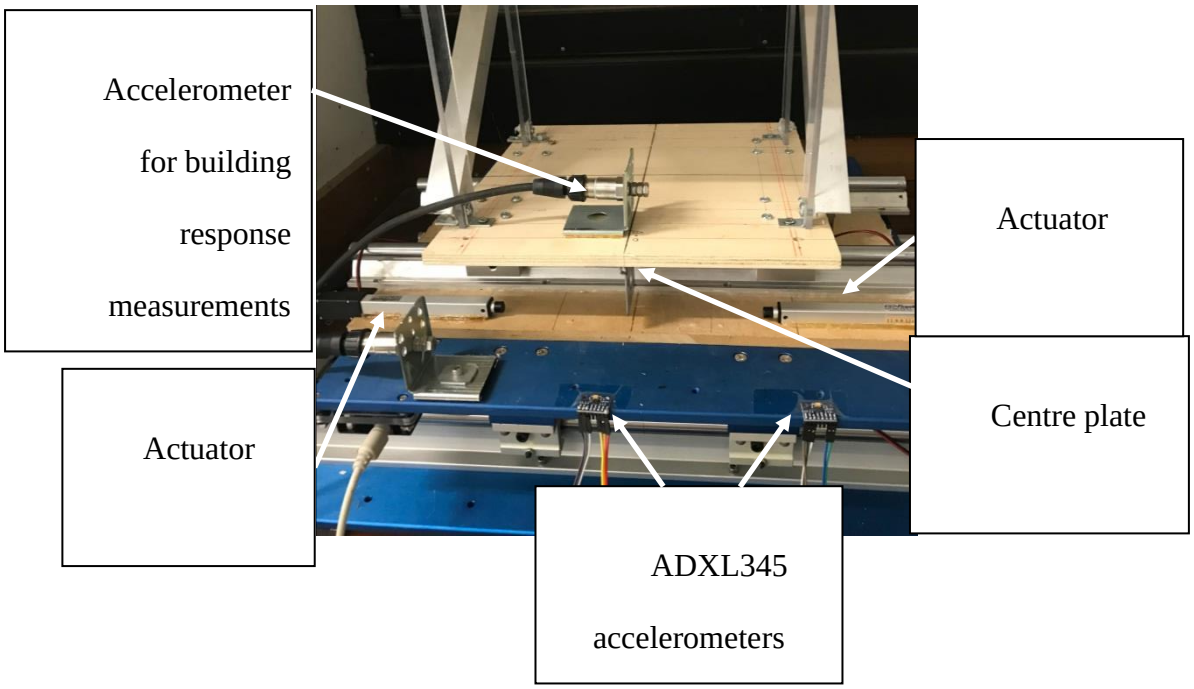

Figure 4-1-3 Front View of Setup

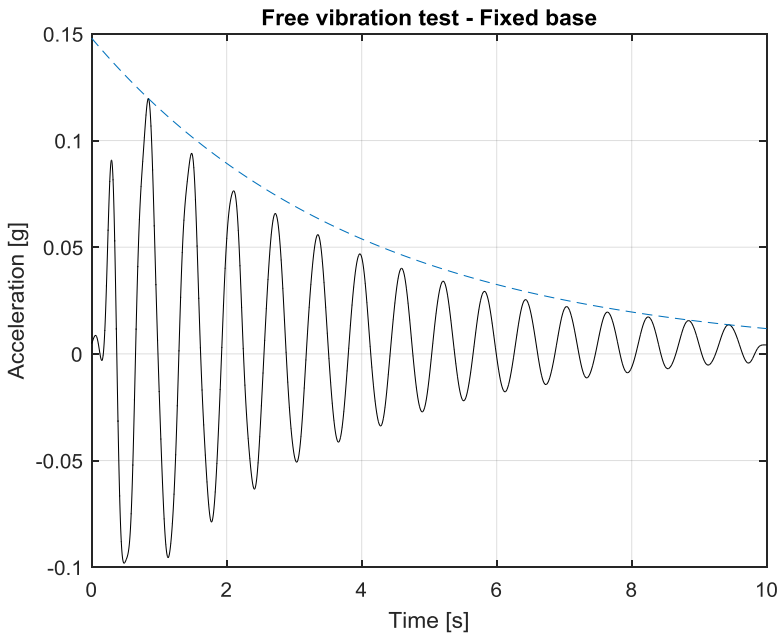

Figure 4-1-4 Free Vibration Test of Model Frame

4.1.2 Controller, sensors and actuators

The smart base isolation requires connectivity between EEWS, network of sensors and actuators. In the experiment, the smart base isolation is controlled by Arduino microcontroller where the baud rate is set to 9600Hz. In order to monitor the status of EEWS, controller keeps reading the data from EEWS until the earthquake statement changes. Internet communication is carried out by an Ethernet shield plugged in the controller. As the backup plan, the proposed system also requires the network of sensors to trigger base isolation in the event which EEWS fails to provide advanced warning. Ground acceleration detection is made via two 3-axis digital accelerometers whose model is ADXL345. These accelerometers are very low cost and factory calibrated, and suitable for the present experiment. For the choice of communication protocols, I^2C is chosen for the network of sensors in this project for its simpler connectivity with controller board because it only requires two signal lines connecting Serial Data Line (SDA) and Serial Clock Line (SCL).

The requirements for the actuator in this smart system are low power supply consumption and fast reaction time. In the experiment, solenoids are chosen as shear keys. An electric solenoid works on the principle of electromagnet. It contains a coil that when energized it produces a controlled magnetic field through its centre. By placing a magnetic armature inside that field, the armature can move in or out of the coil. The use of solenoid is chosen due to its very rapid deployment and its simplicity in circuitry design. However, one drawback is that they require a higher voltage and a separate DC supply is required in the experiment. The solenoids in the experiment are powered by 12V DC and its circuit consists of diode, transistor and resistor. A simple circuit diagram of the experimental setup is shown in Figure 4-1-5.

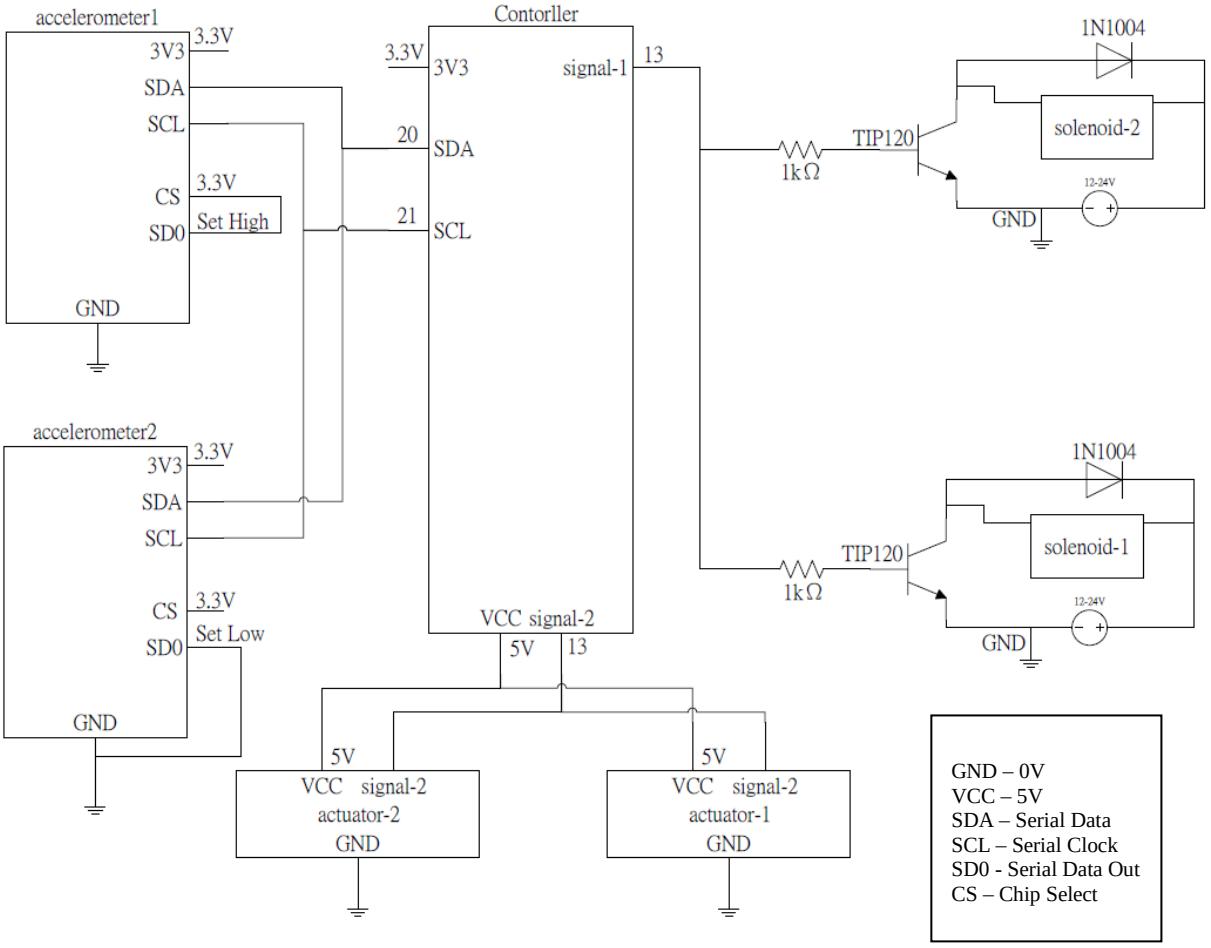

Figure 4-1-5 Circuit Diagram of Smart Base Isolation System

4.1.3 System Initialisation and Activation

In system Initialisation stage the system has to reset the position of the main structure and deploy the shear keys. In the experiment, two electric linear actuators are selected to execute the system Initialisation. They are a kind of electric motors with a feedback signal such that the extension can be fed to microcontroller [81]. They are often used in manufacturing and robotics where linear motion is required. As shown in Figure 4-1-3, two Firgelli 100mm stroke linear actuators (peak force 31N at 7mm/s) are used. They share the

same power supply with the microcontroller board which simplifies the circuit design. In the system Initialisation stage, the actuators are programmed to fully extend (see Figure 6), which will push the main structure via a centre plate to its original position. This simple arrangement eliminates the need of a displacement sensor to monitor position of the main structure. Once shear keys are deployed the actuators will fully retract to avoid making contact with the base isolation system. Subsequently, the system enters service condition in which the microcontroller constantly refreshes the status with EEW and anticipates an earthquake signal.

In the experiment, the base isolation can be activated by three methods: (1) signals from EEW via Ethernet shield, (2) triggered by readings from accelerometers (ADXL345) and (3) a manual switch. The manual switch facilitates adjustments and acts as a manual override, for example by a building manager in a real-life application. The threshold acceleration to trigger base isolation is set to 0.04g. This threshold value is arbitrarily set for the purpose of this experiment and can be programmed to any desirable value. Shear keys are only triggered when the average of both detected acceleration exceed this threshold simultaneously, because high sensitivity may cause unnecessary trigger [82].

4.1.4 Results and Discussions

A total of 12 earthquake simulations were carried out and the test setup is robust and repeatable. Re-centring mechanism performed successfully after each ground motion ceases. Peak values of structural responses are shown in Table 4-1-1 and plotted against time in Figure 4-1-6 to Figure 4-1-9. For clarity only response on roof level is plotted. It should be noted that these readings are independent of those recorded by accelerometers (ADXL345)

connected to the controller board. These measurements are filtered by 6th order Butterworth low-pass filter in MATLAB with cut-off frequency of 25Hz. The figures are arranged in the following sequence: (a) measured shake table accelerations, and roof accelerations - (b) Fixed based; (c) Base isolation triggered by EEW and (d) Base isolation triggered by on-site accelerometers.

		Fixed-base	BI by EEW	BI by sensor
1979 El Centro	Roof	0.6576	0.0908	0.3760
	3rd floor	0.7065	0.1019	0.6280
	Base	1.8112	0.1157	0.7659
1994 Northridge	Roof	0.5879	0.1047	0.4600
	3rd floor	0.6857	0.1011	0.5408
	Base	0.8903	0.1200	0.8383
1995 Kobe	Roof	0.8865	0.1300	0.1142
	3rd floor	0.5818	0.0984	0.1183
	Base	0.1759	0.1371	0.1421
1992 Mendocino	Roof	0.5240	0.1516	0.4113
	3rd floor	0.4897	0.2437	0.4909
	Base	0.557	0.3512	0.5669

Table 4-1-1 Experimental Results (units in *g*)

From Table 4-1-1, it is evident that the base isolation system, if triggered by EEW prior to arrival of ground motion significantly reduce the observed structural responses in all levels. If EEW fails and triggering is carried out by on-site sensor, significant benefits are observed. It should be noted that the measured acceleration at the base of Fixed-base model is larger than the peak acceleration of shake table. This is due to the construction of the model frame

that even when the shear key is deployed, slight movement of the base is unavoidable and ground shaking causes small impacts between shear keys and base.

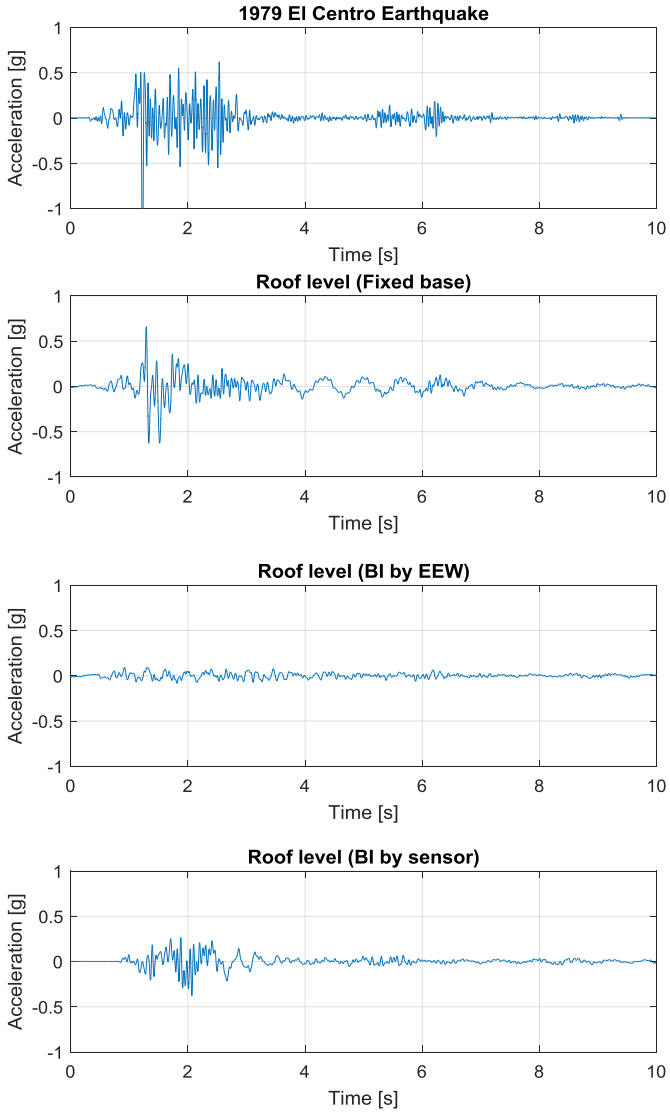

Figure 4-1-6 1979 El Centro Earthquake

In Figure 4-1-6, the 1979 El Centro Earthquake is characterized by a strong motion within the first 2 seconds of the time history, causing the rapid response of the structure almost immediately in the “fixed based” test (the second of Figure 4-1-6). However, when

base isolation is triggered by EEW before the arrival of the shock waves, structural responses are significantly reduced (the third of Figure 4-1-6). On the other hand, when EEW fails to predict and the base isolation is triggered by on-site accelerometer (the forth of Figure 4-1-6), the main structure is excited as a fixed-base structure early in the ground shaking and structural response quickly diminished as the shear keys are disengaged.

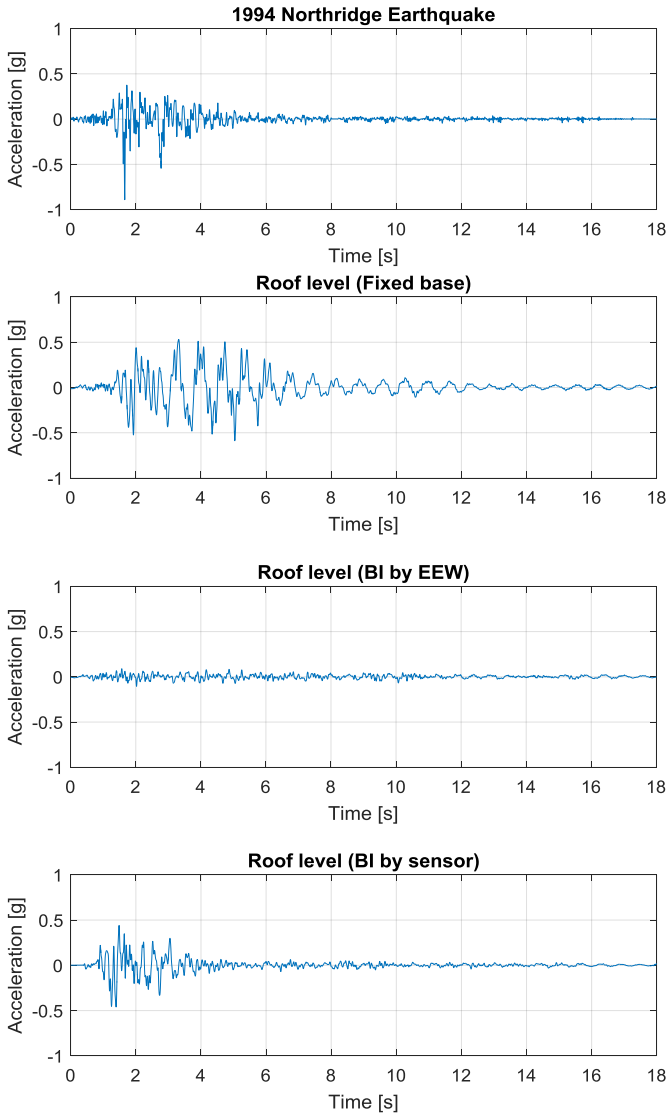

Figure 4-1-7 1994 Northridge Earthquake

In Figure 4-1-7, the 1994 Northridge Earthquake is characterized with a strong shaking early in time history, and overall performance of the smart base isolation system is similar to the previous earthquake time history – the EEW triggered (the third of Figure 4-1-7) shows substantial reduction in structural response, while the sensor triggered (the forth of Figure 4-1-7) shows some strong structural responses early but quickly diminished due to the released shear keys.

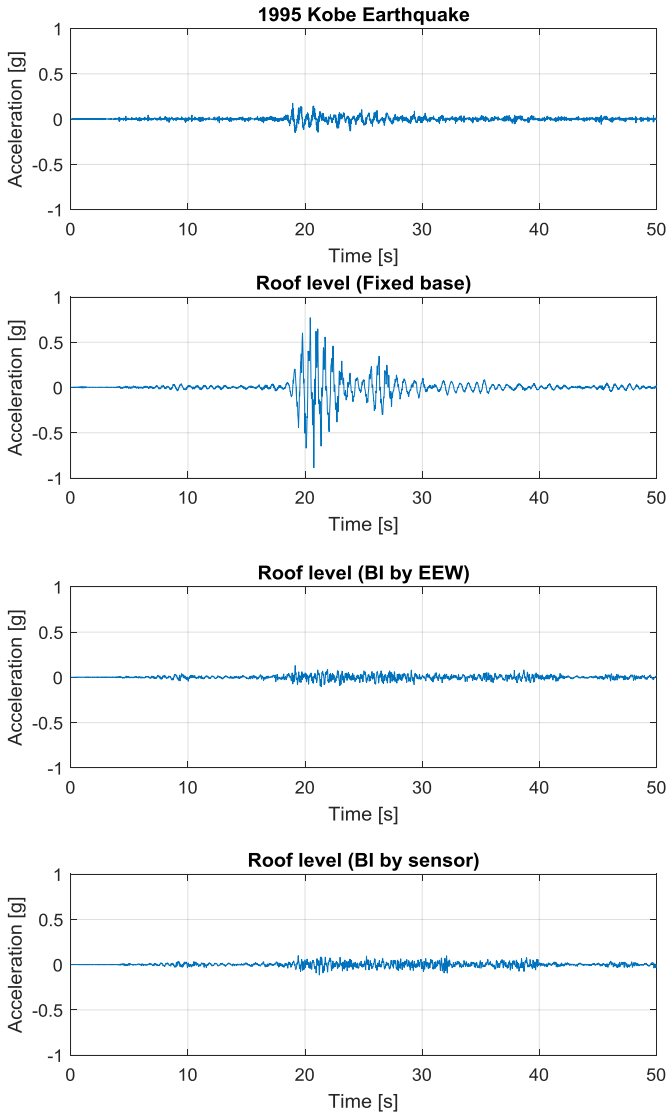

Figure 4-1-8 1995 Kobe Earthquake

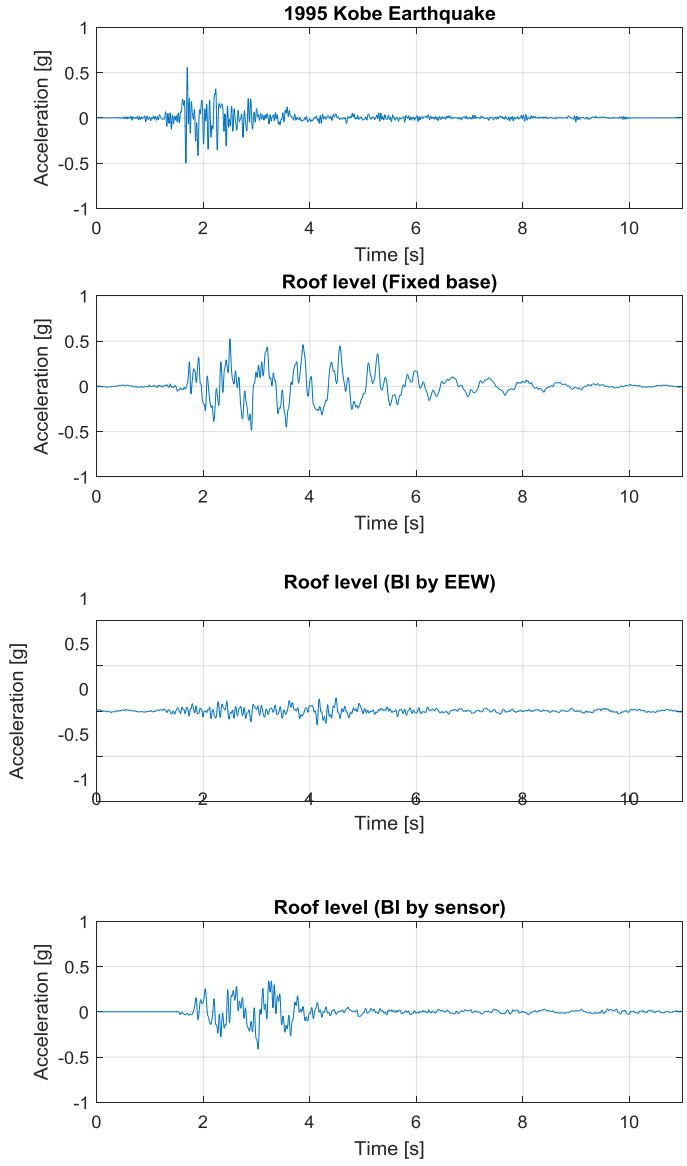

Figure 4-1-9 1992 Mendocino Earthquake

In Figure 4-1-8 the 1995 Kobe Earthquake is characterized by a mild ground shaking followed by a sever shaking in about 18 seconds. Here, the EEW triggered response (the third of Figure 4-1-8) show great similarity to the sensor triggered response (the forth of Figure 4-1-8). This is due to the fact that the sensors have triggered the base isolation prior to the strong ground motion. In Figure 4-1-9, the 1992 Mendocino Earthquake is also characterized

by strong shaking early in the time history, thus the system performance is similar to those in observed in El Centro and Northridge earthquakes.

4.2 Electromagnetic Shear Keys

4.2.1 Experimental Setup

In this experiment, the lightweight 6-layer test model is made of acrylic plastic and aluminium strips. The base plate is made of 3 mm thick wood and attached to the column by aluminium brackets. The steel block for weight gain is located in the centre of each layer so that the total mass of the entire model frame reaches 7.5 kg. The test model is fixed on two layers of mutually orthogonal linear guides, as shown in Figure 4-2-1. Ground motions are simulated by the Quanser Shake Table II. The response of test model is measured independently by three 3-axis 2.4 GHz wireless accelerometers (BeanDevice AX-3D) at three positions: top of shake table, base plate above isolation device, and roof level of the model. The sampling rate is set to 100Hz and the data is exported to MATLAB for further analysis via the BeanScape software.

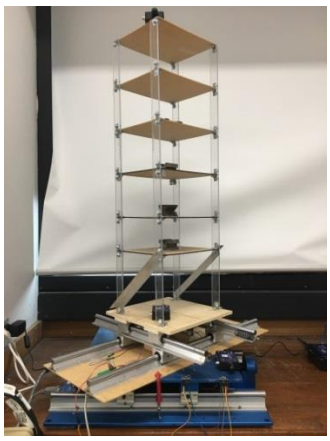

Figure 4-2-1 Overview of Electromagnetic Shear Keys Experiment Setup

Four major scaled historical earthquakes are simulated through the shake table: (1) 1979 Imperial Valley, (2) 1995 Kobe, (3) 1994 Northridge and (4) 1992 Mendocino earthquakes (data provide by Quanser Shake table II). In Table 4-2-1, this experiment will perform three operational modes for analysis and comparison:

Operational mode	Means of trigger	Scenario
1. Fixed base	Nil	Both EEW and on-site sensors fail to detect ground shaking
2. BI by EEW	EEW signal activates the base isolation	EEW signal received prior to arrival of ground shaking
3. BI by sensor	On-site accelerometers detect vibrations higher than predetermined threshold values	EEW fails to detect incoming ground shaking

Table 4-2-1 Operational Modes in Experiment

4.2.2 Controller, Sensors and Actuators

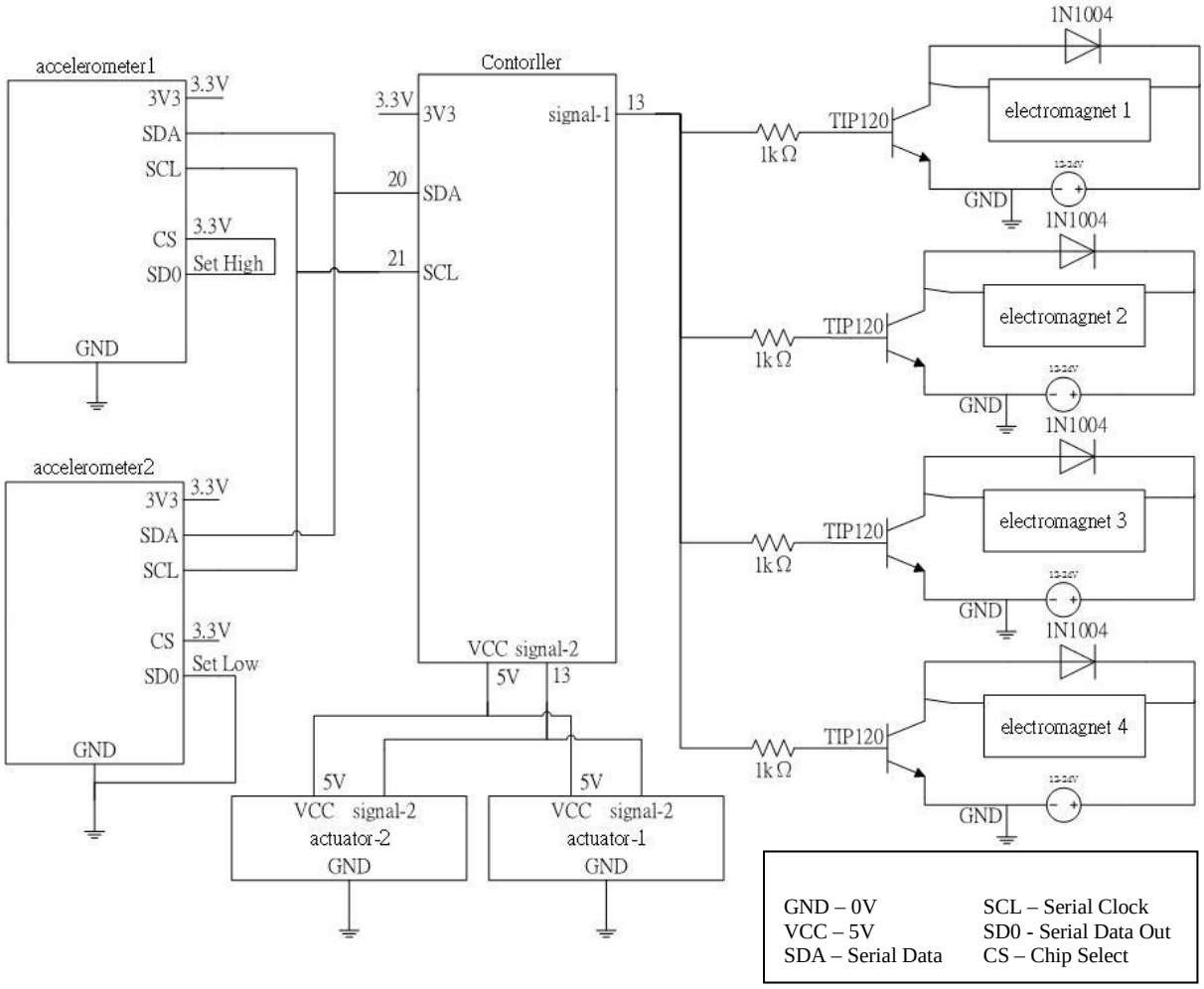

Figure 4-2-2 Circuit Diagram of Smart Base Isolation System

A simple circuit diagram of the experimental setup is shown in Figure 4-2-2. In this experiment, the controller of the smart base isolation system needs to be able to (1) initialise, (2) receive signals from the EEWS/ the network of sensors, and (3) activate the base isolation system. The Arduino MEGA2560 is selected as the control platform and plugged into a network expansion board (called Ethernet Shield) to connect to the Internet. The network of sensors employs two 3-D accelerometers (called ADXL345) for near-field acceleration sensing and selects the I2C protocol based on wiring cost. The shear keys are used to

activate/stop the system are mounted in the isolation device using four electromagnets (shown in Figure 4-2-3). In this experiment, when the electromagnet is energized, the attractive force coupling structure and the foundation is instantly generated, and the attraction is stopped immediately after the power is turned off to activate the base isolation system. However, the more powerful electromagnet is driven by the higher voltage supply and the lower the resistance, which results in higher costs.

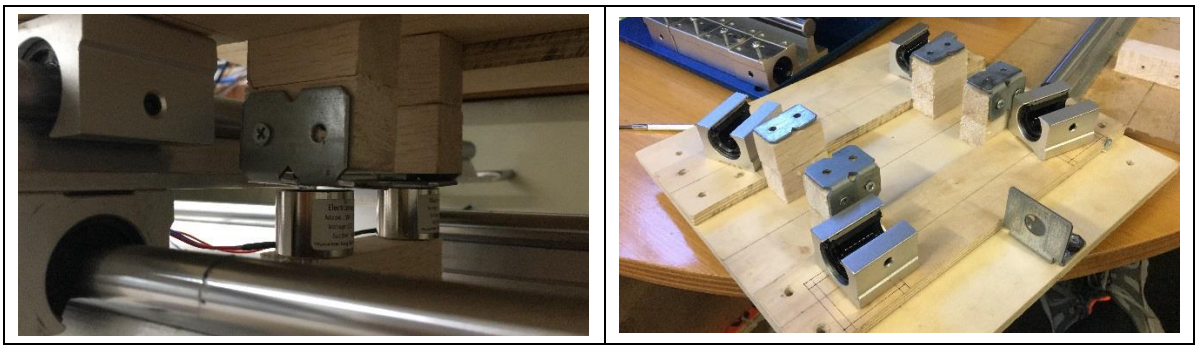

Figure 4-2-3 Electromagnets and The Base of Structure

After the system is activated, the network of sensors still continually senses the vibration. Once the vibration is less than the threshold for a period, the system begins to perform Initialisation. System Initialisation employs two linear motors (peak force 31N at 7mm/s) performing stretch and retract. When the linear motors are fully extended, the structure is pushed back to the origin and fixed to the foundation; when the linear motors are fully retracted, the structure can slide freely on the isolation device after releasing the attractive force from electromagnets.

4.2.3 Initialisation and Activation of Base Isolation System

When the system Initialisation, the controller resets the position of the structure by expanding the linear actuators. In the experiment, two linear actuators are used to perform

system Initialisation. When the linear motors are fully extended, the structure is pushed back to its original position and then the electromagnet is activated to connect the foundation to the structure as the shear keys. In the standby mode, the controller continuously updates the signals from the EEWS and the vibration data from the network of sensors. Once the flag of the earthquake changes, the attractive force from the electromagnet is released to activate the base isolation system.

As a backup plan, sensors network's frequency, detection range, sensing mode, and read/write can be set by code based on the requirements and the actual conditions to avoid unnecessary triggering. Here, this experiment sets the sensitivity range to 5 LSB (about 0.039 g).

4.2.4 Results and discussions

Earthquake	Position	Fixed base	BI by EEW	BI by Sensor
1994 Northridge	Ground level	0.1746	0.1512	0.1095
	Roof level	0.3358	0.2039	0.1805
1995 Kobe	Ground level	0.1303	0.0620	0.0682
	Roof level	0.2961	0.1159	0.1730
1979 Imperial Valley	Ground level	0.1257	0.0593	0.0717
	Roof level	0.2836	0.0837	0.0900
1992 Mendocino	Ground level	0.0936	0.0548	0.1012
	Roof level	01746	0.1047	0.1897

Table 4-2-2 Experimental Results (units in *g*)

Table 4-2-2 shows the structural responses perceived on different modes at different locations. Obviously, the base isolation system triggered by EEWS can effectively improve

the structural response caused by the earthquake and will produce better performance when the seismic energy is large. The base isolation system triggered by sensors is also tested when EEWS fails. Similarly, the base isolation system triggered by the sensor can also effectively reduce the structural response, but the performance is slightly lower than the base isolation system triggered by the EEWS. This problem can be divided into two parts: the setting of the sensor threshold and the hysteresis of the electromagnet. First, low sensor threshold will cause unnecessary system trigger, so vibrations that do not exceed the threshold are still transmitted to the structure. Second, the magnetic force of the magnet depends not only on the strength of the external magnetic field, but also on the magnetization of the original magnet. Therefore, if an opposite magnetic field is not provided, the electromagnet still retains magnetism after the power is turned off.

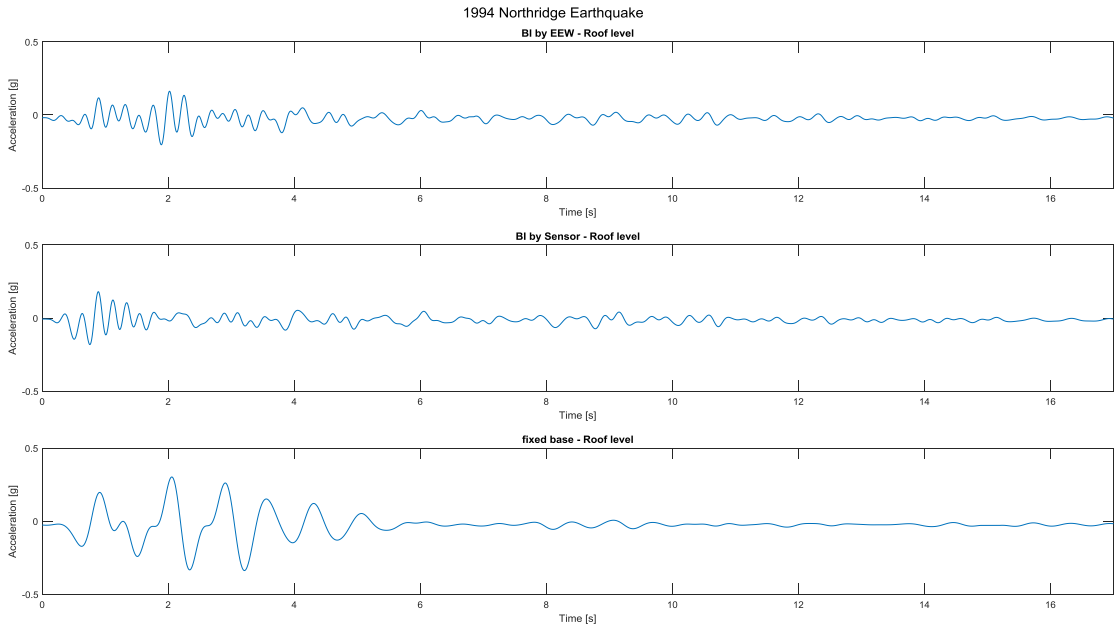

Figure 4-2-4 Structural Responses of 1994 Northridge Earthquake (attack angle = 45^{o})

In Figure 4-2-4, the structural responses of the 1994 Northridge earthquake are shown and compared in the "fixed base", "triggered by EEW " and "triggered by sensors" experiments. In the first row of Figure 4-2-4, the base isolation system triggered by the EEWS was fully activated before the earthquake, so the structural response was improved. When the EEWS fails, in the second row of Figure 4-2-4, some vibrations are still transmitted to the structure due to the late system trigger. It is worth noting that the larger vibrations measured in the 1.9th second of "triggered by EEW " and the 0.5th second in the "triggered by sensors" are caused by the structure hitting the boundary of the slide rails because of the insufficient range of the isolating device.

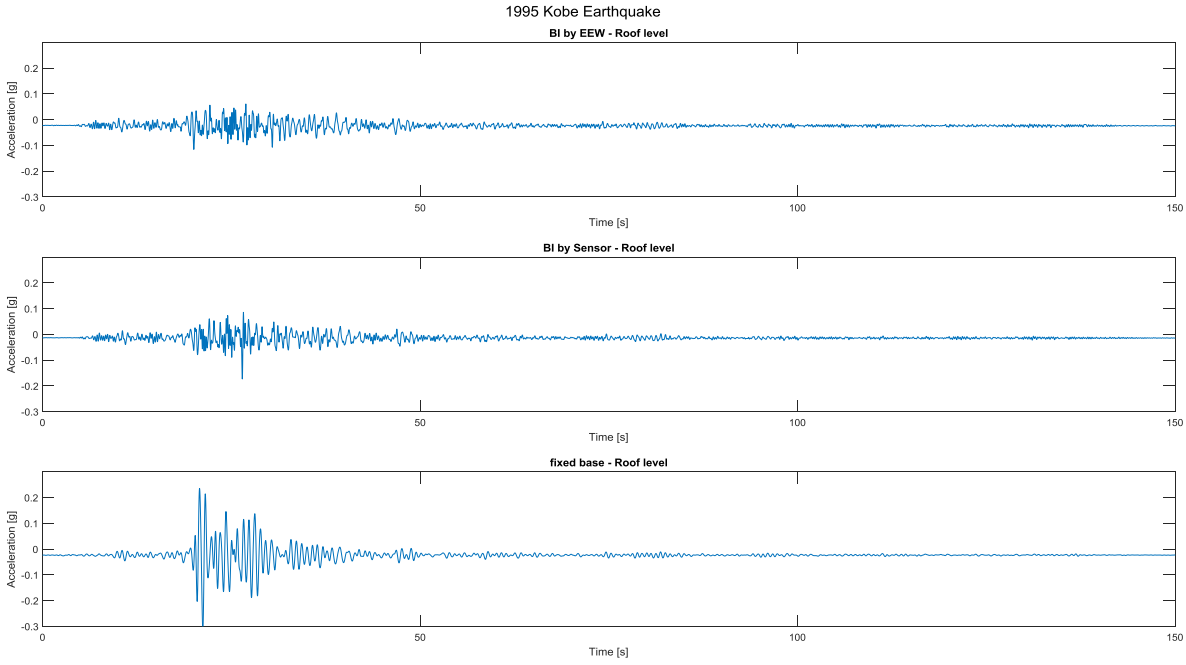

Figure 4-2-5 Structural Responses of 1995 Kobe Earthquake (attack angle = 45^{o})

In Figure 4-2-5, the structural responses of the 1995 Kobe earthquake are shown and compared in the "fixed base", "triggered by EEW " and "triggered by sensors" experiments. In the first row of Figure 4-2-5, the base isolation system triggered by EEWS was fully activated before the earthquake, so the structural response was improved. When EEWS fails, in the second row of Figure 4-2-5, since a small vibration exceeding the sensor threshold occurs before a large vibration, the system triggers earlier, and the base isolation system performs better. It can be seen from this experiment that the earlier the system triggers, the better the system performance.

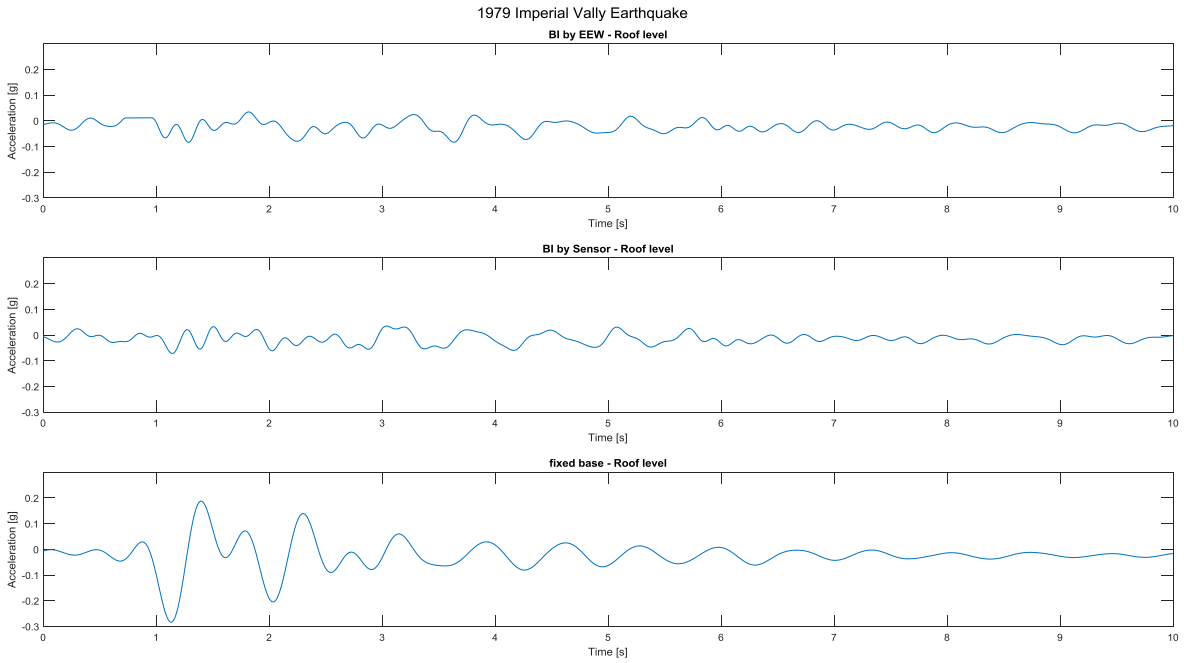

Figure 4-2-6 Structural Responses of 1979 Imperial Valley Earthquake (attack angle = 45^{o})

In Figure 4-2-6, the structural responses of the 1979 Imperial Valley earthquake are shown and compared in the "fixed base", "triggered by EEW" and "triggered by sensors" experiments. In the first row of Figure 4-2-6, the base isolation system triggered by the EEWS

was fully activated before the earthquake, so the structural response was improved. When the EEWS fails, like the 1995 Kobe earthquake, in the second row of Figure 4-2-6, the system triggers earlier because the small vibrations that exceed the sensor threshold occur before a large vibration, so the performance of the base isolation system is better.

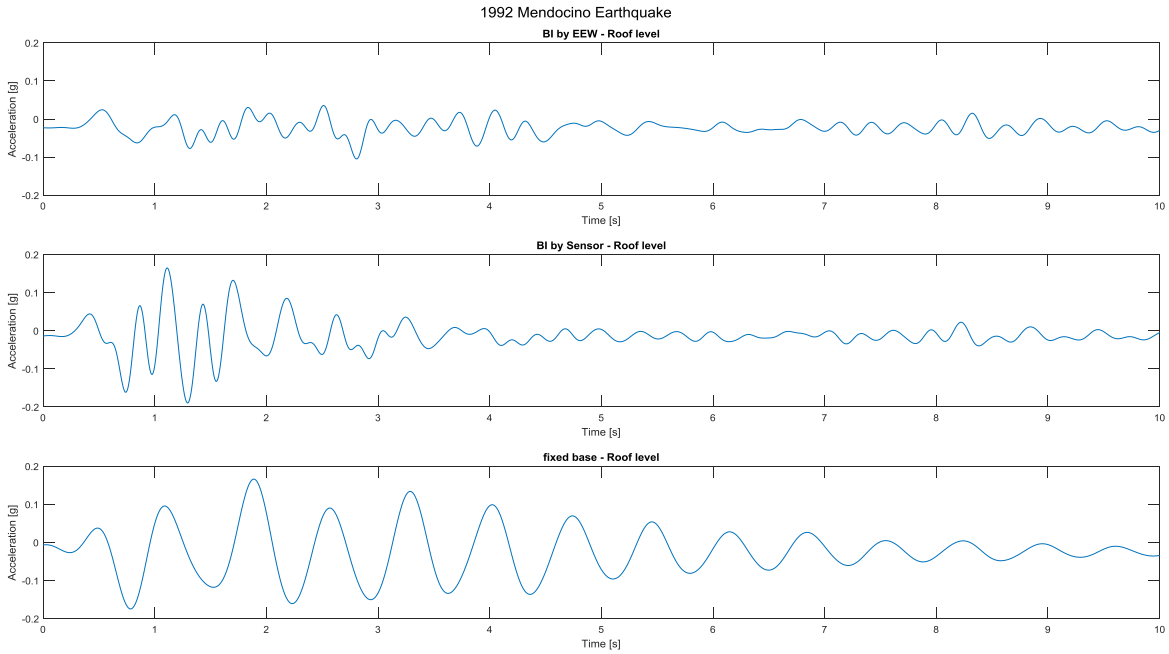

Figure 4-2-7 Structural Responses of 1992 Mendocino Earthquake (attack angle = 45^{o})

In Figure 4-2-7, the structural responses of the 1992 Mendocino earthquake are shown and compared in the "fixed base", "triggered by EEW" and "triggered by sensors" experiments. In the first row of Figure 4-2-7, the base isolation system triggered by the EEWS was fully activated before the earthquake, so the structural response was improved. When EEWS fails, in the second row of Figure 4-2-7, some vibrations are still transmitted to the structure due to delayed system triggering. It is worth noting that the detected larger vibration

starting from the 0.7th second in the "triggered by sensors" is caused by the structure hitting the boundary of the slide rails because of the insufficient vibration range of Isolation device.

4.3 Shear Keys with Linear Actuators

4.3.1 Experimental Setup

A light-weight, 6-level test model made of acrylic plastic and aluminium strips is used in the experimental investigation. Floor plates are made of 3mm thick timber boards and they are connected to columns via aluminium brackets. Steel masses are positioned centrally on each floor and the total mass of the model frame is 7.5kg. The test frame is affixed onto two layers of mutually orthogonal linear guide rails, as shown in Figure 4-3-1. A timber frame is built and secured on the shake table. Ground motions are simulated by the Quanser Shake Table II. The response of the frame is independently measured by three 3-axes 2.4GHz wireless accelerometers (BeanDevice AX-3D) located at three levels: top of shake table, base plate above base isolation, and roof level of the frame. Sampling rate was set to 100Hz and the BeanScape software was used to export data to MATLAB for further analysis.

Figure 4-3-1 The Overview of Experimental Setup

Four major scaled historical earthquakes are simulated through the shake table: (1) 1979 Imperial Valley, (2) 1995 Kobe, (3) 1994 Northridge and (4) 1992 Mendocino earthquakes (data provide by Quanser Shake table II). In order to demonstrate the effectiveness of the two-dimensional base-isolation system, the building was placed at an angle of 45 degrees on the shake table. This experiment will perform three operational modes for analysis and comparison:

Operational mode	Means of trigger	Scenario
1. Fixed base	Nil	Both EEW and on-site sensors fail to detect ground shaking
2. BI by EEW	EEW signal activates the base isolation	EEW signal received prior to arrival of ground shaking
3. BI by sensor	On-site accelerometers detect vibrations higher than predetermined threshold values	EEW fails to detect incoming ground shaking

Table 4-3-1 Operational Modes in Experiment

4.3.2 Controller, Sensors and Actuators

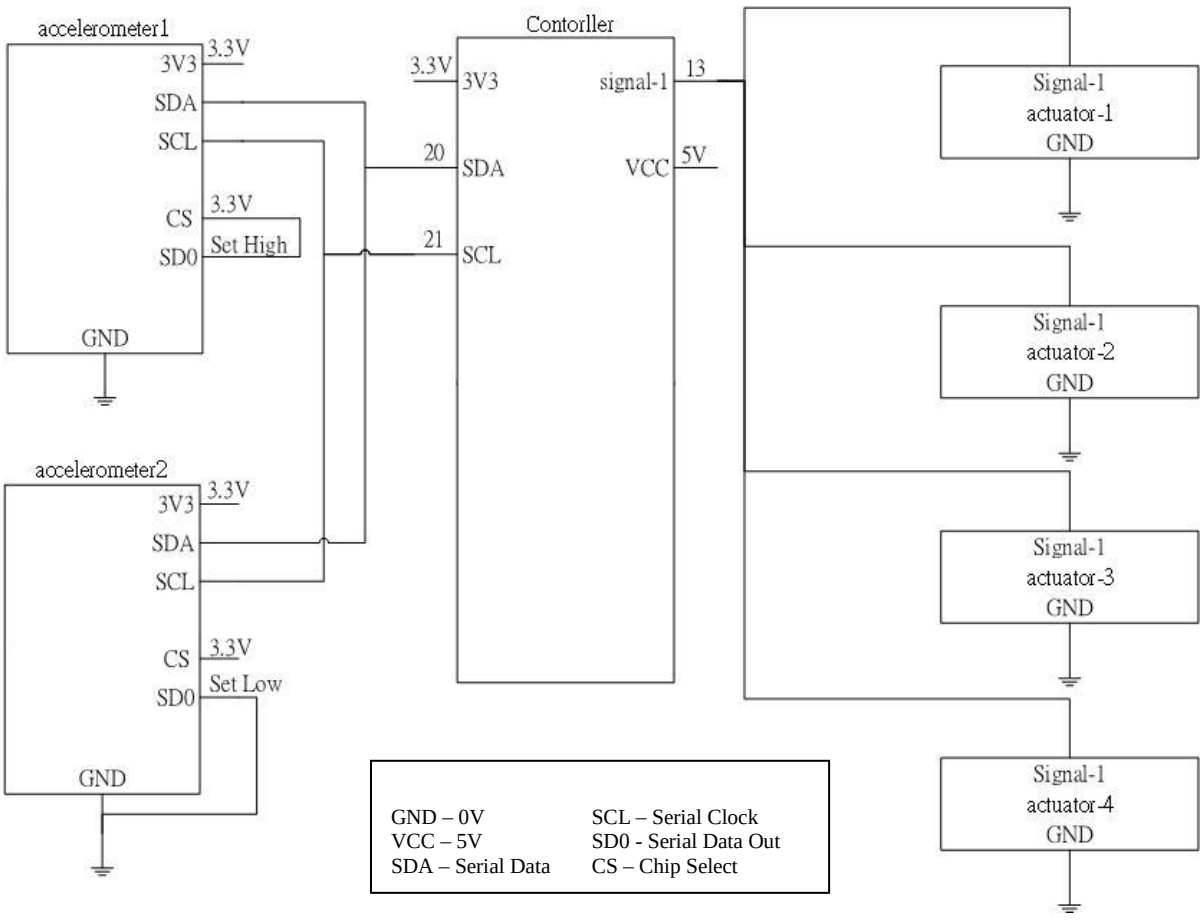

Figure 4-3-2 Electrical Diagram of Experimental Setup

A simple circuit diagram of the experimental setup is shown in Figure 4-3-2. The controller of the proposed system mainly performs three functions: communication, sensing and execution. The experiments are completed on the Arduino MEGA control platform, which has 54 sets of digital input/output ports (14 of which can be used for PWM output), 16

analog inputs and a 16 MHz crystal oscillator. Because of the built-in bootloader, it can be burned directly via USB instead of other external burners. The power supply can be powered by USB directly or by using an AC-to-DC adapter or battery. To obtain the signal of EEW on the Internet, the Ethernet shield is introduced which makes TCP/IP Protocols (TCP, UDP, ICMP, IPv4 ARP, IGMP, PPPoE, Ethernet) on the hardware circuit to reduce the burden of Arduino. An ethernet shield allows up to 4 connections at the same time and achieve transmission speed up to 100MB / s [77]. Furthermore, as a backup and avoiding the effects of blind zone caused by earthquakes nearby, the accelerometers ADXL345 are set up around the building. These sensors are factory calibrated and inexpensive, making them ideal for the experiment.

Finally and most importantly, in order to enable multiple devices to be used simultaneously on the same platform, it is necessary to select the appropriate communication protocol for the requirements and layout. There are currently three communication protocols commonly used on controllers: I2C, SPI, and UART. Firstly, the earliest UART is not a very comprehensive communication method because it needs to be used with different ports and drivers, such as RS-232, RS-422, RS-485 [83]. Among them, RS-232 port is more popular whose advantage is that the line is simple (only two lines), but the disadvantage is that only one-to-one connection and the low speed (up to 115.2kbps). So UART communication protocol is not suitable for high-speed, large-scale transmission. Compared with I2C, SPI is full duplex and the speed of transmission is higher, but more wires are required and execution burden is greater. Because the EEW signal is small (less than 1KB [84]) and the scale is not large, the experiment uses I2C communication protocol.

The execution part of the system is relatively simple. Four linear motors (peak force 31N at 7mm/s) are used as actuators and shear keys to perform extension and retraction. When linear motors are fully extended, the building is pushed back to the starting point and fixed in the frame and on the foundation; when the linear motor is fully retracted, base isolation system is activated and the building can slide freely on the isolation device. The entire system does not require an external power supply, and the power is completely provided by the control platform.

4.3.3 Initialisation and Activation of base isolation system

When the system initialises, the controller resets the position of the structure by extending the shear keys. In the experiment, there will be four linear actuators to perform system Initialisation. They are motors with feedback signals that can be sent back to the controller to access the position of structure [81]. In addition, the device shares the same power supply as the controller, thus simplifying the circuit design. As shown in Figure 4-3-3, four Firgelli 100mm stroke linear actuators (peak force 31N, 7mm / s) are used. During the system Initialisation, the actuators are programmed to fully extend (see the right of Figure 4-3-3), which push the structure back to its original position through the centre plate. The system then enters a service condition in which the controller continuously updates the signals of EEWS and the network of sensors. This simple arrangement can save the need of the displacement sensor to monitor the position of the main structure. Once the flag of earthquake changes, the actuators fully retract to switch on the base isolation system.

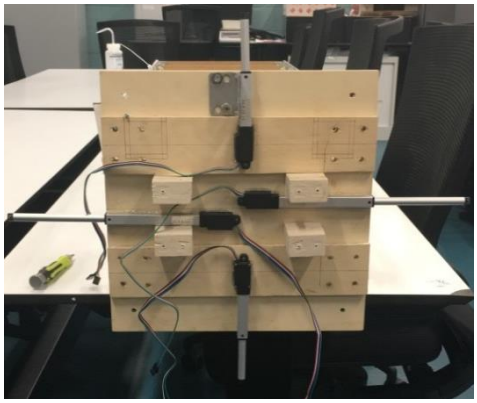

(A) Linear Motors

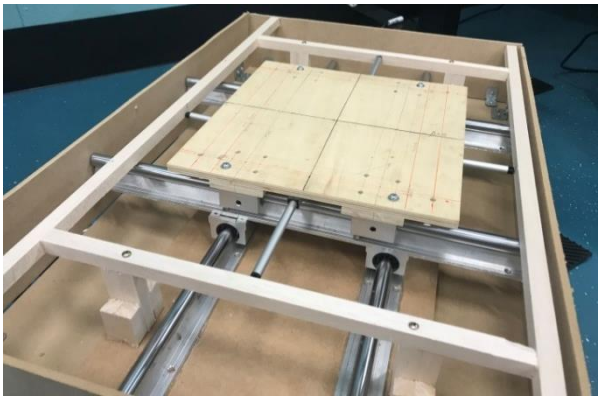

(B)The Base of Structure

Figure 4-3-3 Linear Motors and The Base of Structure

There are two factors to activate the system: (1) the EEW signal from the Internet via Ethernet shield (2) unusual acceleration sensed by accelerometers around the building. First, after the Ethernet shield is turned on, it will continuously update the IP of the EEW signal. Once the earthquake signal is detected, the system will immediately activate the base isolation. Next, ADXL345 accelerometer is a small ultra-low-power 3-axis accelerometer with high resolution (3.9mg/LSB) and a measurement range of ±16g. Its frequency, detection range, sensing mode, and reading and writing can all be set by using the code based on the requirements and actual conditions. Unnecessary triggering often causes problems for users and residents [85]. This experiment sets the range of sensitivity to 5LSB (approximately 0.039g).

4.3.4 Results and Discussions

Since the test object itself is robust and undamaged, after system Initialisation/reset, the experiment can be reproducible. Here, four well-known earthquakes are simulated in three

different scenarios. In order to skip the interference of noise in the environment, all data from sensors is filtered by 6th order Butterworth low-pass filter in MATLAB with cut-off frequency of 25Hz. Then the maximums for the structural responses at different places under different scenarios are shown in Table 4-3-2 and plotted accelerations against time in Figure 4-3-4 to Figure 4-3-7. In figures, from left to right are (a) the Shake table, (b) the ground floor and (c) the roof, and from top to bottom are base isolation triggered (1) by EEWS, (2) by sensors, and no base isolation with (3) the fixed base.

Earthquake	Position	Fixed base	BI by EEW	BI by Sensor
1979 Imperial Valley	Ground level	0.0403	0.0232	0.0366
	Roof level	0.1385	0.0592	0.0795
1992 Mendocino	Ground level	0.0698	0.0300	0.0520
	Roof level	0.1264	0.0662	0.0833
1994 Northridge	Ground level	0.1649	0.0446	0.0448
	Roof level	0.3751	0.0773	0.0833
1995 Kobe	Ground level	0.1302	0.0469	0.0739
	Roof level	0.2940	0.0873	0.0821

Table 4-3-2 Measured Peak Absolute Acceleration (unit in g)

Table 4-3-2 shows the building responses sensed at different locations in different scenarios when simulating four earthquakes. Obviously, the base isolation system triggered by the EEWS can greatly improve the structural response caused by the earthquake, and the better performance happens when the larger earthquake comes. This table also lists the performance of the base isolation system triggered by the sensors when EEWS fails. Similarly, the base isolation system triggered by the sensors can also effectively reduce the structural

response, but the performance is slightly inferior than the base isolation system triggered by the EEWS. This is due to that the retraction of the shear keys takes time. Insufficient range of the base isolation is likely to cause impact between the shear key and the frame, which results in the worse performance of the base isolation system.

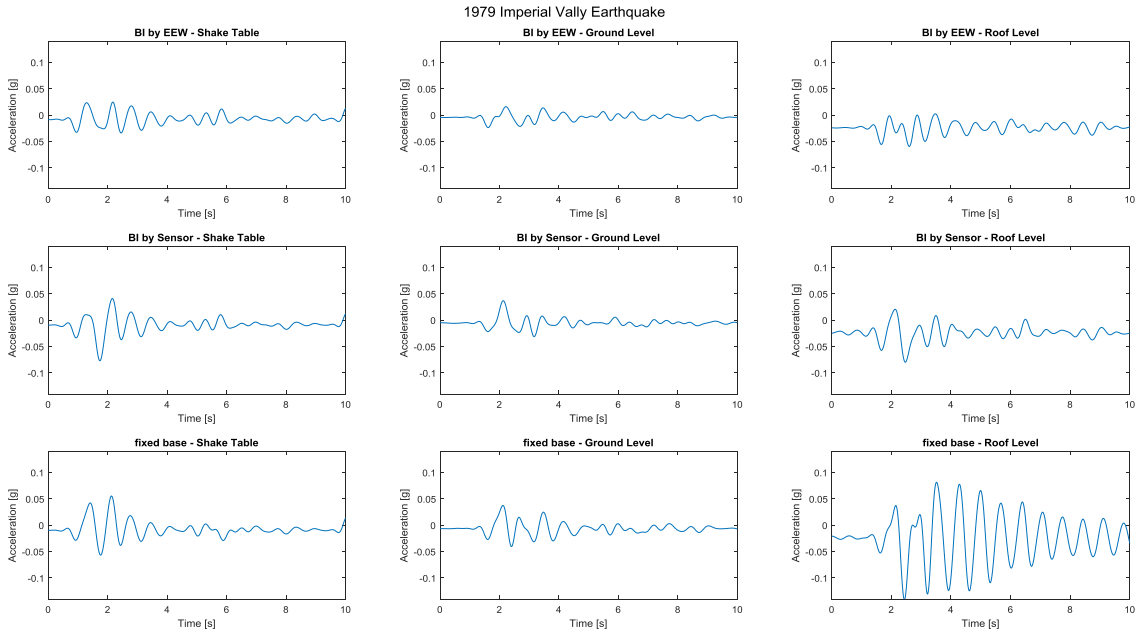

Figure 4-3-4 Structural Responses of 1979 Imperial Valley Earthquake (attack angle = 45^{o})

From the first column of Figure 4-3-4, it is known that the 1979 Imperial Valley earthquake is characterized by strong vibrations starting at the 1.4th second that almost immediately causes a structural response in the "fixed base" experiment (third row). In the first row of Figure 4-3-4, the base isolation system triggered by EEWS has been fully activated before the arrival of the earthquake, so the structural response is greatly improved. When EEWS system fails, in the second row of Figure 4-3-4, the network of sensors detects

the activation threshold of the base isolation system at the 1.6th second and then begins to retract the shear keys. So the stronger structural response still exists when retracting the shear keys because of the insufficient sliding distance of isolation device.

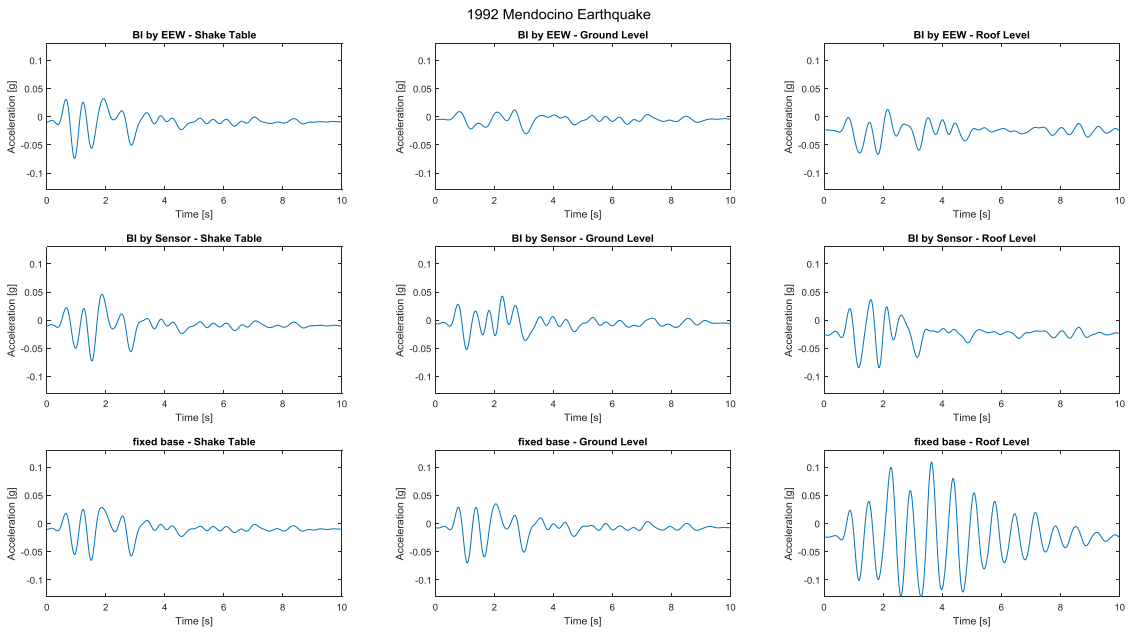

Figure 4-3-5 Structural Responses of 1992 Mendocino Earthquake (attack angle = 45°)

The 1992 Mendocino earthquake is similar to the 1979 Imperial Valley earthquake which is characterized by strong vibration from the first second, as shown in the first column of Figure 4-3-5, the structural responses are shown in the "fixed basis" experiment. In the first row of Figure 4-3-5, the base isolation system triggered by EEWS is fully activated before the earthquake comes, so the structural response is greatly improved. When the EEWS fails, in the second row of Figure 4-3-5, the network of sensors detected the activation threshold of the base isolation system at the 1st second and then began to retract the shear keys. Likewise, due

to insufficient sliding distance of the isolation device, there is still a strong structural response when retracting shear keys.

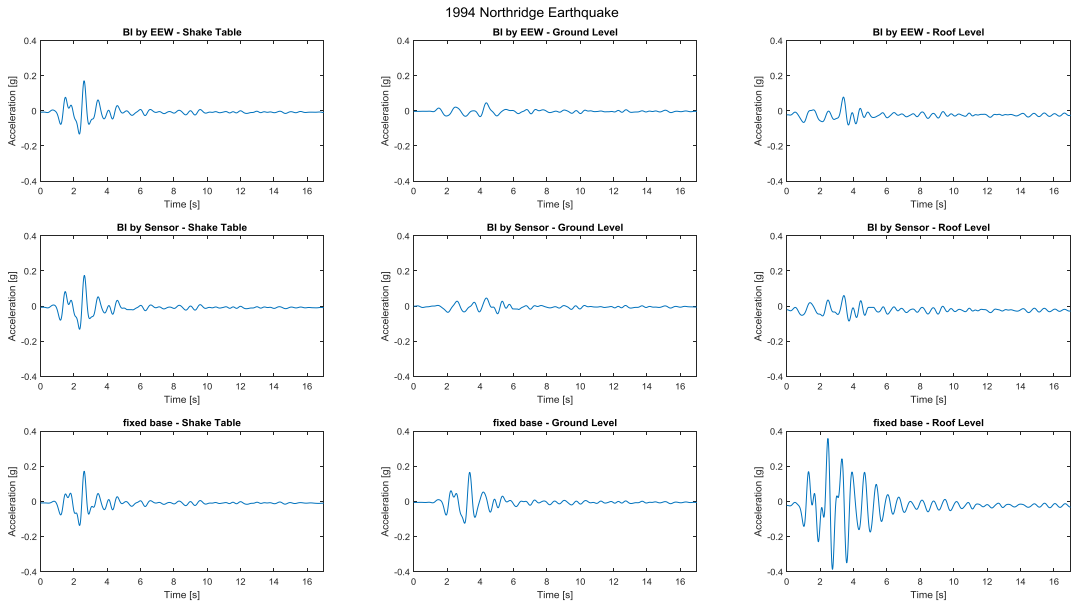

Figure 4-3-6. Structural Responses of 1994 Northridge Earthquake (attack angle = 45^{o})

From the first column of Figure 4-3-6, the 1994 Northridge earthquake is characterized by a slight vibration from the 1.1th second to a strong vibration at the 2.6th second, and the structural responses are shown in the "fixed base" experiment. In the first row of Figure 4-3-6, the base isolation system triggered by EEWS was fully activated before the earthquake, so the structural response was greatly improved. When EEWS fails, in the second row of Figure 4-3-6, because the stronger vibration occurs later, the network of sensors first detects the activation threshold of the base isolation system at the first second and then starts to retract the shear keys, so the system can complete the activation and have a better overall performance before the more destructive seismic wave comes.

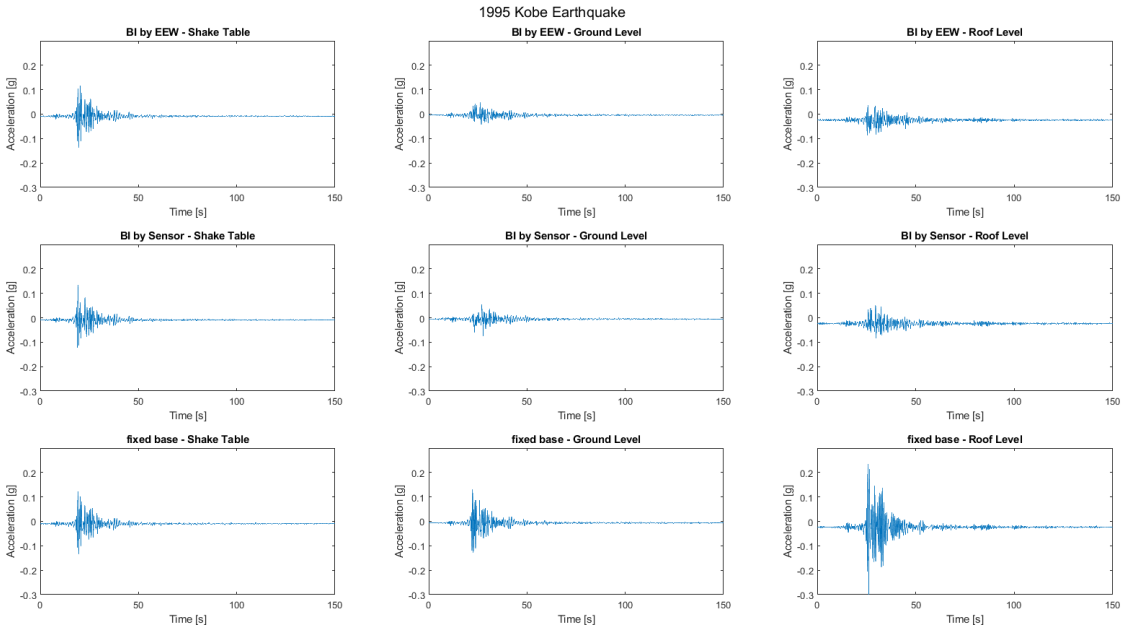

Figure 4-3-7 Structural Responses of 1995 Kobe Earthquake (attack angle = 45^{o})

The 1995 Kobe earthquake is similar to the 1994 Northridge earthquake which is characterized by a slight vibration from the 17th second to a strong vibration at the 19th second. As shown in the first column of Figure 4-3-7, the structural response is shown in the "fixed base" experiment. In the first row of Figure 4-3-7, the base isolation system triggered by EEWS is fully activated before the earthquake arrives, so the structural response is greatly improved. When EEWS fails, in the second row of Figure 4-3-7, because the stronger vibration occurs later, the network of sensors first detects the activation threshold of the base isolation system at the 17th second, and then starts to retract the shear key. Thereby the system can switch on early and have better overall performance before the more destructive seismic wave arrives.

4.4 Summary

In Chapter 4, experimental setups and instruments of (1) solenoid shear keys, (2) electromagnetic shear keys, and (3) shear keys with linear actuators are proposed. Structure model and shake table are used to simulate earthquake experiments to verify the effectiveness of the proposed system. The experimental results show that, when earthquake comes, the structural responses are effectively reduced and the resistance to the load is enhanced.

The main achievements of this chapter are:

(1) The isolation device considers the direction of the earthquake and the possibility of practical application. Therefore, the isolation device is successfully designed that the building model can slide on the isolation device in two dimensions.

(2) In the experiment of electromagnetic shear keys, the principle of the magnet “Like repel each other, unlike attract.” is introduced. The experimental results show that the proposed system effectively reduces the structural response when earthquake comes, but there are still some difficulties that may occur in actual construction.

(3) The function of linear actuators is successfully maximized which not only act the role of shear keys to strengthen the stiffness of the building but also perform system Initialisation. Experimental results show that the system can effectively reduce the structural response of structures caused by earthquakes.

CHAPTER 5

ACTIVE CONTROL

BASE ISOLATION SYSTEM

In chapter 5, the active control system is added to the design. This technology requires an external power source to activate the control devices and utilise actuators to generate the control force. The magnitude of the control force can be adjusted by a control algorithm. The control algorithm uses feedback from the sensors that are placed in strategic locations of the structure which measure excitations and/or responses of structure. Electrohydraulic or electromechanical actuators are typically used to produce active control force. This chapter presents a smart mechatronic base isolation system that employs active control strategy and a network of sensors to improve the structural response in the earthquake. In addition, the conceptual framework of the proposed system is demonstrated and verified by laboratory-scale proof-of-concept experiments.

5.1 State-Space Representation of Active Control System

The equation of motion of a multi-degree-of-freedom system, following section 2-3, is written in state-space as:

$$\dot{x} = Ax + Bu + H\ddot{x}_g \tag{1}$$

in which

$$\mathrm{A} = \begin{bmatrix} 0 & I \\ -M^{-1} & -M^{-1}C \end{bmatrix};\ \mathrm{B} = \begin{bmatrix} 0 \\ M^{-1}D \end{bmatrix};\ \mathrm{H} = \begin{bmatrix} 0 \\ -I \end{bmatrix}$$

where I is an identity matrix of appropriate size; M, C and K are $\mathrm{n} \times \mathrm{n}$ mass, damping and stiffness matrices respectively; D is the location matrix of size $\mathrm{n} \times \mathrm{m}$. u is a vector of control force of size *m*. Since the control of structural response is achieved by applying control forces that depend on the state of the system (that is x and $\dot{\mathrm{x}}$), three factors related to the active control system are extremely important: (1) stability, (2) controllability and (3) observability. In other words, the active control system should be stable, controllable, and observable. These three factors are described in further detail below.

5.1.1 Stability

If u is assumed to be in the form of equation (1), the controlled equation in the state space can be written in the following form:

$$\dot{x} = \bar{A}x + H\ddot{x}_g \tag{2}$$

in which

$$\overline{A} = A + [BK_1 + VC_1];\ \overline{H} = BE + H \tag{3}$$

The stability of a controlled system can be specified as the boundedness of the system state in time. Check the stability of the system by checking the basic dynamics of the system. Therefore, considering the following state equation:

$$\dot{x} = \bar{A}x \qquad x(t_0) = x_0 \tag{4}$$

The equilibrium state of the system is described by:

$$\bar{A}x_e = 0 \tag{5}$$

that is, $x_e = 0$ is its unique equilibrium state if A is non-singular.

An equilibrium state should be stable in the sense of Lyapunov if for any t_0 and any small value $\varepsilon > 0$, there is a real number $\delta > 0$, so that

$$\|x_0 - x_e\| \leq \delta \tag{6}$$

which implies $\|x(t) - x_e\| \leq \varepsilon$ for $t \geq t_0$ and $\| \ \|$ indicates the Euclidean norm.

Therefore, the Lyapunov stability ensures that the state of the system remains close to equilibrium at any time t by the initial state that closes to the equilibrium state [86].

The equilibrium state is asymptotically stable if it is stable and $\delta > 0$ for any t_0, so that again

$$\|x_0 - x_e\| \leq \delta \tag{7}$$

which implies that $\|x(t) - x_e\| \to 0$ as $t \to \infty$.

Therefore, in addition to being stable, when the initial conditions are close enough to the equilibrium state, the state asymptotically converges to x_e [86]. Also, it can be easily shown that the equilibrium state indicates the stability in any solution.

The requirements for the first stability condition are: (1) all eigenvalues of $\bar{A}$ have non-positive real parts; (ii) for any zero real eigenvalues with k, there are exactly k linearly

independent eigenvectors [87]. The second stability condition requires that all eigenvalues of $\bar{A}$ have strictly negative real parts.

5.1.2 Controllability

If the system can be transferred from any initial state $x(t_0)$ to any other state within a limited time interval by unconstrained control vector, the system can be seen as controllable at time t_0. On the other hand, If the system is in state $x(t_0)$ which can be determined by observing the output within a limited time interval, the system can be seen as observable at time t_0.

The concepts of controllability and observability are proposed by Kalman [88]. If the system is uncontrollable, there may be no solution to the control design. Although most physical problems are controllable and observable, the corresponding mathematical model may not always retain the properties of controllability and observability. Therefore, it is necessary to know the mathematical conditions when the model is controllable and observable.

Consider the following system:

$$\dot{\boldsymbol{X}} = AX + Bu \tag{8}$$

Note that Equation 8 does not have any excitation but applies unconstrained control forces to change the state of the system. If the system is controllable, then the controllability matrix given by [86] can be shown:

$$\left[B \vdots AB \vdots \cdots\cdots \vdots A^{n-1}B\right]_{n\times nr} \tag{9}$$

is of rank n; in which n is the size of A matrix and r is the size of the vector of control force u. Alternatively, the matrix contains n linearly independent column vectors.

There is an alternative form under the condition when system state is full controllable, for example, if the eigenvalues of A are different, the eigenvectors are different as well. Then a transformation matrix P can be found such that

$$\boldsymbol{P^{-1}AP = D = daig\lambda} \tag{10}$$

in which $\boldsymbol{daig\lambda}$ is a diagonal matrix of eigenvalues. With this transformation matrix, a new set of variables may be defined as:

$$\mathbf{Z = Px} \tag{11}$$

and a new set of equations in the transformed variable may be obtained as:

$$\boldsymbol{\dot{Z} = DZ + Fu} \tag{12}$$

$$\mathbf{F} = \boldsymbol{P^{-1}B} \tag{13}$$

The system is state-controllable only if the matrix $\mathbf{F}$ does not have a row containing all zero elements.

In the practical design of a control system, the control of the output is more important than the control of the state. Consider the following system:

$$\dot{x} = Ax + Bu \tag{14}$$

$$y = Cx + Du \tag{15}$$

where Y is a vector of size m. Therefore, the sizes of other matrices are determined. If an unconstrained control vector u can be constructed that converts any given initial output $y(t_0)$ to any final output $y(t_1)$ within a limited time interval $t_0 \leq t \leq t_1$, then the systems described in equations 14 and 15 can be seen as completely output controllable. The mathematical condition for the controllability requires the controllability matrix

$$\left[CB \vdots CAB \vdots CA^nB \vdots \cdots\cdots \vdots CA^{n-1}B \vdots D\right]_{n\times(n+1)r} \tag{16}$$

is of rank *m*.

5.1.3 Observability

In order to study observability, the motion equation of the unforced system is employed to check. Consider the equations

$$\dot{\boldsymbol{x}} = \boldsymbol{A}\boldsymbol{x} \tag{17}$$

$$\boldsymbol{y} = \boldsymbol{C}\boldsymbol{x} \tag{18}$$

If each x(t) can be determined from the observation of y(t) over a limited time interval $t_0 \leq t \leq t_1$, the system is completely observable. The concept of observability is important because in practice only a limited number of measurements are possible (of size m) and a complete state of the system may be required to generate control signals by means of control algorithm.

It can be shown that the system in equations 17 and 18 is fully observable if and only if the $n \times nm$ matrix

$$\left[C^* \vdots A^*C^* \vdots \cdots\cdots \vdots (A^*)^{n-1}C^*\right] \tag{19}$$

is of rank n or has *n* linearly independent column vectors.

5.2 Experimental Setup

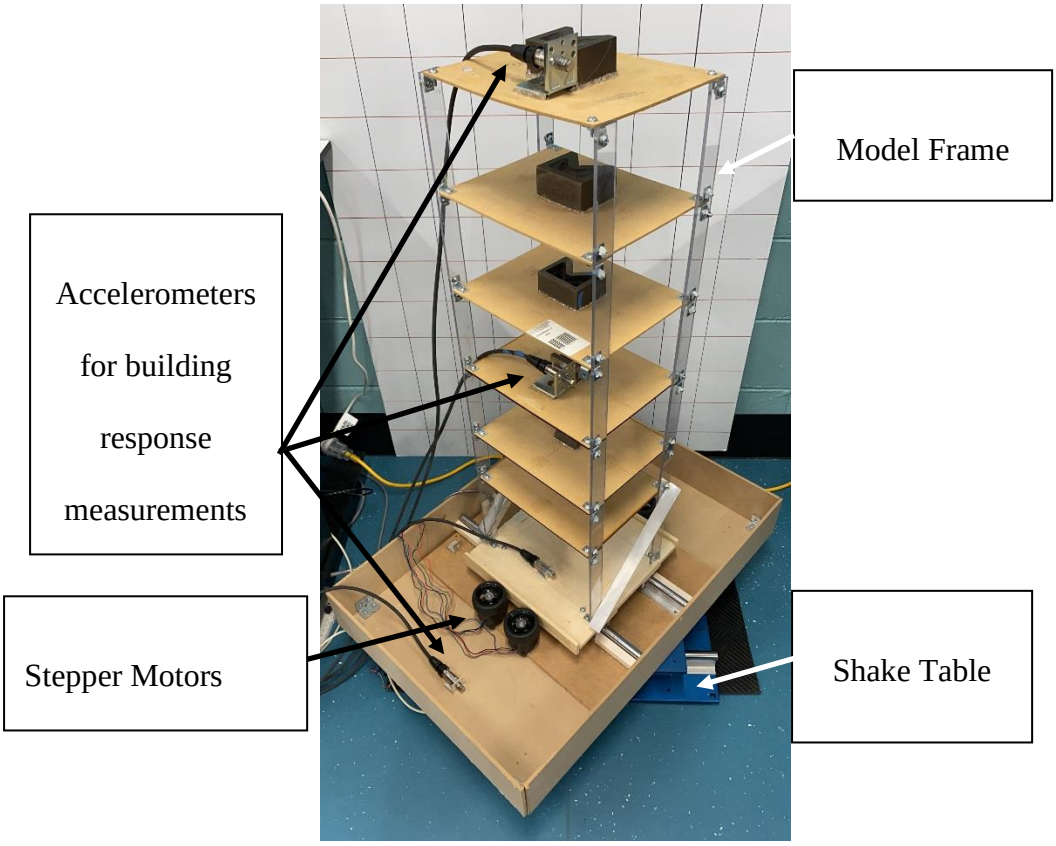

Figure 5-2-1 Overview of Experimental Setup

In this experiment, a lightweight six-story test model made of acrylic plastic, wood and aluminium is used. The floor is made of 3mm thick plank and connected to the four pillars by aluminium brackets. The bottom storey is supported in an out-of-plane direction to avoid torsional movement and steel masses are placed on each floor to increase the weight of structure, thereby the total mass of the model is 7.5 kg. The proposed smart base isolation system consists of two linear steel rails mounted on a 10 mm thick wooden board, four

ball-bearing slide blocks supporting the structure and active control devices, as shown in Figure 5-2-1. The earthquake simulations are performed by the Quanser Shake Table II. The structural responses are measured independently by three 3-axis 2.4 GHz wireless accelerometers (BeanDevice AX-3D) at three locations: the shaker table, the base plate above the isolation device, and the roof of the structure. The sample rate is set to 100 Hz and the data is exported to MATLAB for further analysis via BeanScape software.

Four major scaled historical earthquakes are simulated in one dimension through the shake table: (1) 1979 Imperial Valley, (2) 1995 Kobe, (3) 1994 Northridge and (4) 1992 Mendocino earthquakes (data provide by Quanser Shake table II). In order to prove the effectiveness of the intelligent base isolation system, the experiment will perform two modes of operation for analysis and comparison: (1) base isolation without active control and (2) base isolation with active control

Operational mode	Scenario
1. BI without active control	The structure slides on the isolation device but the active control is disabling.
2. BI with active control	The structure slides on the isolation device and the active control is enabling.

Table 5-2-1 Operational Modes in Experiment

5.3 Controller, Sensors and Actuators

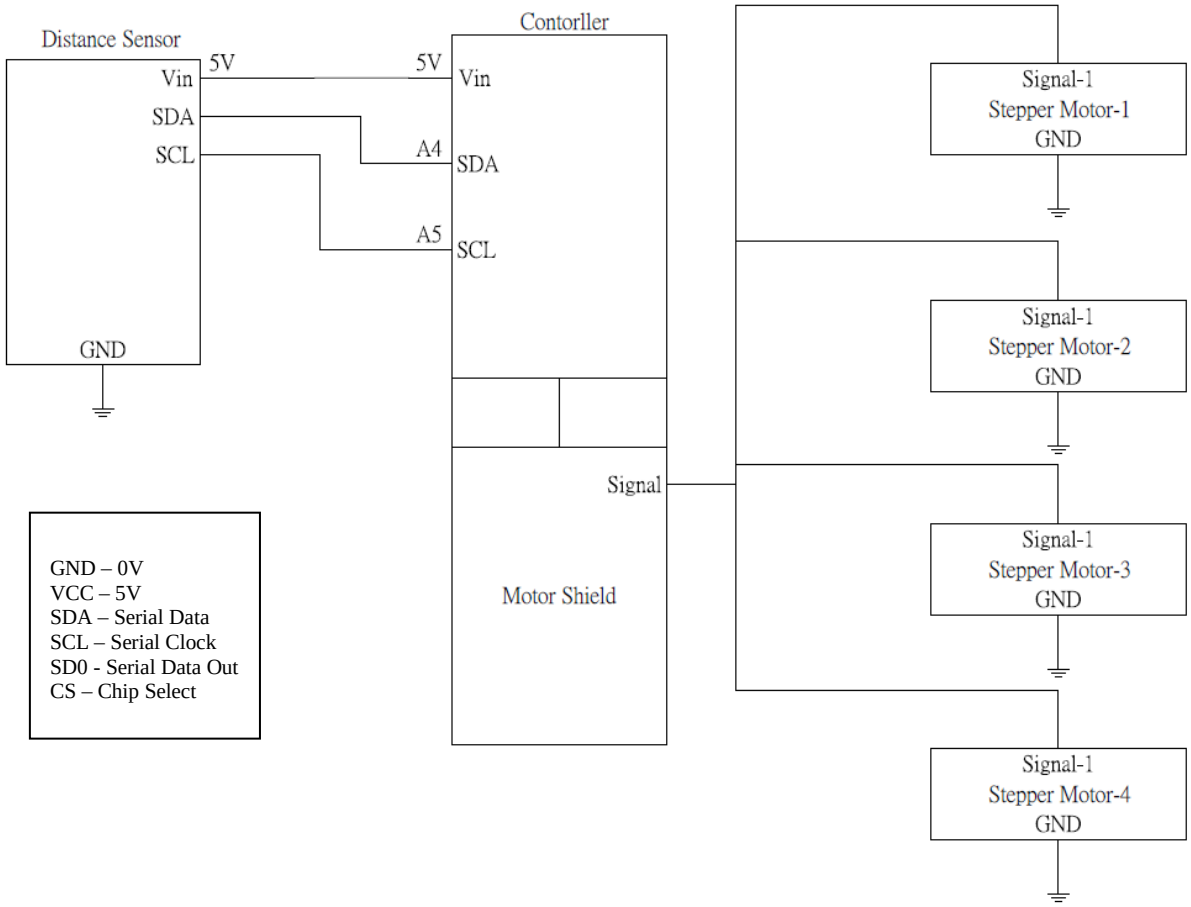

Figure 5-3-1 Electrical Diagram of Experimental Setup

The circuit diagram of this experiment is shown in Figure 5-3-1. In this experiment, the controller of the smart base isolation system needs to be able to (1) receive signals from the network of sensors and (2) perform the active control. The proposed system is controlled by the Arduino MEGA2560 control platform whose baud rate is set at 9600Hz. In addition, an external power supply is connected to compensate for the lack of current provided by the

controller itself. The network of sensors employs a distance sensor to detect the position of the structure on the rails. The actuators work for active control that four stepper motors are mounted in the isolation device (as shown in Figure 5-3-2). This kind of motor can easily realise high-precision positioning only by pulse signal, and there is no electronic component such as an encoder inside. The structure of stepper motor is simple but it's strong with less faulty and high stability. In this experiment, the network of sensors constantly detects the position of the structure on the rails. Based on the position change of the structure on the rails, in conjunction with the control algorithm (described in 5-3 section), the controller adjusts the speed and rotation of the motor to improve the structural response caused by the earthquake and maintains the structure within the system range.

Figure 5-3-2 Stepper Motors and The Base of Structure

5.4 Active Control Strategy

In controller applications, the most widely used control methods are proportional control, integral control and differential control, referred to as PID controllers. The PID controller has become one of the main technologies of industrial controller because of its simple structure, good stability and convenient adjustment.

When the structure and parameters of the object cannot be fully grasped, or the accurate mathematical model cannot be obtained, the PID controller is the most convenient choice, and some applications use PI or PD control. Although the theory and applications of PID controllers are quite mature, there is still no good development in structural vibration control.

There are several active structural vibration control methods that incorporate PID controller but totally different in flexibility and complexity, and each method has its own limitations [89]. In addition to researches based on PID control, discussions on the active structural vibration control are still limited. In the smart base isolation system, the PID controller can be corrected in real time through the proportional controller when the error is detected, but the disadvantage is that the steady-state error will occur after the load distribution changes. [90]. Thereby, the integral controller is to eliminate the steady-state error, but it causes instability because of the increased phase lag. Finally, the differential controller is used to improve the damping of the structure and the stability of the controller.

In simple terms, the PID controller is the systematic error control that the control amount is calculated by using proportional, integral, and differential. If $u(t)$ is defined as the control output, the PID algorithm can be expressed below [91]:

$$u(t) = K_p e(t) + K_i \sum e(t) + K_d[e(t) - e(t-1)] + u0$$

where K_p, K_i and K_d are respectively proportional gain, integral gain, and differential gain. t is the current time, e is the error, and $u0$ is the control amount reference value.

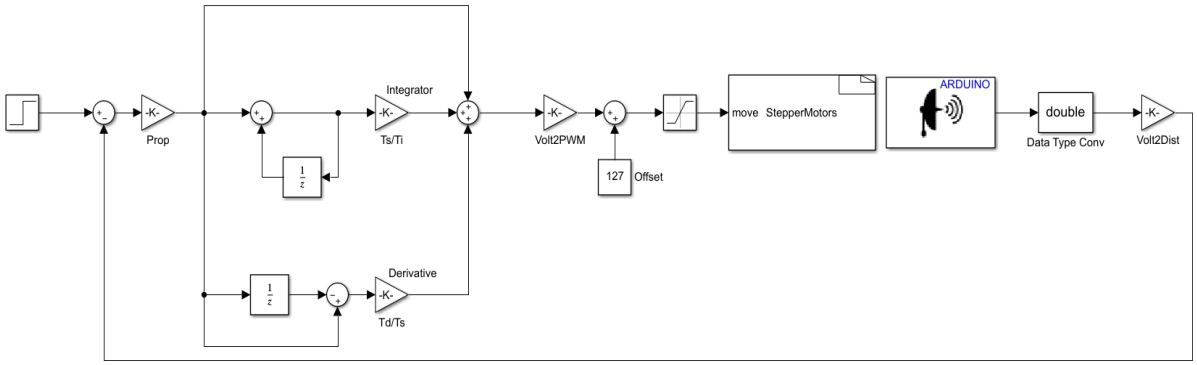

Figure 5-4-1 Simulink of PID Controller in Experiment

In this experiment, as shown in Figure 5-4-1, MATLAB Simulink is used to execute the active control. Before using the controller, the optimal gains for P, I, and D also need to set for the optimal control. Here, the PID Tuner tool in Control System Toolbox is used for system identification.

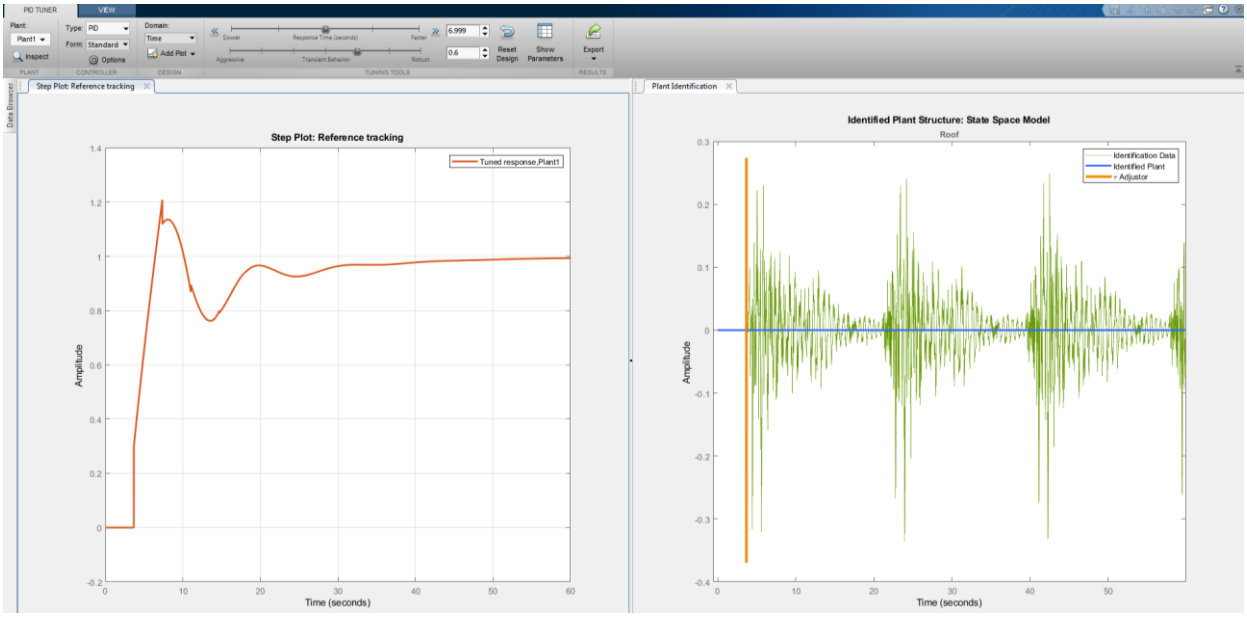

Figure 5-4-2 PID Tuner and System Identification in MATLAB

System identification is performed after the measured input and output data is imported into the PID Tuner. System identification includes selecting the plant model and the parameter values of the structure, which will match the simulated model output to the measured output data. As shown in Figure 5-4-2, after selecting the model, PID Tuner simulates the model and calculates the controller gain to provide a fast and stable response.

5.5 Results and Discussion

		BI without AC	BI with AC
1979 El Centro	Roof Level	0.4672	0.4049
	4th Floor	0.2050	0.2573
	Ground Level	0.0839	0.0965
1994 Northridge	Roof Level	0.0965	0.1014
	4th Floor	0.2058	0.1732
	Ground Level	0.1058	0.1519
1995 Kobe	Roof Level	0.0392	0.0711
	4th Floor	0.0390	0.0721
	Ground Level	0.1604	0.1547
1992 Mendocino	Roof Level	0.1060	0.1103
	4th Floor	0.0647	0.0654
	Ground Level	0.0368	0.0653

Table 5-5-1 Experimental Results (units in *g*)

Table 5-5-1 shows the structural responses sensed at different locations in different scenarios when simulating four earthquakes. Obviously, PID controller does not improve the structural responses of the earthquake, and the measured acceleration is greater than the acceleration measured when the controller is turned off. This is because the controller

continuously adjusts the structure position back to the set value, as shown in Figures 5-5-1 to Figure 5-5-4, the greater vibration results in the greater control output which cause the structural response greater.

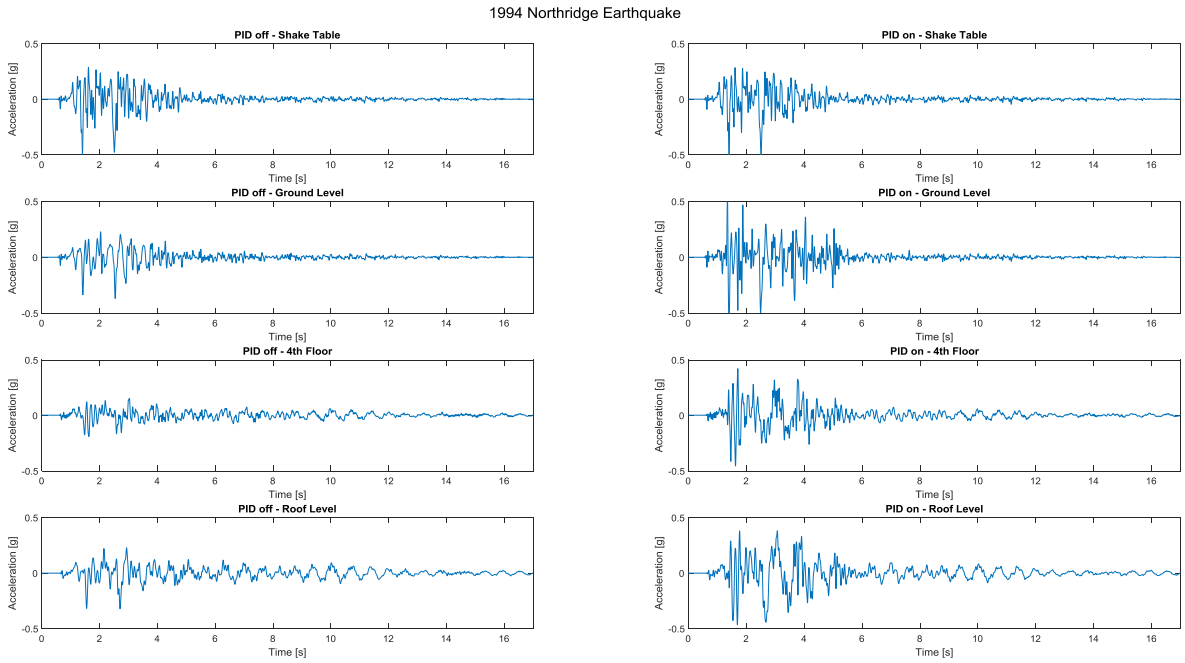

Figure 5-5-1. Structural Responses of 1994 Northridge Earthquake

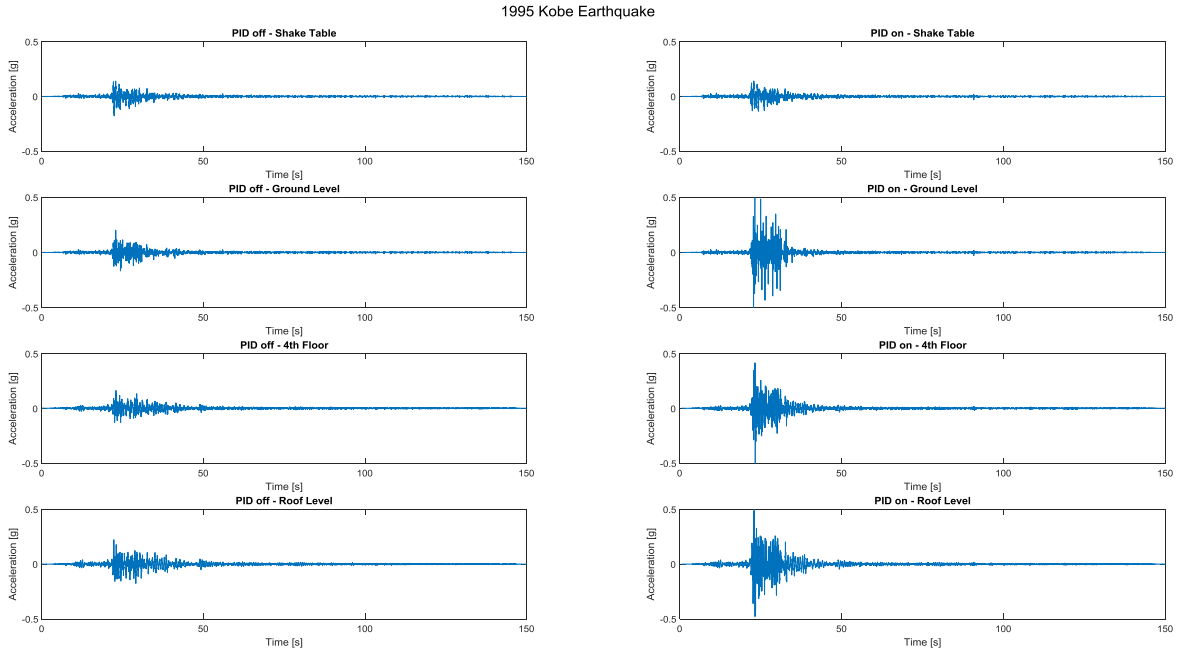

Figure 5-5-2 Structural Responses of 1995 Kobe Earthquake

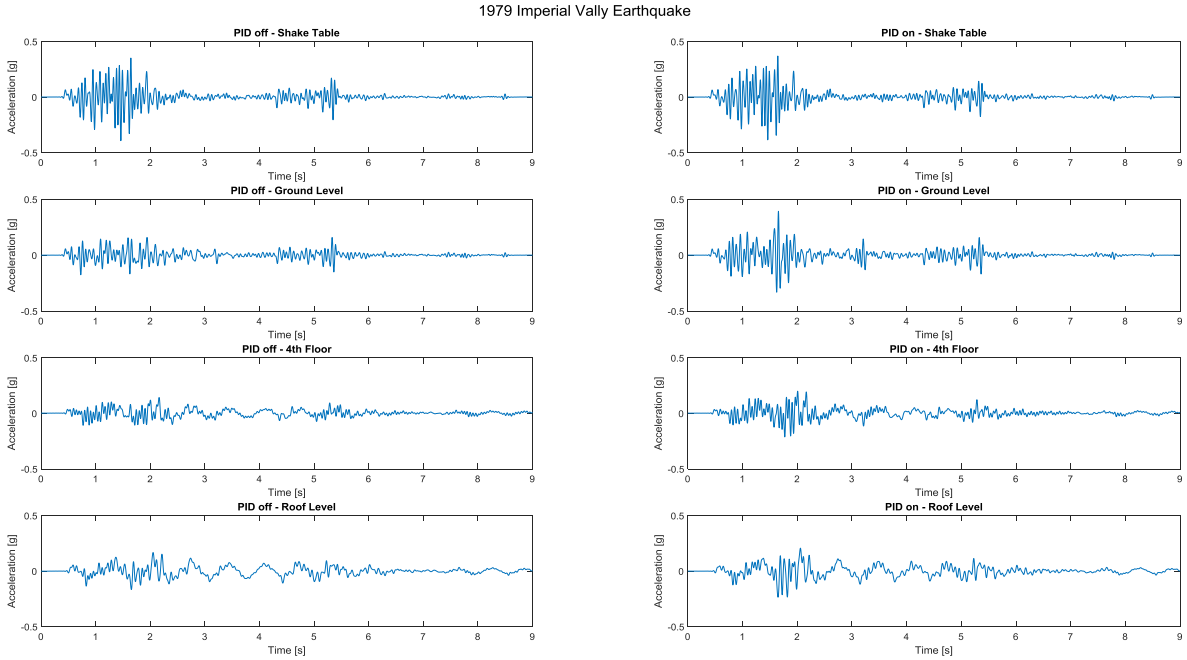

Figure 5-5-3 Structural Responses of 1979 Imperial Valley Earthquake

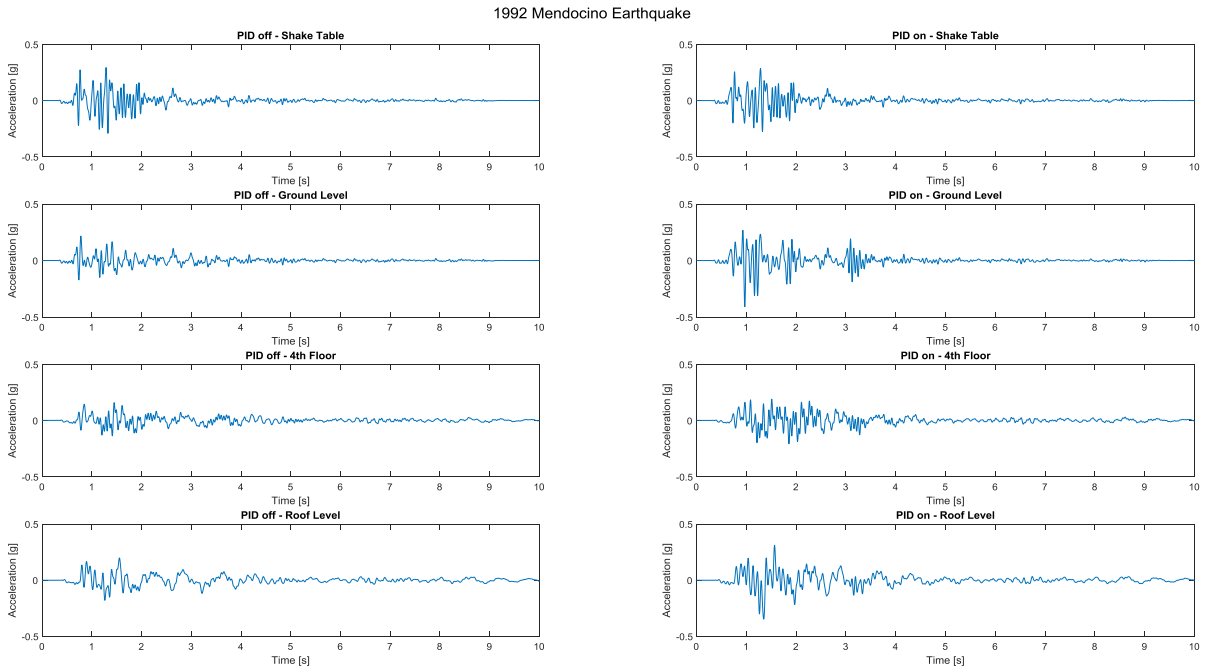

Figure 5-5-4 Structural Responses of 1992 Mendocino Earthquake

5.6 Summary

In Chapter 5, the concept of active control was introduced. The sensors are applied to continuously detect the structural response as the system inputs, and then use stepper motors as actuators to stabilise the structure during the earthquake through the PID controller. Experimental results show that the system is capable of resisting loads caused by the external environment and keeping the building within a safe operating range. However, experiments have also shown that the application of PID controller to base isolated structure does not improve the structural response caused by earthquakes.

CHAPTER 6

SUMMARY, CONCLUSIONS AND FUTURE WORKS

6.1 Summary

The main purpose of this research is to mechanize the traditional base isolation system. Existing seismic and construction methods have been reviewed and classified as passive control, active control and semi-active control. The earthquake early warning system is introduced as a popular topic in recent years and explored its application. Then, the motion equation of the base isolation system is reviewed and described.

In order to realise the possibility of electro-mechanization, the seismic structural response monitoring system is organized, including control platform, network communication, handshake nodes and sensors. The software program is also coded according to the experiment requirements and objectives.

In the experimental part, the earthquake simulation is performed by the Quanser Shake Table II, and the wireless sensors are installed in different positions of the structure. Finally, the data is imported into MATLAB through BeanScape software for data analysis.

The beginning of electro-mechanization of the base isolation system is to use the shear keys to switch modes of different structural characteristics to make up for the deficiency of the traditional base isolation device. Experiments have shown that the base isolation system triggered by EEWS has a significant improvement in the structural response caused by the earthquake. Then, according to the principle of magnet, the frictional force formula is used to investigate the possibility of electromagnet as shear key. Experiments have shown that the hysteresis effect of the electromagnet has little effect on the proposed system, but overall it performs well. Finally, considering the direction of the earthquake and the function of the base isolation system, a two-dimensional base isolation device is introduced, and four linear motors are used for the activation and Initialisation of the proposed system. Experiments show that the execution speed of the linear motors affects the system performance, but the base isolation system triggered by EEWS still performs well.

The final goal is to achieve active control of the base isolation system. In conjunction with the motors and the sensors, the controller cooperates with the PID control algorithm to perform structural vibration control. Experiments show that the PID controller cannot effectively reduce the structural responses caused by earthquakes, but this controller can maintain the structure within the system range.

6.2 Conclusion

This thesis proposes a smart mechatronic base isolation system that connects to the Earthquake Early Warning (EEW) system. When there is no earthquake, the structure on the sliding isolation device can be locked to achieve a strong lateral force resistance against the wind load. Therefore, excessive deformation due to strong wind can be prevented. The system includes a controller that can be programmed to continuously update signals from the EEWS and the network of sensors. When the controller receives the signal from the EEWS indicating that ground motion is about to occur, the shear keys which lock the structure and the isolation device will be released, allowing the superstructure to slide freely. After the ground motion stops, the actuator can be used to re-centre the superstructure to complete the system Initialisation. The system is fully automatic and repeatable. The isolation device uses very low friction linear guides. The performance of isolating ground vibrations is very good without adding stiffness or damping to the structure. As backup plan, the proposed system also includes the network of sensors for detecting ground motion. These sensors will replace the triggering in the event of EEW failure to activate the base isolation system. In addition, this thesis introduces the shake tables to simulate the vibration and a conceptual design laboratory-scaled model. The system is installed on the shake table for earthquake simulation. The tests are carried out under the following three conditions: (1) fixed base – when the shear keys lock the structure when ground motion; (2) base isolation triggered by EEW, and (3) base isolation triggered by the network of sensors. The experiment results show that the proposed smart mechatronic base isolation system can significantly reduce the structural response when earthquake occurs. This research suggests that the system can represent the next generation of seismic structures.

6.3 Research Questions

RQ1. What benefits do mechatronics and control systems add to the base isolation systems?

Zuk presented the earliest notion of active controlled structure in 1968. He distinguished between the active control, which is designed to reduce structural motion and that which generates structural motion. Kinetic structures belong to the second category, which control enclosed space through structural manipulation[92]. Earliest works on active structural control include prestressed tendon to stabilise tall structures, control of tall buildings by cables attached to jacks[87], and use of active systems which can provide increased strength to the structure to counter exceptional over-loading[93].

As shown in Figure 6-3-1, feedback structure is quite common in most of the control concepts. External energy resources are essential for actuators to produce the required control force. According to the control strategy, active control can be classified as: open loop control system (when the left side loop of Figure 6-3-1 is operative); close loop control (when the right loop of Figure 6-3-1 is operative); and open–close loop control (when the both loops of Figure 6-3-1 are operative). An adaptive control system is a variation of open-close loop control with a controller which can adjust parameters of the system. The adaptive systems are generally used to control structures whose parameters are unknown and are based on tracking error between the measured response and the observed response. A learning control system can learn and switch over from open loop control system to close control system depending upon the requirements.

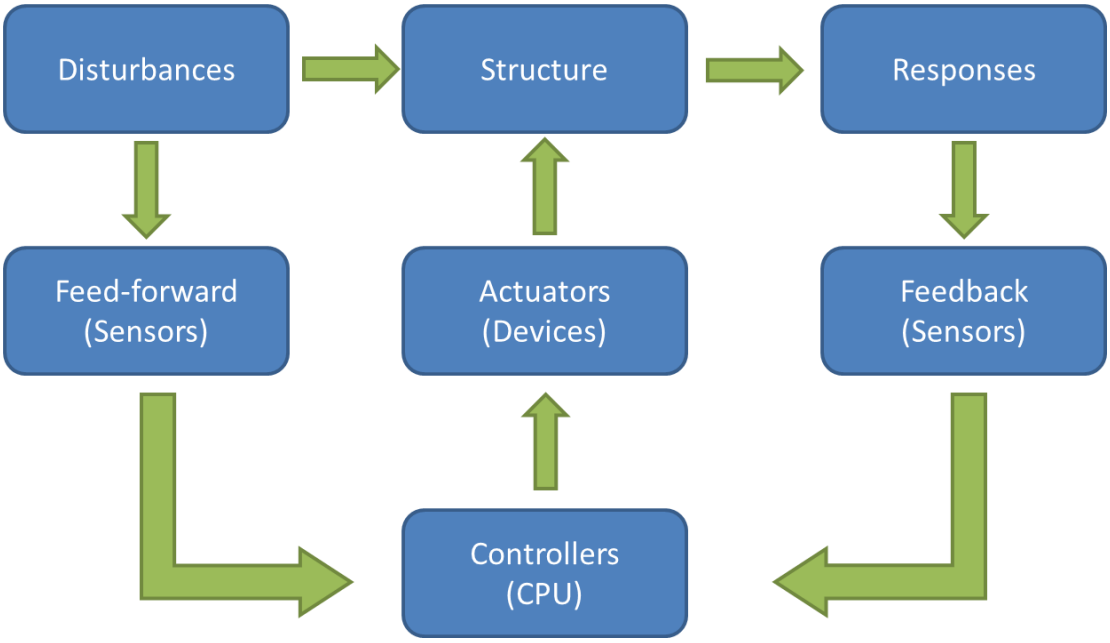

Figure 6-3-1 Active Control Flow Chart

For the semi-active control, various devices have been used for the analysis, which involve (i) Stiffness control devices; (ii) Electro-rheological dampers/magneto-rheological dampers; (iii) Friction control devices; (iv) Fluid viscous devices; and (v) TMDs and TLDs. However, when implemented in the real world of engineering, many problems would still occur during the application, such as (i) Modelling error; (ii) Time delay; (iii) Limited sensor and controller; (iv) Parameter uncertainties and system identification; (v) Discrete time control; (vi) Reliability; and (vii) Cost-effectiveness and hardware requirement. As a result, the corresponding applications of the active control have also been studied.

Control device and controller design are the main focus of the traditional active vibration control systems[94, 95]. Since the force exerted by the earthquake and wind on the structures are very huge and uncertain, these large civil structures require a large amount of energy to control it. The structural control can be classified as passive control which does not require an

external power source[16], and active control which uses sensors and active actuators to control the unwanted vibrations[44]. There are many active control devices designed for structural control applications[96]. The active mass damper (AMD) is the most popular actuator, which uses a mass without spring and dashpot[97].

In order to achieve a good performance, it is essential to design an effective control strategy, which should be simple, robust, and fault tolerant. Many attempts have been made to introduce advanced controllers for the active vibration control of building structures. Instead of changing the structure stiffness, a pole-placement H_∞ control corresponding to a target damping ratio is proposed by Park[98]. In order to avoid the higher order problem in H_∞ control, the balanced truncation is applied by [99]. According to [100], the genetic algorithm is used to determine the feedback control. There are several optimal control algorithms applied for the active vibration control of building structures, for example filtered linear quadratic control (LQ)[101], linear quadratic regulator (LQR)[102], and linear quadratic Gaussian (LQG)[103]. All these controllers are model-based, complex and demand the exact model of the building structure. Some model-free controllers, such as sliding mode control (SMC)[104], neural network control[105], and fuzzy logic control[106] are still complex.

In recent years, PID control is widely used in industrial applications. Without model knowledge, PID control may be the best controller in real-time applications[107]. The great advantages of PID control over the others are that they are simple and have clear physical meanings. Although theory research in PID control algorithms is well established, it is still not well developed in structural vibration control. A simple proportional control is applied to reduce the building displacement due to wind excitation[108]. PD and PID controllers were used in the numerical simulations[109, 110]. A Proportional-integral (PI) controller with an

AMD is used to attenuate the structural motion due to earthquake[111]. However, these control results are not satisfactory, because it is difficult to tune PID gains to guarantee good performances such as rise-time, overshoot, settling time, and steady-state error[109]. Moreover, these works do not discuss the stability analysis of these active control systems.

While there is no doubt about the advances in the structural control field, there still exist some areas which need more exploration[112]. The active devices have the ability to add force onto the building structure. A poorly designed controller will lead to an undesirable control performance, which can even damage the building. So it is desired to study the stability of the closed-loop system. Only a few structural controllers such as H_∞ and SMC considers the stability in their design, whereas the other control strategies do not. However, these designs have concerned only the linear stiffness, since it represents a simple and efficient model at least for a small operational range. In practice, these building structures possess nonlinear behaviour like the hysteresis phenomenon[113]. Also, there is a lack of experimental verification of these controllers. The practical implementation of a controller will be challenging if these issues were not addressed.

RQ2. How to effectively trigger the base isolation system by Earthquake Early Warning System and network of accelerometers?

The technology of Earthquake Early Warning System (EEWS) is different from the traditional seismic report technology [114-120]. Traditionally, rapid determination of seismic parameters mainly depends on the P-wave and S-wave arrival time differences to determine the epicentre distance and position, so it usually takes at least several minutes or longer[121]. Instead, the signal of EEWS needs to be generated in few seconds after the seismic wave

reaches the station, and then there are three kinds of information which are interpretable: (1) whether it is an earthquake; (2) whether it is a large earthquake; (3) the location of the earthquake; (4) the earthquake strength. At present, the most common method is to use the first 3 seconds of P-wave data [64], which is mainly based on the fact that the waveforms and displacement peaks of seismic waveforms of earthquakes are not the same for rapid processing.

In this project, EEWS is used to activate the base isolation system before earthquake waves arrived. In the experiment, controller keeps updating the data from EEWS centre until the earthquake statement changes. Signal is received by Ethernet shield mounted on controller whose transmission speed can reach 100MB/s [77], and the size of a warning is much less than 1KB (about 24 bytes)[84]. Currently, many mainstream SoCs (System on Chip) have built in the controllers for three popular communication protocols: I2C, SPI, and UART. Similarly, various sensors, touch controllers, fingerprint modules, Bluetooth modules, and WIFI modules are also compatible with one or more of these three methods[122]. The UART can only connect one-to-one, and the transmission speed is not fast (up to 115.2 kbps). The existing version is not only popular but also suitable for high-speed, high-volume transmission. Here, it is recommended to make trade-offs based on system requirements between the cost of topology and transmission speed. I2C requires only two signal wires, while SPI needs at least four. If there are multiple slave devices, more wires are inevitable; The general speed of I2C is 100kbs, 400kbps, and 1Mbps, while the speed of SPI can reach several Mbps or 10+ Mbps. After the earliest EEW signal received, the base isolation system is triggered.

As a substitute when the signal of earthquake early warning system fails receiving, accelerometers have the advantage of compensating for the blind area of earthquake early warning system. This device can measure acceleration by the deflection and the circuit. It consists of one cantilever and one weight whose working principle is to change the microstructure of the internal complementary metal oxide semiconductor (CMOS) when the accelerometer moves or rotates[123]. The capacitance value will change and then converts the signal to a specific output voltage. Namely, these sensors have the ability to keep monitoring the situation around including the vibration starts and finishes. In the experiment, accelerometers are arranged around the equipment and keeping sending the data to the controller. Once the data received shows the abnormal vibration, the base isolation system will be triggered immediately. The other issue is sensitivity. High sensitivity may cause unnecessary trigger which makes users troubled[82]. The range of vibration of the network of sensors is set in 0.04g. When the data detected is over, controller activates the base isolation system. At other time, system will not be triggered and check if the system is reset because this kind of vibration doesn't cause any damage.

RQ3. How to improve engineering properties of the isolators?

Most of the base isolation system cannot avoid the isolation layer directly contacting the building, so one of the most important things is how to effectively reduce the friction force. According to the friction formula, the friction force is directly proportional to the friction coefficient and the normal force, so these two factors are the main directions we explore. In this project, choosing a low coefficient of friction is one of the most direct methods, but it still suffers from several shortcomings such as poor performance under strong wind due to its low lateral stiffness, limitations on axial capacity, P-delta effects, and poor re-centring properties,

etc. Therefore, the concept of magnet is proposed to improve the engineering properties of the isolators[124].

Magnetic levitation, a method follows “The same polarity x repels each other, the opposite polarity attracts each other”, can float objects in the air without other external forces. At first step, solenoid is used to play a role as shear key which can firmly fix on the foundation. Normally, solenoid fully extends iron core making the structure not isolated for countering the effects of lateral load acting on a structure. In the event of earthquake, controller receives the signal and then solenoid attracts the iron core back from the foundation. Next, electromagnet is applied. The principle of polarity after power on causes the building and the isolator the same polarity and mutually exclusive. Under the conditions, the building can float on the isolator to eliminate friction. However, the weight of the building makes the normal force very large, so it needs huge power to generate enough repulsive force. Because this project is limited by the availability of funding and large-scale testing facilities, we can only achieve the normal force decreasing to partly eliminate friction.

On the other hand, because earthquakes come from different directions, one-dimensional conceptual framework of proposed system is upgraded to be two-dimensional make it more comprehensive. At the same time, considering the possibility of construction and cost, the linear actuators are mounted above the isolation layer below the structure and the entire system is surrounded by a frame as the limitation of base isolation system. Normally, the actuators will extend completely to fix the building to the frame to achieve enough lateral stiffness. When earthquake occurs, the actuators will be retracted in time to start the base isolation like the most commonly used hydraulic actuators. As a result, the system can perform well when the earthquake at the beginning of the earthquake is small.

RQ4. Does active control help improve the base isolation system?

Recently, Base Isolation systems are improved by control strategies that some kind of active forces are delivered to the main structure. Smart control has been researched in the last two decades. Ramallo et al (2002) presented a theoretical investigation into the topic and Yoshioka et al (2002) demonstrated experimentally the use of magneto-rheological (MR) dampers with laminated rubber base isolators. Clipped-optimal controller utilises H-square (H2)/Linear–quadratic–Gaussian (LQG) control strategy. Chang et al [125] experimentally investigated an active base-isolation system which and low-friction pendulum bearing integrated with hydraulic actuators. Oliveira et al compared four different control strategies and concluded that the Integral control algorithm outperform others based on numerical simulations [126].

However, actively controlled base isolation systems may imply difficulties in practical implementation. In particular, the force-delivering devices such as hydraulic actuators will need to be switched on. Earthquake events are relatively rare in nature and having the system turned on will incur problems such as overheating and other maintenance issues[127]. For semi-active controlled systems, for example, the use of MR dampers[128], the problem of large power consumption seemed to be solved. However, semi-active control still requires careful system identification[12], tuning and control algorithm are complex to implement. This article describes the conceptual framework and experimental investigation of a simple version of active control which is only activated when there is an earthquake.

Next, active control of civil engineering structures has following components: (1) control devices should be large and strong enough to provide active control forces to act on massive and heavy civil engineering structures; (2) The structures are stationary, safe, and stable

without external dynamic disturbances; (3) Structural vibrations are mainly caused by external dynamic loads, which should be kept under control. These characters make civil engineering structures differ from other industries. The classical control theory only focuses on the initial conditions, such as the initial displacements and velocities. Consequently, there are usually no external loadings in the equations of motion. However, environmental loads, such as strong earthquake, wind gust, wave forces, etc. exist in practical situation in nature.

6.4 Future Works

The experiments have already proven that the proposed smart mechatronic basis isolation is feasible. However, full scale implementation still needs to be carried out in conjunction with other professional fields. They are briefly discussed below.

First, traditional passive base isolation is a mature technology, and many different applications (such as lead-core laminated rubber bearings and friction pendulum) are commercially available. Although existing base isolation device can be considered, the proposed concept is to eliminate the requirement for lateral stiffness, so a special design can be conceived with the goal of minimizing lateral stiffness or friction.

Second, regarding the power supply, in the experiment, the controller is running at 5.5V DC, and the power consumption of the sensors and actuators is very low. They can even run on batteries in fully scale implementation. However, the shear keys require sufficient stiffness to withstand all transverse shear of the primary structure, and of course represent a considerable mass. Therefore, a large amount of power is required to activate them, and uninterruptible power supply (UPS) needs to be considered to prevent power outages.

Third, the shear keys are mechanically operated by electromagnet. In a full-scale implementation, as discussed, the shear keys will provide sufficient stiffness, so it may be made of steel in forms of hollow pipes or even solid cross sections. As their weight increases, mechanical operation by electromagnets and electric/hydraulic linear actuators becomes increasingly infeasible. In addition, modern actuators have stall protection (stalling occurs when the load torque is greater than the shaft torque) to prevent hardware damage. The horizontal movement of main structure may cause slight misalignment between shear keys and the shafts that eventually causes the linear brake to stall.

Fourth, since the proposed system requires the internet between the EEWS and the base isolation system, there may be network security issues. In future developments, encryption and decryption techniques can be used to ensure the correctness of the signals, or a separate network connection can be established between buildings and the EEWS.

Last but not least, the controller and electronic devices including actuators may be inference to electromagnetic pulse (EMP), so the protection is required such as Faraday cage.

REFERENCE

[1] I. G. Buckle and R. L. Mayes, "Seismic isolation: history, application, and performance—a world view," *Earthquake spectra*, vol. 6, no. 2, pp. 161-201, 1990.

[2] V. A. Matsagar and R. Jangid, "Base isolation for seismic retrofitting of structures," *Practice Periodical on Structural Design and Construction*, vol. 13, no. 4, pp. 175-185, 2008.

[3] P. B. Rao and R. Jangid, "Performance of sliding systems under near-fault motions," *Nuclear Engineering and Design*, vol. 203, no. 2-3, pp. 259-272, 2001.

[4] R. Emil Simiu and P. DongHun Yeo, *Wind effects on structures*. Wiley Online Library, 1986.

[5] P. Henderson and M. Novak, "Response of base-isolated buildings to wind loading," *Earthquake Engineering & Structural Dynamics*, vol. 18, no. 8, pp. 1201-1217, 1989.

[6] Y. Chen and G. Ahmadi, "Wind effects on base-isolated structures," *Journal of engineering mechanics*, vol. 118, no. 8, pp. 1708-1727, 1992.

[7] B. Liang, X. Shishu, and T. Jiaxiang, "Wind effects on habitability of base-isolated buildings," *Journal of Wind Engineering and Industrial Aerodynamics*, vol. 90, no. 12-15, pp. 1951-1958, 2002.

[8] T. T. Soong and M. C. Costantinou, *Passive and active structural vibration control in civil engineering*. Springer, 2014.

[9] J. Ramallo, E. Johnson, and B. Spencer Jr, "“Smart” base isolation systems," *Journal of Engineering Mechanics*, vol. 128, no. 10, pp. 1088-1099, 2002.

[10] H. Yoshioka, J. Ramallo, and B. Spencer Jr, "“Smart” base isolation strategies employing magnetorheological dampers," *Journal of engineering mechanics*, vol. 128, no. 5, pp. 540-551, 2002.

[11] C.-M. Chang, Z. Wang, and B. F. Spencer, "Application of active base isolation control," in *Sensors and Smart Structures Technologies for Civil, Mechanical, and Aerospace Systems 2009*, 2009, vol. 7292, p. 729239: International Society for Optics and Photonics.

[12] D. Shook, P.-Y. Lin, T.-K. Lin, and P. N. Roschke, "A comparative study in the semi-active control of isolated structures," *Smart Materials and Structures*, vol. 16, no. 4, p. 1433, 2007.

[13] J.-H. Yoo and N. M. Wereley, "Performance of a magnetorheological hydraulic power actuation system," *Journal of Intelligent Material Systems and Structures*, vol. 15, no. 11, pp. 847-858, 2004.

[14] B. Spencer Jr and S. Nagarajaiah, "State of the art of structural control," *Journal of Structural Engineering*, vol. 129, no. 7, pp. 845-856, 2003.

[15] F. Wang, Z. Weng, and L. He, "Active and Passive Hybrid Vibration Isolation," in *Comprehensive Investigation on Active-Passive Hybrid Isolation and Tunable Dynamic Vibration Absorption*: Springer, 2019, pp. 19-45.

[16] M. D. Symans and M. C. Constantinou, "Semi-active control systems for seismic protection of structures: a state-of-the-art review," *Engineering structures*, vol. 21, no. 6, pp. 469-487, 1999.

[17] Z. Ying, W. Zhu, and T. Soong, "A stochastic optimal semi-active control strategy for ER/MR dampers," *Journal of Sound and Vibration*, vol. 259, no. 1, pp. 45-62, 2003.

[18] W. L. Qu, Z. H. Chen, and Y.-L. Xu, "Dynamic analysis of wind-excited truss tower with friction dampers," *Computers & structures*, vol. 79, no. 32, pp. 2817-2831, 2001.

[19] G. P. Cimellaro and A. M. Reinhorn, "Algorithm for optimal design of adjacent buildings connected by fluid viscous devices," in *Structures Congress 2008: Crossing Borders*, 2008, pp. 1-10.

[20] R. Bairrao, L. Guerreiro, and R. C. Barros, "Shaking table tests on semi-active tuned mass and tuned liquid dampers," in *The 14th World Conference on Earthquake Engineering, Beijing, China*, 2008.

[21] S. Dyke, B. Spencer Jr, M. Sain, and J. Carlson, "Experimental verification of semi-active structural control strategies using acceleration feedback," in *Proc. of the 3rd Intl. Conf. on Motion and Vibr. Control*, 1996, vol. 3, pp. 291-296.

[22] F. Marazzi, "Semi-active control of civil structures: implementation aspects," *Ph. D. Dissertation, Università di Pavia*, 2002.

[23] Z.-D. Xu, Y.-P. Shen, and Y.-Q. Guo, "Semi-active control of structures incorporated with magnetorheological dampers using neural networks," *Smart materials and structures*, vol. 12, no. 1, p. 80, 2003.

[24] F. Y. Cheng, H. Jiang, and K. Lou, *Smart structures: innovative systems for seismic response control*. CRC press, 2008.

[25] Y. Kim, C. Kim, and R. Langari, "Novel bio-inspired smart control for hazard mitigation of civil structures," *Smart Materials and Structures,* vol. 19, no. 11, p. 115009, 2010.

[26] J. P. Amezquita-Sanchez, A. Dominguez-Gonzalez, R. Sedaghati, R. de Jesus Romero-Troncoso, and R. A. Osornio-Rios, "Vibration control on smart civil structures: A review," *Mechanics of Advanced Materials and Structures,* vol. 21, no. 1, pp. 23-38, 2014.

[27] K. Doi, "The operation and performance of Earthquake Early Warnings by the Japan Meteorological Agency," *Soil Dynamics and Earthquake Engineering,* vol. 31, no. 2, pp. 119-126, 2011.

[28] G. P. Warn and K. L. Ryan, "A Review of Seismic Isolation for Buildings: Historical Development and Research Needs," *Buildings,* vol. 2, no. 3, pp. 300-325, 2012.

[29] P. Henderson and M. Novak, "Wind effects on base isolated buildings," *Journal of Wind Engineering & Industrial Aerodynamics,* vol. 36, pp. 559-569, 1990.

[30] Y. Chen and G. Ahmadi, "Wind Effects on Base- Isolated Structures," *J. Eng. Mech.,* vol. 118, no. 8, pp. 1708-1727, 1992.

[31] A. Vulcano, "Comparative study of the earthquake and wind dynamic responses of base- isolated buildings," *Journal of Wind Engineering & Industrial Aerodynamics,* vol. 74, pp. 751-764, 1998.

[32] J. S. Love, M. J. Tait, and H. Toopchi-Nezhad, "A hybrid structural control system using a tuned liquid damper to reduce the wind induced motion of a base isolated structure," *Engineering Structures,* vol. 33, no. 3, pp. 738-746, 2011.

[33] L. Chung, A. Reinhorn, and T. Soong, "Experiments on active control of seismic structures," *Journal of Engineering Mechanics,* vol. 114, no. 2, pp. 241-256, 1988.

[34] A. Nishitani and Y. Inoue, "Overview of the application of active/semiactive control to building structures in Japan," *Earthquake engineering & structural dynamics,* vol. 30, no. 11, pp. 1565-1574, 2001.

[35] M. Utkucu, H. S. Kuyuk, and I. H. Demir, "Expanding Horizons in Mitigating Earthquake Related Disasters in Urban Areas: Global Development of Real-Time Seismology," *Disaster Science and Engineering,* vol. 1, no. 2, pp. 44-49, 2015.

[36] B. R. Ellingwood, "Earthquake risk assessment of building structures," *Reliability Engineering & System Safety,* vol. 74, no. 3, pp. 251-262, 2001.

[37] D. J. Mead and D. Meador, *Passive vibration control*. Wiley Chichester, 1998.

[38] F. Casciati, J. Rodellar, and U. Yildirim, "Active and semi-active control of structures–theory and applications: A review of recent advances," *Journal of Intelligent Material Systems and Structures*, vol. 23, no. 11, pp. 1181-1195, 2012.

[39] Y. Li, R. Song, and J. W. Van De Lindt, "Collapse fragility of steel structures subjected to earthquake mainshock-aftershock sequences," *Journal of Structural Engineering*, vol. 140, no. 12, p. 04014095, 2014.

[40] W. Y. H. Y. S. Yongjiu and C. H. W. Siqing, "Finite element analysis on dynamic characteristics and seismic resistance of super high-rise steel structures [J]," *China Civil Engineering Journal*, vol. 5, 2006.

[41] R. W. Clough, K. Benuska, and E. Wilson, "Inelastic earthquake response of tall buildings," in *Proceedings, Third World Conference on Earthquake Engineering, New Zealand*, 1965, vol. 11.

[42] P. Chandurkar and D. P. Pajgade, "Seismic analysis of RCC building with and without shear wall," *International journal of modern engineering research*, vol. 3, no. 3, pp. 1805-1810, 2013.

[43] Z. T. C. Zhong-gui, "On the consolidation of the residential houses with the brick-concrete structure after earthquakes [J]," *Shanxi Architecture*, vol. 6, 2009.

[44] B. Spencer and M. K. Sain, "Controlling buildings: a new frontier in feedback," *IEEE Control Systems*, vol. 17, no. 6, pp. 19-35, 1997.

[45] H. Stuttle, "Joint-clamp," ed: Google Patents, 1907.

[46] S. Krenk, "Frequency analysis of the tuned mass damper," *Journal of applied mechanics*, vol. 72, no. 6, pp. 936-942, 2005.

[47] F. Sadek, B. Mohraz, A. W. Taylor, and R. M. Chung, "A method of estimating the parameters of tuned mass dampers for seismic applications," *Earthquake Engineering & Structural Dynamics*, vol. 26, no. 6, pp. 617-635, 1997.

[48] N. A. Alexander and F. Schilder, "Exploring the performance of a nonlinear tuned mass damper," *Journal of Sound and Vibration*, vol. 319, no. 1-2, pp. 445-462, 2009.

[49] K. Ghaedi, Z. Ibrahim, H. Adeli, and A. Javanmardi, "Invited Review: Recent developments in vibration control of building and bridge structures," *Journal of Vibroengineering*, vol. 19, no. 5, pp. 3564-3580, 2017.

[50] K. Maebayashi, K. Shiba, A. Mita, and Y. Inada, "Hybrid mass damper system for response control of building," in *Proc. Tenth World Conference on Earthquake Engineering*, 1992, pp. 2359-64.

[51] S. Chesné and C. Collette, "A simple hybridization of active and passive mass dampers," in *ISMA conference*, 2016.

[52] K. D. Pham, M. K. Sain, S. R. Liberty, and B. Spencer, "First generation seismic-AMD benchmark: Robust structural protection by the cost cumulant control paradigm," in *Proceedings of the 2000 American Control Conference. ACC (IEEE Cat. No. 00CH36334)*, 2000, vol. 1, no. 6, pp. 1-5: IEEE.

[53] M. Abdel-Rohman and H. H. Leipholz, "Active control of tall buildings," *Journal of Structural Engineering*, vol. 109, no. 3, pp. 628-645, 1983.

[54] T. Soong and A. Reinhorn, "An overview of active and hybrid structural control research in the US," *The structural design of tall buildings*, vol. 2, no. 3, pp. 193-209, 1993.

[55] T. T. Soong and W.-F. Chen, *Active structural control: theory and practice*. Longman Scientific & Technical New York, 1990.

[56] N. R. Bhatt and D. C. Chase, "Instrument rack," ed: Google Patents, 1981.

[57] S. Chesné and C. Collette, "Experimental validation of fail-safe hybrid mass damper," *Journal of Vibration and Control*, vol. 24, no. 19, pp. 4395-4406, 2018.

[58] M. Li, J. Ou, G. Wang, and L. Gui, "Experimental Study on A Full Scale AVS Device," *Earthquake Engineering and Engineering Vibration*, vol. 20, no. 4, pp. 96-105, 2000.

[59] P. Tan and F.-l. Zhou, "Structural active variable stiffness-damping control system and its optimal design," *J. Architect. Civil Eng*, vol. 24, pp. 6-12, 2007.

[60] J. N. Yang and A. K. Agrawal, "Semi-active hybrid control systems for nonlinear buildings against near-field earthquakes," *Engineering structures*, vol. 24, no. 3, pp. 271-280, 2002.

[61] M. Spizzuoco and A. Ochiuozi, "Performance of a semi-active MR control system for earthquake protection," in *Proceedings of the 13th WCEE*, 2004, pp. 1-6.

[62] H. Li and L. Huo, "Advances in structural control in civil engineering in China," *Mathematical Problems in Engineering*, vol. 2010, 2010.

[63] F. Zhou, P. Tan, W. Yan, and L. Wei, "Theoretical and experimental research on a new system of semi-active structural control with variable stiffness and damping," *Earthquake Engineering and Engineering Vibration*, vol. 1, no. 1, pp. 130-135, 2002.

[64] Y. M. Wu and L. Zhao, "Magnitude estimation using the first three seconds P-wave amplitude in earthquake early warning," *Geophysical Research Letters*, vol. 33, no. 16, 2006.

[65] R. M. Allen, P. Gasparini, O. Kamigaichi, and M. Bose, "The status of earthquake early warning around the world: An introductory overview," *Seismological Research Letters*, vol. 80, no. 5, pp. 682-693, 2009.

[66] C. Satriano, Y.-M. Wu, A. Zollo, and H. Kanamori, "Earthquake early warning: Concepts, methods and physical grounds," *Soil Dynamics and Earthquake Engineering*, vol. 31, no. 2, pp. 106-118, 2011.

[67] P. Gasparini, G. Manfredi, and J. Zschau, *Earthquake early warning systems*. Springer, 2007.

[68] Y. K. Wen, "Method for Random Vibration of Hysteretic Systems," (in English), *Journal of the Engineering Mechanics Division-Asce*, vol. 102, no. 2, pp. 249-263, 1976.

[69] A. S. Whittaker and M. Kumar, "SEISMIC ISOLATION OF NUCLEAR POWER PLANTS," *Nuclear Engineering and Technology*, vol. 46, no. 5, pp. 569-580, 2014.

[70] S. Nagarajaiah, A. M. Reinhorn, and M. C. Constantinou, "Nonlinear Dynamic Analysis of 3-D-Base-Isolated Structures," *J. Struct. Eng.*, vol. 117, no. 7, pp. 2035-2054, 1991.

[71] B. R. Hacker, G. A. Abers, and S. M. Peacock, "Subduction factory 1. Theoretical mineralogy, densities, seismic wave speeds, and H2O contents," *Journal of Geophysical Research: Solid Earth*, vol. 108, no. B1, 2003.

[72] E. Yamasaki, "What We Can Learn From Japan's Early Earthquake Warning System," *Momentum*, vol. 1, no. 1, 18/4/2012 2012.

[73] A. Zollo, O. Amoroso, M. Lancieri, Y.-M. Wu, and H. Kanamori, "A threshold-based earthquake early warning using dense accelerometer networks," *Geophysical Journal International*, vol. 183, no. 2, pp. 963-974, 2010.

[74] M. Banzi and M. Shiloh, *Getting started with Arduino: the open source electronics prototyping platform*. Maker Media, Inc., 2014.

[75] A. Saraò, M. Clocchiatti, C. Barnaba, and D. Zuliani, "Using an Arduino seismograph to raise awareness of earthquake hazard through a multidisciplinary approach," *Seismological Research Letters*, vol. 87, no. 1, pp. 186-192, 2016.

[76] R. Nicolau Vidal, "Omnidirectional scanner using a time of flight sensor," Universitat Politècnica de Catalunya, 2018.

[77] S. Monk, *Programming Arduino: getting started with sketches*. Tab Books, 2016.

[78] N. Semiconductors, "UM10204 I2C-bus specification and user manual," *User Manual*, vol. 4, 2014.

[79] A. Devices, "ADXL345 datasheet," *USA: Analog Devices*, 2010.

[80] L. Ada, "Adafruit VL53L0X Time of Flight Micro-LIDAR Distance Sensor Breakout," ed: Recuperado a partir de https://learn. adafruit. com/adafruit-vl53l0x-micro …, 2018.

[81] J.-D. Warren, J. Adams, and H. Molle, "Arduino for robotics," in *Arduino robotics*: Springer, 2011, pp. 51-82.

[82] N. Zhao, "Full-featured pedometer design realized with 3-axis digital accelerometer," *Analog Dialogue,* vol. 44, no. 06, pp. 1-5, 2010.

[83] C.-M. Lu, "Communication system for devices with UART interfaces," ed: Google Patents, 2010.

[84] R. R. Friedlander and J. R. Kraemer, "System and method for detection of earthquakes and tsunamis, and hierarchical analysis, threat classification, and interface to warning systems," ed: Google Patents, 2010.

[85] G. Martindale, "Earthquake Monitor," 2011.

[86] D. R. Choudhury, *Modern control engineering*. PHI Learning Pvt. Ltd., 2005.

[87] T. Soong, "State-of-the-art review: active structural control in civil engineering," *Engineering Structures,* vol. 10, no. 2, pp. 74-84, 1988.

[88] R. E. Kalman, "Canonical structure of linear dynamical systems," *Proceedings of the National Academy of Sciences of the United States of America,* vol. 48, no. 4, p. 596, 1962.

[89] S. Tavakoli and P. Fleming, "Optimal tuning of PI controllers for first order plus dead time/long dead time models using dimensional analysis," in *European Control Conference (ECC), 2003*, 2003, pp. 2196-2200: IEEE.

[90] S. Etedali, M. R. Sohrabi, and S. Tavakoli, "Optimal PD/PID control of smart base isolated buildings equipped with piezoelectric friction dampers," *Earthquake Engineering and Engineering Vibration,* vol. 12, no. 1, pp. 39-54, 2013.

[91] A. O'Dwyer, *Handbook of PI and PID controller tuning rules*. Imperial college press, 2009.

[92] W. Zuk, "Kinetic structures, civil engineering," in *ASCE*, 1968, vol. 39, pp. 62-64.

[93] W. Nordell, "Active systems for blast-resistant structures," NAVAL CIVIL ENGINEERING LAB PORT HUENEME CA1969.

[94] N. Fisco and H. Adeli, "Smart structures: part I—active and semi-active control," *Scientia Iranica,* vol. 18, no. 3, pp. 275-284, 2011.

[95] N. Fisco and H. Adeli, "Smart structures: part II—hybrid control systems and control strategies," *Scientia Iranica,* vol. 18, no. 3, pp. 285-295, 2011.

[96] T. Datta, "A state-of-the-art review on active control of structures," *ISET Journal of earthquake technology,* vol. 40, no. 1, pp. 1-17, 2003.

[97] J. C. Chang and T. T. Soong, "Structural control using active tuned mass dampers," *Journal of the Engineering Mechanics Division,* vol. 106, no. 6, pp. 1091-1098, 1980.

[98] W. Park, K.-S. Park, and H.-M. Koh, "Active control of large structures using a bilinear pole-shifting transform with H∞ control method," *Engineering Structures,* vol. 30, no. 11, pp. 3336-3344, 2008.

[99] R. Saragih, "Designing active vibration control with minimum order for flexible structure," in *Control and Automation (ICCA), 2010 8th IEEE International Conference on*, 2010, pp. 450-453: IEEE.

[100] H. Du and N. Zhang, "H∞ control for buildings with time delay in control via linear matrix inequalities and genetic algorithms," *Engineering Structures,* vol. 30, no. 1, pp. 81-92, 2008.

[101] K. Seto, "A structural control method of the vibration of flexible buildings in response to large earthquakes and strong winds," in *Decision and Control, 1996., Proceedings of the 35th IEEE Conference on*, 1996, vol. 1, pp. 658-663: IEEE.

[102] A. Alavinasab, H. Moharrami, and A. Khajepour, "Active Control of Structures Using Energy-Based LQR Method," *Computer-Aided Civil and Infrastructure Engineering,* vol. 21, no. 8, pp. 605-611, 2006.

[103] C.-C. Ho and C.-K. Ma, "Active vibration control of structural systems by a combination of the linear quadratic Gaussian and input estimation approaches," *Journal of Sound and Vibration,* vol. 301, no. 3-5, pp. 429-449, 2007.

[104] J. N. Yang, J. Wu, A. Agrawal, and Z. Li, "Sliding mode control for seismic-excited linear and nonlinear civil engineering structures," 1994.

[105] J.-T. Kim, H.-J. Jung, and I.-W. Lee, "Optimal structural control using neural networks," *Journal of engineering Mechanics,* vol. 126, no. 2, pp. 201-205, 2000.

[106] D. A. Shook, P. N. Roschke, P.-Y. Lin, and C.-H. Loh, "GA-optimized fuzzy logic control of a large-scale building for seismic loads," *Engineering structures,* vol. 30, no. 2, pp. 436-449, 2008.

[107] K. J. Åström and T. Hägglund, "Revisiting the Ziegler–Nichols step response method for PID control," *Journal of process control,* vol. 14, no. 6, pp. 635-650, 2004.

[108] A. Nerves and R. Krishnan, "Active control strategies for tall civil structures," in *Industrial Electronics, Control, and Instrumentation, 1995., Proceedings of the 1995 IEEE IECON 21st International Conference on*, 1995, vol. 2, pp. 962-967: IEEE.

[109] R. Guclu, "Sliding mode and PID control of a structural system against earthquake," *Mathematical and Computer Modelling,* vol. 44, no. 1-2, pp. 210-217, 2006.

[110] R. Guclu and H. Yazici, "Vibration control of a structure with ATMD against earthquake using fuzzy logic controllers," *Journal of Sound and Vibration,* vol. 318, no. 1-2, pp. 36-49, 2008.

[111] M. Tinkir, M. Kalyoncu, and Y. Şahin, "Deflection control of two-floors structure against northridge earthquake by using PI controlled active mass damping," in *Applied Mechanics and Materials*, 2013, vol. 307, pp. 126-130: Trans Tech Publ.

[112] S. Thenozhi and W. Yu, "Advances in modeling and vibration control of building structures," *Annual Reviews in Control*, vol. 37, no. 2, pp. 346-364, 2013.

[113] F. Naeim, "Dynamics of Structures, Theory and Applications in Earthquake Engineering," *Earthquake Spectra*, vol. 17, no. 3, pp. 549-550, 2001.

[114] J. D. Elkins, "Earthquake early warning system," ed: Google Patents, 1997.

[115] Y. Nakamura and J. Saita, "UrEDAS, the earthquake warning system: Today and tomorrow," in *Earthquake Early Warning Systems*: Springer, 2007, pp. 249-281.

[116] Y.-M. Wu and H. Kanamori, "Development of an earthquake early warning system using real-time strong motion signals," *Sensors*, vol. 8, no. 1, pp. 1-9, 2008.

[117] N. C. Hsiao, Y. M. Wu, T. C. Shin, L. Zhao, and T. L. Teng, "Development of earthquake early warning system in Taiwan," *Geophysical Research Letters*, vol. 36, no. 5, 2009.

[118] P.-Y. Lin, "Earthquake early warning systems," *International Journal of Automation and Smart Technology*, vol. 1, no. 2, pp. 27-34, 2011.

[119] E. Yamasaki, "What we can learn from Japan's early earthquake warning system," *Momentum*, vol. 1, no. 1, p. 2, 2012.

[120] Y.-M. Wu and T.-L. Lin, "A test of earthquake early warning system using low cost accelerometer in Hualien, Taiwan," in *Early Warning for Geological Disasters*: Springer, 2014, pp. 253-261.

[121] A. Ben-Menahem and S. J. Singh, *Seismic waves and sources*. Springer Science & Business Media, 2012.

[122] A. Z. Abbasi, N. Islam, and Z. A. Shaikh, "A review of wireless sensors and networks' applications in agriculture," *Computer Standards & Interfaces*, vol. 36, no. 2, pp. 263-270, 2014.

[123] P. Michalik, A. Napieralski, D. Fernández, and J. Madrenas, "Technology-portable mixed-signal sensing architecture for CMOS-integrated z-axis surface-micromachined accelerometers," in *Mixed Design of Integrated Circuits and Systems (MIXDES), 2010 Proceedings of the 17th International Conference*, 2010, pp. 431-435: IEEE.

[124] E. A. Johnson, J. C. Ramallo, B. F. Spencer Jr, and M. K. Sain, "Intelligent base isolation systems," in *Proceedings of the Second World Conference on Structural Control*, 1998, vol. 1, no. June, pp. 367-76.

[125] C. M. Chang and B. F. Spencer, "Active base isolation of buildings subjected to seismic excitations," *Earthquake Engineering & Structural Dynamics*, vol. 39, no. 13, pp. 1493-1512, 2010.

[126] F. Oliveira, P. Morais, and A. Suleman, "A comparative study of semi- active control strategies for base isolated buildings," *Earthquake Engineering and Engineering Vibration*, vol. 14, no. 3, pp. 487-502, 2015.

[127] A. Kashiwazaki, T. Shimada, T. Fujiwaka, and K. Umeki, "Feasibility tests on a three-dimensional base isolation system incorporating hydraulic mechanism," in *ASME 2002 Pressure Vessels and Piping Conference*, 2002, pp. 11-18: American Society of Mechanical Engineers.

[128] M. Braz-César and R. Barros, "Properties and numerical modeling of MR dampers," in *ICEM15-15 th International Conference on Experimental Mechanics*, 2012.